

Random surfaces and lattice Yang-Mills

Sky Cao Minjae Park Scott Sheffield
MIT and IAS Princeton University of Chicago MIT and IAS Princeton

July 14, 2023

Abstract

We study Wilson loop expectations in lattice Yang-Mills models for $G = \mathrm{U}(N)$. Using tools recently introduced in a companion paper [PPSY23], we provide alternate derivations, interpretations, and generalizations of several recent theorems about Brownian motion limits (Dahlqvist), lattice string trajectories (Chatterjee and Jafarov) and surface sums (Magee and Puder). We show further that one can express Wilson loop expectations as sums over embedded planar maps in a manner that applies to any matrix dimension $N \geq 1$, any inverse temperature $\beta > 0$, and any lattice dimension $d \geq 2$.

The embedded maps we consider are pairs (M, ϕ) where M is a planar (or higher genus) map and ϕ is a graph homomorphism from M to a lattice such as \mathbb{Z}^d . The faces of M come in two partite classes: *edge-faces* (each mapped by ϕ onto a single edge) and *plaquette-faces* (each mapped by ϕ onto a single plaquette). When $G = \mathrm{U}(N)$ the weight of a lattice edge e is the Weingarten function applied to the Young tableau whose row lengths are the boundary lengths of the faces in $\phi^{-1}(e)$. (The Weingarten function becomes quite simple in the $N \rightarrow \infty$ limit.) The overall weight of an embedded map is proportional to N^χ (where χ is the Euler characteristic) times the product of the edge weights. There are several variants of this construction, which yield different embedded map models. In this context, we present a list of relevant open problems spanning several disciplines: random matrix theory, representation theory, statistical physics, and the theory of random surfaces, including random planar maps and Liouville quantum gravity.

Contents

1	Introduction	2
1.1	Overview	2
1.2	Random matrices	5
1.3	Continuum Yang-Mills	6
1.4	Lattice models and planar maps	7
1.5	Main results	8
2	Notation and background	12
2.1	Poisson point process on strand diagrams	12
2.2	Representation theory and other preliminaries	18
3	Poisson process exploration, the $T \rightarrow \infty$ limit, and recovery of Weingarten calculus	27
3.1	Strand-by-strand exploration	27
3.2	Extension to general values of N	43
4	Schwinger-Dyson/Master loop equation	47

5	Wilson loop expectations as sums over edge-plaquette embeddings	54
6	Open problems	57

1 Introduction

1.1 Overview

On a heuristic level, Euclidean Yang-Mills theory is a “probability measure” defined by

$$d\mu_{\text{YM}}(\omega) = \frac{1}{Z} e^{-\frac{1}{2g^2} S_{\text{YM}}(\omega)} d\omega$$

where ω ranges over a space \mathcal{A} of Lie-algebra-valued connection forms on some Riemannian manifold, the Yang-Mills action S_{YM} is the L^2 -norm of the curvature of ω , g is a coupling constant, and $d\omega$ is a “Lebesgue measure” on \mathcal{A} . Making precise sense of the heuristic definition above is a famous open problem that we will not solve here [JW06].

Instead, we will study *lattice Yang-Mills theory* (a.k.a. *lattice gauge theory*), an approximation to the continuum theory introduced in 1974 by Wilson [Wil74] who also credits Polyakov and Smit for similar ideas [Wil04]. An online search for scholarly work on “lattice gauge theory” turns up tens of thousands of articles in physics and mathematics, and we cannot cover all of the variants and applications here. Wilson’s memoir and Chatterjee’s recent survey for probabilists are good places to start [Wil04, Cha19b]. See also Yang’s account of his early work with Mills in 1954 [WG01].

Lattice Yang-Mills assigns a random N -by- N matrix from some compact Lie group G — usually $U(N)$, $SO(N)$, $SU(N)$ or $Sp(N/2)$ — to each directed edge of a graph Λ , which is usually \mathbb{Z}^d or a finite induced subgraph of \mathbb{Z}^d . We require this assignment to have an edge-reversal symmetry: if Q_e is the matrix assigned to a directed edge $e = (v, w)$, then $Q_{(w,v)} = Q_{(v,w)}^{-1}$. If $p = (e_1, e_2, \dots, e_k)$ is a directed path, then we write $Q_p = Q_{e_1} Q_{e_2} \dots Q_{e_k}$. A *loop* is a directed cycle ℓ defined modulo cyclical reordering (which amounts to repositioning the starting point of the loop). We define a set \mathcal{P} of directed loops in Λ that we call *plaquettes*. Usually \mathcal{P} is the set of directed unit squares in Λ (i.e., directed cycles with four distinct vertices), but in principle \mathcal{P} can be any collection of loops that is closed under reversal (i.e. $p \in \mathcal{P}$ implies that the orientation reversal of p is in \mathcal{P}).

Define the **normalized trace** by $\text{tr}(M) := \frac{1}{N} \text{Tr}(M) = \frac{1}{N} \left(\sum_{j=1}^N M_{j,j} \right)$ and write $\text{Re}(z)$ for the real part of z . Note that if M is the identity, then $\text{Re}(\text{tr}(M)) = 1$ and $\text{Re}(\text{tr}(-M)) = -1$. In some sense $\text{Re}(\text{tr}(M)) \in [-1, 1]$ is a measure of how close M is to the identity matrix. It is large (close to 1) if M is near the identity. Note also that for unitary matrices M , we have that $\frac{1}{2}(\text{tr}(M) + \text{tr}(M^{-1})) = \text{Re}(\text{tr}(M))$. If ℓ is a loop then $\text{tr}(Q_\ell)$ is well-defined because the conjugacy class of $Q_{e_1} Q_{e_2} \dots Q_{e_k}$ (and hence the trace) does not change if we cyclically reorder the e_i . If ℓ^{-1} is the orientation reversal of ℓ then $\text{tr}(Q_{\ell^{-1}}) = \overline{\text{tr}(Q_\ell)}$. This is because inverting a matrix inverts its eigenvalues, and (for matrices in compact Lie groups) each eigenvalue z satisfies $|z|^2 = z\bar{z} = 1$ so that $1/z = \bar{z}$.

The lattice Yang-Mills measure is the probability measure

$$Z^{-1} \prod_{p \in \mathcal{P}} \exp(N\beta \text{Tr}(Q_p)) \prod_{e \in E_\Lambda^+} dQ_e \tag{1.1}$$

where $\beta > 0$ is an inverse temperature, Z is a normalizing constant and (to avoid counting an undirected edge twice) E_Λ^+ is the set of oriented edges of Λ for which the endpoint is lexicographically after the starting point. This is a positive measure because \mathcal{P} is closed under direction-reversal.

Similarly, we can define a set \mathcal{P}^+ of “positively oriented plaquettes” containing exactly one element of $\{\ell, \ell^{-1}\}$ for each $\ell \in \mathcal{P}$, and then rewrite (1.1) as

$$Z^{-1} \prod_{p \in \mathcal{P}^+} \exp(2N\beta \operatorname{Re}(\operatorname{Tr}(Q_p))) \prod_{e \in E_\Lambda^+} dQ_e. \quad (1.2)$$

Remark 1.1. We note here that the above action differs from previous work [Cha19a, CJ16, SSZ22] by a factor of 2: where we have 2β the previous works have just β . This slightly simplifies many of our formulas later on, where β appears instead of $\frac{\beta}{2}$.

Informally, the Yang-Mills measure on (Q_e) configurations corresponds to i.i.d. *Haar measure* (one instance of Haar measure for each positively directed edge of Λ) modified by a *weighting* that favors configurations for which Q_p is close to the identity whenever $p \in \mathcal{P}$. A *Wilson loop observable* is a quantity of the form

$$W_{\mathcal{L}}(Q) := \prod_{\ell \in \mathcal{L}} \operatorname{tr}(Q_\ell),$$

where \mathcal{L} is some finite collection of loops in Λ . A *Wilson loop expectation* is a quantity of the form

$$\mathbb{E}[W_{\mathcal{L}}(Q)]$$

Remark 1.2. In contrast to previous works [Cha19a, CJ16, SSZ22], our Wilson loops are defined with the normalized trace rather than the trace. Thus, our Wilson loop expectations are $N^{-|\mathcal{L}|}$ (here $|\mathcal{L}|$ denotes the number of loops in \mathcal{L}) times the Wilson loop expectations of the previous works. This is the more natural scaling for large N limits.

The fundamental goal of lattice Yang-Mills theory is to understand these quantities. That is, one seeks to compute

$$\int \prod_{\ell \in \mathcal{L}} \operatorname{tr}(Q_\ell) Z^{-1} \prod_{p \in \mathcal{P}} \exp(N\beta \operatorname{Tr}(Q_p)) \prod_{e \in E_\Lambda^+} dQ_e \quad (1.3)$$

which we can Taylor expand and write as

$$Z^{-1} \int \prod_{\ell \in \mathcal{L}} \operatorname{tr}(Q_\ell) \prod_{p \in \mathcal{P}} \left(\sum_{k=0}^{\infty} \frac{(N\beta)^k}{k!} \operatorname{Tr}(Q_p)^k \right) \prod_{e \in E_\Lambda^+} dQ_e. \quad (1.4)$$

Given $K : \mathcal{P} \rightarrow \mathbb{Z}_+$, write $K! = \prod_{p \in \mathcal{P}} K(p)!$ and $\beta^K = \prod_{p \in \mathcal{P}} \beta^{K(p)}$. Using this notation, write (1.4) as

$$Z^{-1} \sum_{K: \mathcal{P} \rightarrow \mathbb{Z}_+} \frac{(N\beta)^K}{K!} \int \prod_{\ell \in \mathcal{L}} \operatorname{tr}(Q_\ell) \prod_{p \in \mathcal{P}} \left(\operatorname{Tr}(Q_p) \right)^{K(p)} \prod_{e \in E_\Lambda^+} dQ_e. \quad (1.5)$$

This leads to a classical problem in random matrix theory, which is somehow at the heart of this subject. How can we best compute and understand the individual summand in (1.5), which can be described in words as “expected products of traces of products of Haar-distributed matrices and their inverses”?

Variants of this question have a long history, beginning with the foundational work of 't Hooft and Brézin et al and Itzykson, Parisi, Zuber from the 1970's [tH93, BIPZ78] and expanding greatly over subsequent decades, encompassing various types of random matrices, including Gaussian ensembles (such as GUE or GOE) as well as Haar measure on compact Lie

groups [Eyn11a, IZ80, Meh81, GPW91, DFGZJ95, Zvo97, BIZ80, Oko00, BDFG02, ZJZ03, GMS05, GMS05, MS06, CMSS07, EO08, CGMS09, Eyn11b, GN15, E⁺16]. These papers make connections to the random planar map theory developed by Tutte (and many others)[Tut68] and the continuum random surface theory developed by Polyakov (and many others) [Pol81]. The third author’s recent random surface survey contains many additional references on both sides [She22].

Despite these decades of work, fundamental advances continue to be made. For example, the precise question above was recently addressed in the groundbreaking work of Magee and Puder [MP19, MP22], as explained further in Section 1.2 below. The analog of Λ in their setting is a “blossom graph” which contains a single vertex and an edge set E_Λ that consists of finitely many (distinct and labeled) self-loops. This is somehow the most general setting, because in this scenario *any* element of the free group generated by (Q_e) can be written as Q_ℓ for a loop ℓ in Λ . Their analysis treats this as a fundamental random matrix question (not necessarily motivated by Yang-Mills) and builds on the classical work of Collins and Śniady on the so-called *Weingarten calculus* which in turn builds on earlier work by Weingarten himself [Wei78, CŚ06, CMN22]. See also the representation-theoretic ideas due to Dahlqvist and others [CDK18, Dah16]. Further analysis on this theme appears in recent work by Buc-d’Alché which in particular describes the $N \rightarrow \infty$ asymptotic behavior of Wilson loop expectations in terms of so-called *unitary maps* [Bd23] while also considering generalizations to mixtures of deterministic and unitary matrices.

A series of papers by Chatterjee and/or Jafarov has provided a different approach to identities involving (1.5) including the *Schwinger-Dyson Master Loop equations*. This approach enables them to describe the $N \rightarrow \infty$ behavior of (1.5) in terms of the so-called *lattice string trajectories* [CJ16, Cha19b, Jaf16, Cha19a], see also another recent derivation by [SSZ22] and several generalizations due to Diez and Miaskiwy [DM22]. These works build on a vast literature in this area, including early works of Makeenko and Migdal [MM79]. Although they work in the setting where Λ is an induced subgraph of \mathbb{Z}^d , one may also recall a standard “gauge fixing” argument that allows one to reduce to the case that Q_e is fixed to be the identity for all e within some spanning tree of Λ . This is equivalent to identifying that entire tree with a single vertex, which reduces Λ to a blossom graph that (in the case $\beta = 0$) agrees exactly with the setting discussed by Magee and Puder.

We will provide an alternate derivation of some of the blossom graph results of Magee and Puder [MP19, MP22] as well as the master field and string trajectory results of Chatterjee and Jafarov [CJ16, Cha19b, Jaf16, Cha19a]. Our statements along these lines will be slightly more general than those in previous works. We allow for any matrix dimension $N \geq 1$ (the results in [MP19, MP22] are stated for N sufficiently large; one has to use a slightly different definition of the Weingarten function for smaller N). We consider general Λ and \mathcal{P} in our derivation of the Schwinger-Dyson relations (in [CJ16, Cha19b, Jaf16, Cha19a] the plaquettes \mathcal{P} are taken to be squares, though this is not fundamental to the argument) and we also derive a slightly more general form of those relations (allowing one to somehow explore a single edge instead of exploring all edges at once; Chatterjee once suggested in private conversation that this should be possible). Another straightforward generalization would be to include some deterministic matrices in the words; this is done e.g. in [Bd23] but we will not discuss this here. While [CJ16, Cha19b, Jaf16, Cha19a] first frame their results in terms of $O(N)$ and $SU(N)$ we will frame our results and discussion in terms of $U(N)$, which from our point of view is the simplest case. In a forthcoming revision, we will explain how our results change if one instead considers $SU(N)$, $SO(N)$, or $Sp(N/2)$. See Remark 1.14 for more discussion.

In addition, we will explain how to express Wilson loop expectations in terms of random lattice-embedded planar maps in various ways, which give rise to convergent sums for any Λ , any $N \geq 1$, and any β . These are closely related to the surface sums in [MP19, MP22], but our derivation and interpretation will be rather different.

Remark 1.3. One of the long-term goals of this theory is to construct and understand a continuum scaling limit of quantities like (1.5) as $\beta \rightarrow \infty$ and the lattice mesh size simultaneously goes to zero at an appropriate rate. Thus, ideally one desires an understanding of the terms of (1.5) that is sufficiently robust that it allows one to make predictions about these limits.

Remark 1.4. When β is large, the function $x \rightarrow \exp(2\beta x)$, defined for $x \in [-1, 1]$, is largest for x near 1 and *much smaller* in the rest of $[-1, 1]$. In principle, one could replace the \exp in (1.3) by a different function with this property: say $x \rightarrow \frac{1}{2}(x^b + x^{b+1})$ for some large b . If we took this approach, then the analog of (1.5) would have only finitely many summands, but we would still expect it to have a similar scaling limit behavior as $b \rightarrow \infty$ and the lattice mesh size simultaneously goes to zero. Somehow b is playing the role of β here: instead of taking the number of plaquettes of a given type to be *a priori* Poisson with parameter β we can take the number to be either b or $b + 1$ (each with probability $1/2$). Alternatively, one can replace (1.1) with

$$Z^{-1} \left[\left(|\mathcal{P}|^{-1} \sum_{p \in \mathcal{P}} \text{tr}(Q_p) \right)^b + \left(|\mathcal{P}|^{-1} \sum_{p \in \mathcal{P}} \text{tr}(Q_p) \right)^{b+1} \right] \prod_{e \in E_\lambda^+} dQ_e \quad (1.6)$$

which somehow fixes the *total* number of plaquettes to be b or $b + 1$. This approach might also have a similar scaling limit if $b \rightarrow \infty$ at the right rate. If one is working toward the goal of “constructing a candidate continuum theory” one is allowed to use whatever approach turns out to be most computationally tractable.

Acknowledgements. We thank Sourav Chatterjee, Bjoern Bringmann, Hao Shen, and Tom Spencer for helpful conversations. We thank the Institute for Advanced Study for hosting us while this work was completed. The first author was supported by the Minerva Research Foundation at IAS, as well as by NSF Award: DMS 2303165. The third author is supported by NSF Award: DMS 2153742.

1.2 Random matrices

At the heart of our analysis are two classical questions about the traces of random matrices. The first is the one we discussed in Section 1.1 and the second is a close variant.

1. Suppose M_1, M_2, \dots, M_k are i.i.d. samples from Haar measure on $U(N)$ (or a similar Lie group) and that W_1, \dots, W_m are words in the M_i and M_i^{-1} . Can we compute the expectation

$$\mathbb{E} \left[\prod_{i=1}^k \text{tr}(W_i) \right]$$

in a “nice” way? For example, can we express $\mathbb{E} \left[\text{tr}(M_1 M_2 M_1^{-1} M_2^{-3}) \text{tr}(M_1^3 M_2 M_1^{-1} M_2^{-1}) \right]$ as a simple function of N ?

2. How does the answer to the previous question change if instead of sampling from Haar measure, we obtain each M_i by running a Brownian motion on the Lie group for t_i units of time, starting with the identity?

The second question can be understood as an “external field” version of the first question. This is because when the t_i are small, the M_i are more likely to be close to the identity, and this “bias toward the identity” is similar in spirit to the “bias toward positive spin” imposed in e.g. an Ising

model with an external field. The second question also arises naturally in *two-dimensional* Yang-Mills theory and has been heavily studied in that context [GKS89, Dri89, Fin91, Wit91, Mig96, Sen97, Lév03, Lév10, Lév17, DHK17, She21, Che19, Dri19, CCHS20, DN20, DL22].

In two dimensions, the fine-mesh scaling limit of Yang-Mills theory is well understood, but if one attempts to compute the Wilson loop expectation for a complicated collection of loops (perhaps with many intersections and self-intersections) one obtains precisely an instance of the second problem above—indeed, the problems are equivalent since one can obtain *any* instance of the second problem for *some* two-dimensional loop.

In a recent companion paper [PPSY23] (including some of the authors of this paper), it was shown that the answer to the second question can be expressed as an expectation w.r.t. a certain Poisson point process. In this paper, we will explain how the answer to the first question can be derived directly from the analysis in [PPSY23] by taking $t_i \rightarrow \infty$. This is our first main result, which we state informally as follows. For a precise version, see Theorem 2.5.

Theorem 1.5. *The expectations of traces of words of Unitary Brownian motion converge as the time parameter goes to infinity to an explicit limit given in terms of the Weingarten function. Similar results hold for the other classical Lie groups.*

Remark 1.6. We note that Theorem 2.5 has previously appeared in [Dah17], albeit stated in slightly different (but equivalent) terms – see Sections 4 and 5 of the paper. Dahqvist’s proof relies heavily on representation theory. On the other hand, our proof is essentially entirely probabilistic (involving the analysis of a certain stochastic process), and we will explain all the representation theory prerequisites that are needed. For these reasons, we believe that our proof may be easier to read for those who have a solid probability background but perhaps are not that familiar with representation theory.

Our approach to this result is in some sense very straightforward. The analysis in [PPSY23] notes that when all of the t_i are less than infinity, the noise generating the Lie group Brownian motion is a Gaussian white noise on a Lie algebra; because all randomness is Gaussian, all of the relevant quantities can be easily deduced from Wick’s formula and planar maps (see the overview of these techniques [Zvo97]) which leads to a Poisson point process formulation of the theory. The analysis in this paper begins with the Poisson point process formulation obtained in [PPSY23] and shows that geometric cancellations simplify in the $t_i \rightarrow \infty$ limit, so that the *Weingarten function* (as originally introduced in [Wei78]) appears naturally without any difficult computation. This approach also provides other insights – for instance, certain single-edge analogs of the string-exploration steps in [CJ16] can be interpreted in terms of the so-called Jucys-Murphy elements [Juc74, Mur81, ZJ09, Nov10, App11, MN13].

1.3 Continuum Yang-Mills

The famous continuum *Yang-Mills problem* [JW06] is (roughly speaking) to construct and understand the basic properties of a continuum analog of the lattice model described above, which should somehow make rigorous sense of the measure in 1.1. This problem remains open for $d \geq 3$ and its solution for $d = 4$ would in some sense also yield a solution to the quantum Minkowski version of Yang-Mills that forms the basis of the standard model in physics, see the Millennium Prize description [JW06].

This paper is focused on understanding a *lattice* version of Yang-Mills theory in terms of sums over surfaces, with the aim of gaining insight into a possible continuum theory. It is not clear what kind of fine-mesh scaling limit one should expect the lattice models to have, but our hope is that

the lattice analysis presented here will provide some clues, and we present several open problems along these lines in Section 6.

We remark that a number of purely continuum approaches to this problem are also being actively pursued. For example, there is an *SPDE-based approach* which aims to construct a dynamical version of continuum Yang-Mills (on a torus, say) and show that it converges to a stationary law in the large time limit. One can take as the initial value a “Lie-algebra-valued Gaussian free field connection” that one expects to approximate the correct continuum theory at small scales and try to argue that the behavior at large scales converges to a limit over time. See e.g. [CCHS20, CC21, CC23, CCHS22a, CCHS22b, Che22, BC23]. There has been some significant recent progress in this area, especially in two and three dimensions.

Alternatively, one can also work directly in the continuum *without* attempting to understand a dynamical process. One might regularize the continuum model in some other way—perhaps starting with a continuum Gaussian. Some form of this was implemented by Magnen, Rivasseau, and Sénéor [MRS93]. Some approaches along these lines might also be amenable to the type of random surface analysis discussed in this paper; see Section 6.

1.4 Lattice models and planar maps

Consider a pair (\mathcal{M}, ϕ) where \mathcal{M} is a planar (or higher genus) map and $\phi : \mathcal{M} \rightarrow \Lambda$ is a graph homomorphism. We call this pair a **semi-folded map** or **edge-plaquette embedding** if the following hold:

1. The dual graph of \mathcal{M} is bipartite. The faces of \mathcal{M} in one partite class designated as “edge-faces” (shown blue in figures) and those in the other class are called “plaquette faces” (shown yellow in figures).
2. ϕ maps each plaquette-face of \mathcal{M} isometrically *onto* a plaquette in \mathcal{P} .
3. ϕ maps each edge-face of \mathcal{M} onto a single edge of Λ .

See Figures 1-4 for examples and intuition.

In order to construct a model of random edge-plaquette-embedding that is useful in Yang-Mills theory. We will need to assign a “weight” to every face of Λ (depending on the number of plaquettes there) and every edge (depending on the number and type of blue faces there). This weight is closely related to the so-called Weingarten function, which we discuss next.

1.4.1 Weingarten function

Note that a complex-valued function on S_n can be identified as an element in the group algebra $\mathbb{C}[S_n]$, that is $\sigma \mapsto f(\sigma)$ is identified as $\sum_{\sigma \in S_n} f(\sigma)\sigma$. Let $\mathbb{Q}[N] \subset \mathbb{C}[N]$ be the field of rational functions with rational coefficients in the variable N . When $N \geq n$ the **Weingarten function** Wg_N^1 can be defined as the inverse in the group ring of $\mathbb{Q}(N)[S_n]$ of the function $\sigma \rightarrow N^{\#\text{cycles}(\sigma)}$. (There is a slightly different definition for $N < n$, see Section 2.) Note that $\text{Wg}_N(\sigma)$ depends only on the conjugacy class of σ —i.e. on the cycle structure of σ . We can order cycles from biggest to smallest, and represent this by a Young diagram, and interpret Wg_N as a function on Young diagrams. It is not the simplest function but it does have an explicit form (see the overview and additional references in [MP19]):

$$\text{Wg}_N(\sigma) = \frac{1}{(n!)} \sum_{\lambda \vdash n} \left[\chi_\lambda(\text{id}) \chi_\lambda(\sigma) \prod_{(i,j) \in \lambda} (N + j - i)^{-1} \right] \quad (1.7)$$

¹We omit the dependence on n for brevity.

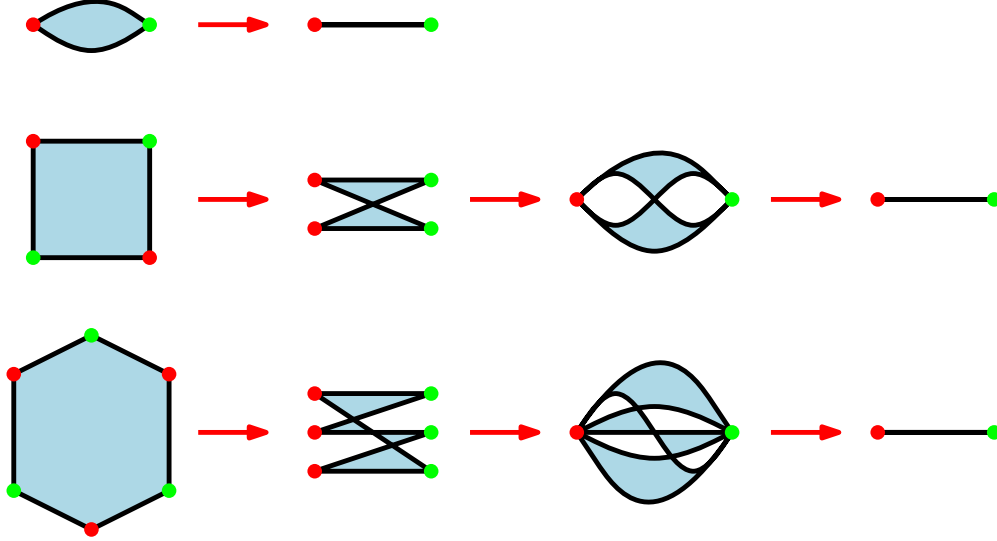


Figure 1: In an edge-plaquette embedding, we can imagine that each blue face is “twisted and collapsed” onto a single edge, see Figure 2. In the sequence above, we first twist, then collapse matching vertices, then collapse edges.

where id is the identity permutation, $\lambda \vdash n$ denotes that λ is a partition of n , $\chi_\lambda(\sigma)$ is the character (trace of σ in the irreducible representation indexed by λ). As will be explained in Section 5, we interpret σ as a collection of blue faces (one blue face of length $2k$ for each cycle of σ of length k). Then $\text{Wg}_N(\sigma)$ is essentially the *weight* associated to given collection of blue faces at an edge. Actually, as we detail in Section 5, the edge weights are given by the *normalized Weingarten function*, which we define as

$$\overline{\text{Wg}}_N(\sigma) := N^{2n - \#\text{cycles}(\sigma)} \text{Wg}_N(\sigma).$$

This is the normalization which leads to a nontrivial $N \rightarrow \infty$ limit (see Remark 5.2).

Given an edge-plaquette embedding (\mathcal{M}, ψ) and an edge e of our lattice Λ , we will write $\overline{\text{Wg}}_N(e)$ as shorthand for $\overline{\text{Wg}}_N(\mu_e(\mathcal{M}, \psi))$, where $\mu_e(\mathcal{M}, \psi)$ is the partition given by half the degrees of the blue faces mapped to e .

1.5 Main results

We already informally stated the first of our main results – recall Theorem 1.5. In this subsection, we proceed to state the remaining main results of this paper.

First, when computing Wilson loop expectations, we imagine the simplest setting in which we fix the number of yellow faces of each type (i.e. assign weight 1 to that number and 0 to all others). This corresponds to focusing on a single summand in (1.5), or equivalently to taking $\beta = 0$ in (1.5). In this case we have the following:

Theorem 1.7. *When the gauge group is $U(N)$, the expected trace product is proportional to $\sum (\prod_e \overline{\text{Wg}}_N(e)) \cdot N^{\chi - 2k}$ where the sum is over spanning edge-plaquette embeddings with given plaquette numbers, χ is the Euler characteristic and $k = |\mathcal{L}|$ is the number of loops.*

Remark 1.8. We regard Theorem 1.7 and the upcoming Corollary 1.10 as the main conceptual contribution of this paper. These results introduce the new concept of an edge-plaquette embedding,

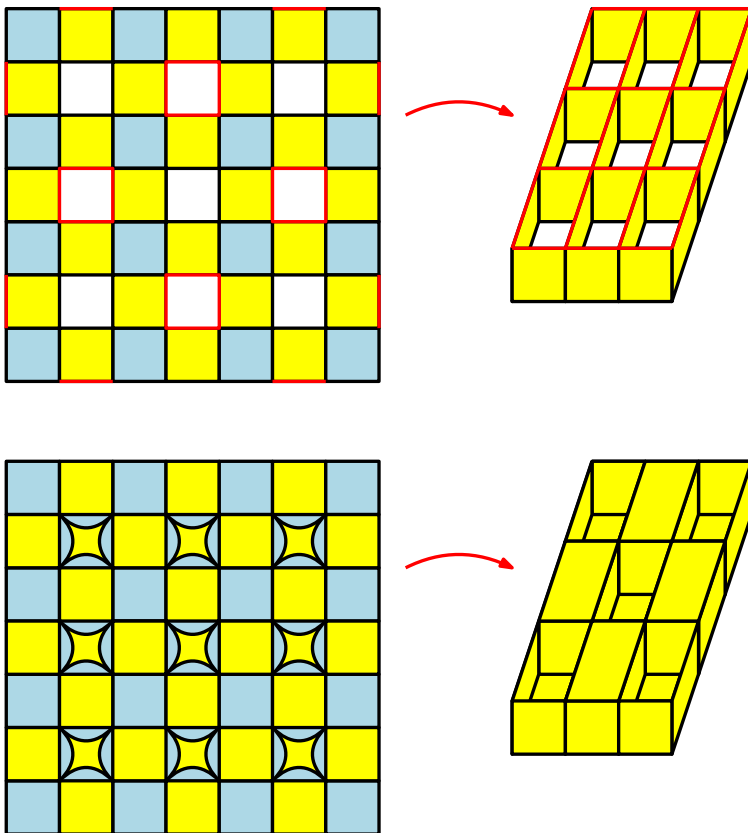


Figure 2: **Edge-plaquette embedding example:** Each of the 16 blue faces on the upper left gets mapped to a single vertical edge in the upper right, while each yellow face on the upper left gets mapped to a vertical yellow face on the upper right—the edge colored red is the one mapped to the top. On the lower left, additional yellow faces are added; their images on the right alternate between upper and lower layers in checkerboard fashion. Going from left to right requires “folding up” the blue squares and collapsing the blue 2-gons.

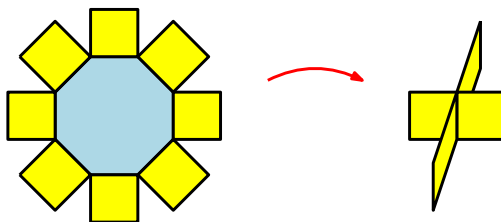


Figure 3: **Edge-plaquette embedding example:** If the blue face is an octagon, then there will be 8 yellow plaquettes meeting at the corresponding edge. In this example shown, the pre-image of each yellow face on the right may consist of two yellow faces on the left. In other words, there are two “copies” of each of the four plaquettes shown on the right.

and give a fundamentally new description of Wilson loop expectations in terms of random planar maps², thereby connecting two very different areas of research. Ultimately, we hope to prove new results about lattice gauge theories via analysis of these random planar maps, in particular building

²This is rather loose terminology, as our surface sums are signed, and in general higher genus surfaces may appear.

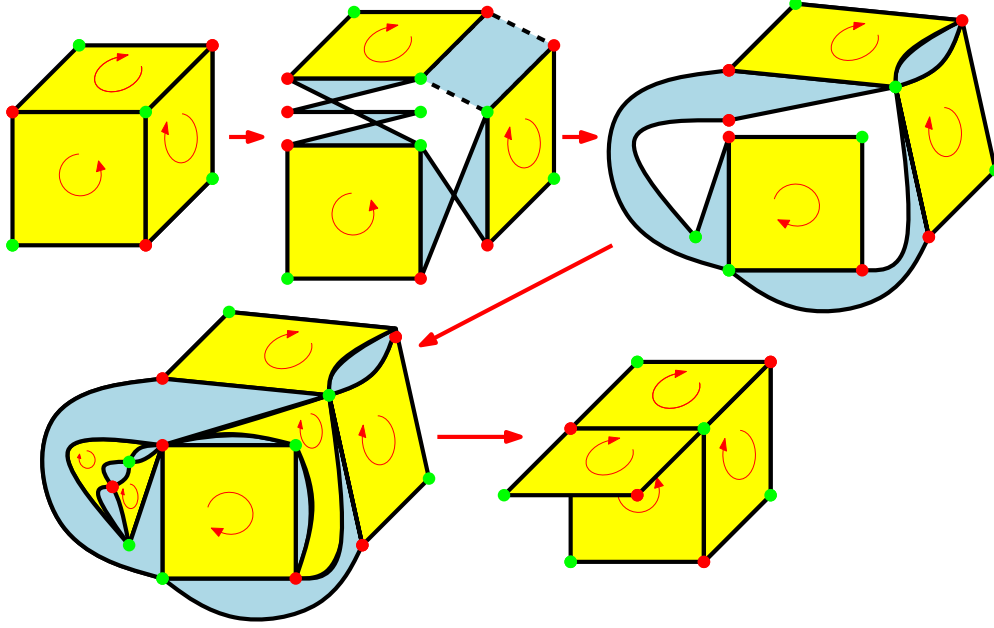


Figure 4: **Edge-embedding example showing orientations:** (1) Three oriented plaquette images in $\phi(M)$. (2) The blue faces connecting them have different types. (3) “Untwist” by flipping the lower-left plaquette across its red-red diagonal so that the three red and three blue faces are orientably embedded in the plane. (4) Add some new faces (three yellow squares and five blue 2-gons) to fill in the hole. Interpret the resulting colored map as a portion of \mathcal{M} orientably embedded in the plane. (5) Map this portion back into the lattice. Not all six yellow plaquettes are visible on the right because some overlap each other.

on the many advances in their understanding – see Section 6 for some open problems. See also Remark 1.11.

Remark 1.9. The results of Magee and Puder [MP19, MP22] could also be applied here to give a surface sum representation of the terms in (1.5). However, the relation to random planar maps is not as clear in their formulation. As mentioned in Remark 1.8, this is the main point of our result. For more comparison with Magee and Puder, see Section 1.5.1.

For a precise statement of this theorem, see Theorem 5.6. Even in the $U(N)$ case there are several variants to this result. The various “string trajectory moves” in [CJ16] can be interpreted in terms of the exploration of a surface built out of blue 2-gons and 4-gons and yellow squares. One can also interpret the individual Jucys-Murphy elements in these terms.

By applying Theorem 1.7 to every term in the series appearing in equation (1.5), we obtain that Wilson loop expectations may be expressed as a weighted sum over edge-plaquette embeddings. We state this informally as the following corollary.

Corollary 1.10 (Wilson loop expectations as surface sums). When the gauge group is $U(N)$, the Wilson loop expectation $\mathbb{E}[W_{\mathcal{L}}(Q)]$ is equal to $\sum \frac{\beta^{\text{area}}}{K!} \prod W(e) \cdot N^{\chi-2k}$, where the sum is over spanning edge-plaquette embeddings with arbitrary plaquette numbers, area is the total number of plaquettes in the edge-plaquette embedding, $K!$ is a combinatorial factor depending only on the plaquette counts, χ is the Euler characteristic, and $k = |\mathcal{L}|$ is the number of loops.

For a precise statement of this corollary, see Corollary 5.8.

Remark 1.11. Recently, Taggi and coauthors [LT20, LT21, QT23] have succeeded in proving various results about spin $O(n)$ and related models by analyzing a certain related random path (or random loop) model. Starting from the spin $O(n)$ model, they arrive at their random path model in exactly an analogous manner as how we arrive at Corollary 1.10. Namely, starting from the action for the spin $O(n)$ model, which at a single edge is of the form $\exp(\beta\sigma_x \cdot \sigma_y)$, where $\sigma_x, \sigma_y \in S^n$, they expand $\exp(\beta(\sigma_x \cdot \sigma_y)) = \sum_k \frac{\beta^k}{k!} (\sigma_x \cdot \sigma_y)^k$ for each edge (x, y) , and then compute the resulting S^n -integrals. The S^n -integrals may be easily computed, with the resulting expressions only involving very explicit quantities such as factorials and Gamma functions (see [LT21, equation (2.12)]). This is one simplification compared to our setting, where the $U(N)$ -integrals lead to the appearance of the Weingarten function, which is much more complicated to understand. Another key difference is that while the S^n -integrals are always positive, the $U(N)$ -integrals may be both positive and negative. Thus the random path model of Taggi et al. may be interpreted as a genuine probability measure, while our surface sums may only be interpreted as signed measures.

Next, we give an informal statement of the Schwinger-Dyson relations/Master loop equations satisfied by Wilson loop expectations. The corresponding precise statement is Theorem 4.6.

Theorem 1.12 (Schwinger-Dyson relation/Master loop equation). *Wilson loop expectations satisfy the following recursion:*

$$\mathbb{E}[W_{\mathcal{L}}(Q)] = \text{splitting} + \text{merger} + \text{deformation}$$

Here, splitting, merger, and deformation correspond to certain types of operations we may apply to a given collection of loops \mathcal{L} to obtain a new collection of loops. They will be precisely defined in Section 4.

Remark 1.13. As previously mentioned, versions of this recursion for various Lie groups have previously appeared [CJ16, Cha19b, Jaf16, Cha19a, SSZ22]. We note that the precise form of our recursion is slightly different from (and more general than) the existing literature – see Remark 4.4. Ultimately, the reason for this difference is due to our proof method. Whereas previous approaches are based on integration-by-parts³, our approach is essentially equivalent to applying a certain recursion that is satisfied by the Weingarten function (see e.g. [CM17, Proposition 2.2]), although we don't phrase our argument in this way – we prefer to proceed more probabilistically via our aforementioned Poisson process formulation.

Having completed the statements of our main results, we next remark how we expect our results to change when we consider other Lie groups such as $SU(N)$, $SO(N)$, or $Sp(N/2)$. In a forthcoming revision, we will include results for these other cases.

Remark 1.14 (Other Lie groups). First, the results of [PPSY23] also include the cases of $SU(N)$, $SO(N)$, or $Sp(N/2)$. That is, expectations of products of words of independent Brownian motions are expressed as certain Poisson process expectations. In particular, [PPSY23] explains the key differences in terms of how one associates weights (depending on the Lie group) to a given realization of a Poisson process. Once these different weights are accounted for, the proof of Theorem 1.12 would proceed in exactly the same manner. On the other hand, with regards to Theorem 1.7 and Corollary 1.10, the analogs of the Weingarten function one obtains (and the corresponding planar map interpretation) are different – see e.g. [CŠ06, Dah16, MP22].

³The method of [SSZ22] does not directly use integration by parts, rather it proceeds by applying Itô's formula to the lattice Langevin dynamics and computing the quadratic variation term that arises. However, one still needs integration by parts to show that the lattice Yang-Mills measure is invariant with respect to the lattice Langevin dynamics. This is why we say that the approach of [SSZ22] is based on integration by parts.

1.5.1 Discussion of Magee and Puder

The vocabulary in [MP21, MP19] is somewhat different from ours, but the results can be expressed in similar terms. We won't give a detailed account of those results, but let us briefly outline a couple of key ideas. The approach in [MP21, MP19] makes heavy use of commutator words. Suppose a loop ℓ in \mathcal{L} corresponds to a commutator word $ABA^{-1}B^{-1}$ (where A and B could in principle describe paths of length longer than one). Imagine then that we have a surface S with a single boundary loop, whose boundary is mapped to ℓ . We can turn this surface into a closed surface in two ways. First, we can identify the boundary of an ordinary disk with circular boundary of S , thereby gluing a circular disk onto S . Second we can glue the boundary of S to itself by first gluing the pre-images of the A and A^{-1} segments to each other and then gluing the pre-images of the B and B^{-1} segments to each other—which somehow turns the disk bounded by ℓ into a torus. It is not hard to see that the second approach produces a surface whose genus is 1 higher than the surface produced by the first approach: it effectively “adds a handle” to the surface. If we write long loop ℓ as a product of n commutator words, then those words provide us a recipe for turning a disk bounded by ℓ into an n -holed torus (by performing gluings of the type mentioned above for each commutator).

Theorem 1.7 is closely related to [MP19, Theorem 2.8]. We remark that one could also interpret [MP19, Theorem 2.9] in terms of embedded maps (somehow involving multiple layers of blue faces). We note that [MP19, Theorem 2.9] is in some ways simpler than [MP19, Theorem 2.8] (it does not involve the Weingarten function) and in other ways more complicated (it involves another quantity called the L^2 Euler characteristic, which is in general not so trivial). We note that [MP19, Theorem 2.9] is derived from [MP19, Theorem 2.8] and we will not give an alternate derivation of this step.

2 Notation and background

In this section, we introduce some basic notation and background that will be needed throughout this paper.

- For $n \in \mathbb{N}$, we denote the set $[1, n] \cap \mathbb{Z} = \{1, \dots, n\}$ by $[n]$.
- For $a, b \in \mathbb{Z}$, $a < b$, we denote $[a : b] := \{a + 1, \dots, b\}$. So $[n] = [0 : n]$.
- For a set A , we let $\binom{A}{2}$ denote the unordered set of ordered pairs of elements of A .

2.1 Poisson point process on strand diagrams

In this section, we review a result in the companion paper [PPSY23] that is necessary for this paper. In particular, we express the expected trace of unitary Brownian motions in terms of a certain Poisson point process, which we encode in a strand diagram (Definition 2.1).

Let $\mathbf{\Gamma} = (\Gamma_1, \Gamma_2, \dots, \Gamma_k)$ be a collection of words Γ_i on letters $\{\lambda_1, \dots, \lambda_L\}$ where

$$\Gamma_i = \lambda_{c_i(1)}^{\varepsilon_i(1)} \dots \lambda_{c_i(M_i)}^{\varepsilon_i(M_i)}$$

for some $c_i : [M_i] \rightarrow [L]$ and $\varepsilon_i : [M_i] \rightarrow \{-1, 1\}$. By letting $M = M_1 + \dots + M_k$ and concatenating c_i 's and ε_i 's, we may define $c : [M] \rightarrow [L]$ and $\varepsilon : [M] \rightarrow \{-1, 1\}$. Our goal is to compute

$$\mathbb{E}[\text{Tr}(B(\mathbf{\Gamma}))],$$

where

$$\text{Tr}(B(\mathbf{\Gamma})) := \text{Tr}(B(\Gamma_1)) \dots \text{Tr}(B(\Gamma_k)), \text{ and } B(\Gamma_i) = B_T^{\varepsilon_i(1)} \dots B_T^{\varepsilon_i(M_i)},$$

and where $\{B_T\}_{\ell \in [L]}$ is a collection of independent Brownian motions on $U(N)$ run for time $T > 0$. We also define

$$\mathcal{C} = \bigcup_{\ell \in [L]} \binom{c^{-1}(\ell)}{2} = \{(m, m^*) : m < m^* \text{ and } c(m) = c(m^*)\},$$

and

$$\mathcal{D} = \bigsqcup_{(m, m^*) \in \mathcal{C}} [0, T_{c(m)}],$$

equipped with some parametrizing bijection $\eta : \mathcal{C} \times [0, 1] \rightarrow \mathcal{D}$.⁴ Given a point $x \in \mathcal{D}$, let $l(x) \in \mathcal{C}$ be the index of the interval which contains x . We now consider the Poisson point process Σ on \mathcal{D} with intensity given by the Lebesgue measure. Equivalently, Σ has the same law with $\Sigma_\infty \cap \mathcal{D}$ where Σ_∞ is the Poisson point process on

$$\mathcal{D}_\infty = \bigsqcup_{(m, m^*) \in \mathcal{C}} [0, \infty)$$

with intensity given by the Lebesgue measure. In other words, Σ_∞ is a disjoint union of i.i.d. rate 1 Poisson processes on $[0, \infty)$.

As we previously alluded to, expectations of Unitary Brownian motion may be represented by a certain diagram which is obtained from a Poisson process on \mathcal{D} . To begin to make this statement precise, in the following definition, we describe how to associate a diagram to a given collection of points of \mathcal{D} .

Definition 2.1 (Strand diagram). Let $\Gamma = \lambda_{c(1)}^{\varepsilon(1)} \cdots \lambda_{c(M)}^{\varepsilon(M)}$ be a word on $\{\lambda_1, \dots, \lambda_L\}$ and Σ be a collection of points in \mathcal{D} . Then $\eta^{-1}(\Sigma)$ be a collection of points $((m, m^*), t) \in \mathcal{C} \times [0, 1]$ for $(m, m^*) \in \mathcal{C}$ and $t \in [0, 1]$. Let $n_\ell = |c_i^{-1}(\ell)|$ for each $\ell \in [L]$. The **strand diagram of** (Γ, Σ) is an array of right- or left-directed arrows, each of which is identified as the unit interval $[0, 1]$, placed as follows.

- There are L columns and each column is labelled by λ_ℓ for $\ell \in [L]$;
- The column labeled by λ_ℓ consists of a stack of n_ℓ unit-length arrows, each of which corresponds to an element of $c_i^{-1}(\ell)$;
- If an arrow corresponds to $m = c_i^{-1}(\ell) \in [M]$, it is right-directed (resp. left-directed) if $\varepsilon(m) = 1$ (resp. $\varepsilon(m) = -1$);
- The end of arrow corresponding to m is connected to the origin of the arrow corresponding to $m + 1$, modulo M ;
- For each point $((m, m^*), t) \in \eta^{-1}(\Sigma)$, if $\varepsilon(m)\varepsilon(m^*) = 1$, we insert a green crossing (called the “same-direction swap”) on two arrows corresponding to m and m^* at location $t \in [0, 1]$. Otherwise, we put a blue double bar (called the “opposite-direction swap”) on two arrows corresponding to m and m^* at location $t \in [0, 1]$.

In general, if $\mathbf{\Gamma} = (\Gamma_1, \dots, \Gamma_k)$ is an ordered collection of words Γ_i on $\{\lambda_1, \dots, \lambda_L\}$, we define the strand diagram of $(\mathbf{\Gamma}, \Sigma)$ as a collection of strand diagrams of $(\Gamma_1, \Sigma_1), \dots, (\Gamma_k, \Sigma_k)$ where $\Sigma = \bigsqcup_{i=1}^k \Sigma_i$ with the same labelled columns. See Figure 5 for an example.

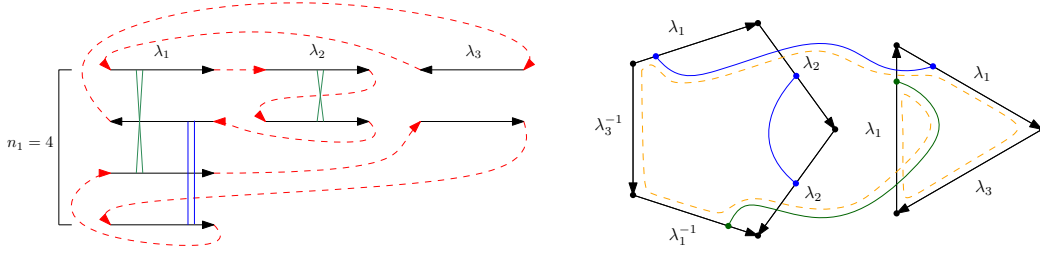


Figure 5: **Left:** The strand diagram for $((\Gamma_1, \Gamma_2), \Sigma)$ with $\Gamma_1 = \lambda_1 \lambda_2 \lambda_2 \lambda_1^{-1} \lambda_3^{-1}$, $\Gamma_2 = \lambda_1 \lambda_3 \lambda_1$, and $\eta^{-1}(\Sigma) = \{((1, 6), 1/4), ((2, 3), 1/2), ((4, 8), 3/4)\}$. For example, the first and sixth alphabet in the word Γ are λ_1 's, so we put a green crossing at the $1/4$ location of two unit intervals representing those. Similarly, we put a blue double bar at the $3/4$ location of two unit intervals representing λ_1^{-1} and λ_1 . **Right:** The CW-complex constructed from the left strand diagram. By following each 1-cells and closing each cycle by adding a new 2-cell, we obtain a closed surface whose Euler characteristic defines the Euler characteristic of the strand diagram. The orange dashed line is an example of a 2-cell we add. Including this face, we need 3 faces in total to obtain a closed surface with the minimum genus. Therefore, the Euler characteristic of this surface is equal to $V - E + F = 14 - 17 + 5 = 2$, and the resulting surface is a sphere.

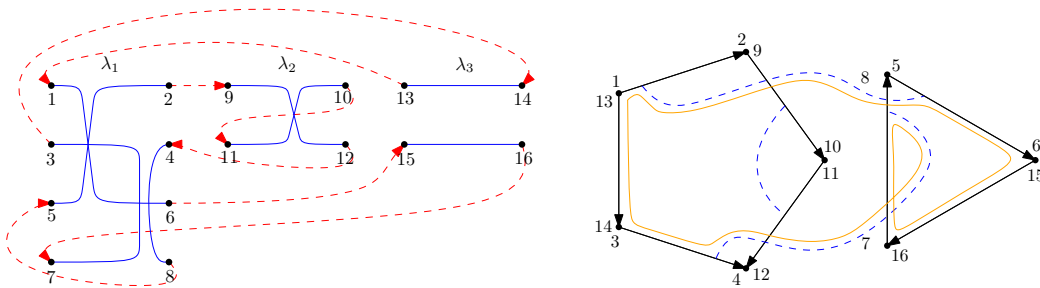


Figure 6: **Left:** The same strand diagram as Figure 5 but with ends of arrows labelled. By following all swaps, each row of the strand diagram defines a matching on $[2n_\ell]$ for $\ell = 1, 2, 3$. **Right:** The corresponding CW complex picture with labels. It is straightforward that the number of components in the left picture is exactly the number of faces in this picture.

We define a CW-complex from a strand diagram as in Figure 5. Each word Γ_i can be represented by a regular polygon with unit-length arrows (preserving the orientation), and each same-direction swap or opposite-direction swap corresponds to a path connecting two arrows at the specified location in the strand diagram. As a result, we have k 2-cells for each polygon, $M + 2|\Sigma|$ 1-cells, and $M + 2|\Sigma|$ 0-cells, where $M = n_1 + \dots + n_L$. Then there exists a *closed* surface with the minimum genus constructed by adding extra F 2-cells, that is by following every 1-cell and adding a 2-cell whenever they form a cycle. (Equivalently, it can be viewed as a *ribbon graph*.) By Euler's formula, the number F of extra 2-cells determines the minimum genus, that is $\chi = (M + 2|\Sigma|) - (M + 3|\Sigma|) + (k + F) = k + F - |\Sigma|$. We define the Euler characteristic χ of the strand diagram as the Euler characteristic of this surface with the minimum genus.

We now give a precise statement of how Unitary Brownian motion expectations reduce to certain diagrammatic sums. We quote the following result from [PPSY23].

⁴The bijection η is only to record the location of points. In [PPSY23], the interval $[0, T_{c(m)}]$ is identified as the interior of each loop (so that η is a space-filling curve) for more geometric interpretation, but the Lebesgue measures are identical in the end.

Lemma 2.2 (Expected trace as Poisson sums [PPSY23]). Let $\mathbf{\Gamma}$ be a collection of words on $\{\lambda_1, \dots, \lambda_L\}$ and $T > 0$. Let Σ be the Poisson point process on \mathcal{D} . Consider the strand diagram S for $(\mathbf{\Gamma}, \eta^{-1}(\Sigma))$. Then

$$\mathbb{E}[\mathrm{Tr}(B(\mathbf{\Gamma}))] = \exp\left(-\frac{1}{2} \sum_{m=1}^M T + \sum_{(m, m^*) \in \mathcal{C}} T\right) \mathbb{E}\left[\varepsilon(\Sigma)(-1)^{|\Sigma|} N^{-k+\chi(S)}\right].$$

Lemma 2.2 may be interpreted as follows. First, observe that for each individual letter λ_ℓ , the portion of the strand diagram corresponding to λ_ℓ may be thought of as a matching on $[2n_\ell]$, see Figure 6. In order to compute the Euler characteristic $\chi(S)$ of a given strand diagram S , it suffices to give the partitions π_1, \dots, π_L of $[2n_1], \dots, [2n_L]$, respectively. In particular, the number of vertices $V(S)$ is precisely the number of components of the diagram given by combining the exterior connections (which we have been drawing as dashed red lines) with the interior connections specified by $\pi = (\pi_1, \dots, \pi_L)$. Let $\#\mathrm{comp}(\mathbf{\Gamma}, \pi)$ be the number of components of the diagram arising from $\mathbf{\Gamma}, \pi$. Define also

$$w_T(\pi) := \exp\left(\sum_{\ell \in [L]} \left(\binom{n_\ell}{2} - n_\ell\right) T\right) \mathbb{E}\left[\varepsilon(\Sigma)(-1/|N|)^{|\Sigma|} \mathbb{1}(\pi(S) = \pi)\right], \quad (2.1)$$

which is interpreted as the partition function of all point configurations which results in the collection of partitions π . From these considerations, combined with Lemma 2.2, we have the following.

Lemma 2.3. Let $\mathbf{\Gamma}$ be a collection of words on $\{\lambda_1, \dots, \lambda_L\}$. Let Σ be the Poisson point process on \mathcal{D} . Consider the strand diagram S for $(\mathbf{\Gamma}, \eta^{-1}(\Sigma))$. Then

$$\mathbb{E}[\mathrm{Tr}(B_T(\mathbf{\Gamma}))] = \sum_{\pi=(\pi_1, \dots, \pi_L)} w_T(\pi) N^{\#\mathrm{comp}(\mathbf{\Gamma}, \pi)}. \quad (2.2)$$

Lemma 2.3 says that in order to compute the expectations of traces of words of Unitary Brownian motion, we may perform a weighted sum over all partitions of the corresponding strand diagram, where the weights are given by $w_T(\pi)$, and the statistic we are averaging over is N raised to the number of components of the diagram made from the exterior connections specified by the collection of words $\mathbf{\Gamma}$ and the interior connections specified by the collection of partitions π . See also Figure 7 for a visualization.

We proceed to give a precise statement of Theorem 1.5, which is we are able to obtain the $T \rightarrow \infty$ limit of the right-hand side of (2.2). First, we make the following definition.

Definition 2.4 (Balanced collection of words). A collection of words $\mathbf{\Gamma} = (\Gamma_1, \dots, \Gamma_k)$ on letters $\{\lambda_1, \dots, \lambda_L\}$ is balanced if for each letter λ_i , the number of times that λ_i appears in $\mathbf{\Gamma}$ is equal to the number of times λ_i^{-1} appears in $\mathbf{\Gamma}$.

Next, we describe a certain special set of partitions that plays a key role in the limiting formula. Suppose that $\mathbf{\Gamma}$ is balanced. Then n_ℓ is even for all $\ell \in [L]$. Given a pair of bijections $\sigma, \tau : [n_\ell/2] \rightarrow [n_\ell/2 : n_\ell]$, we may obtain a partition $[\sigma \tau]$ of $[2n_\ell]$ as in Figure 8.

Clearly, the set of all partitions that arise this way is a strict subset of the set of all partitions of $[2n_\ell]$. Observe that $\sigma\tau^{-1} : [n_\ell/2] \rightarrow [n_\ell/2]$ is a bijection, and thus we may view $\sigma\tau^{-1} \in \mathcal{S}_{n_\ell/2}$. It turns out that as $T \rightarrow \infty$, these are the only partitions that have a non-vanishing weight. This is inherent in the following theorem. Its proof is the subject of Section 3.

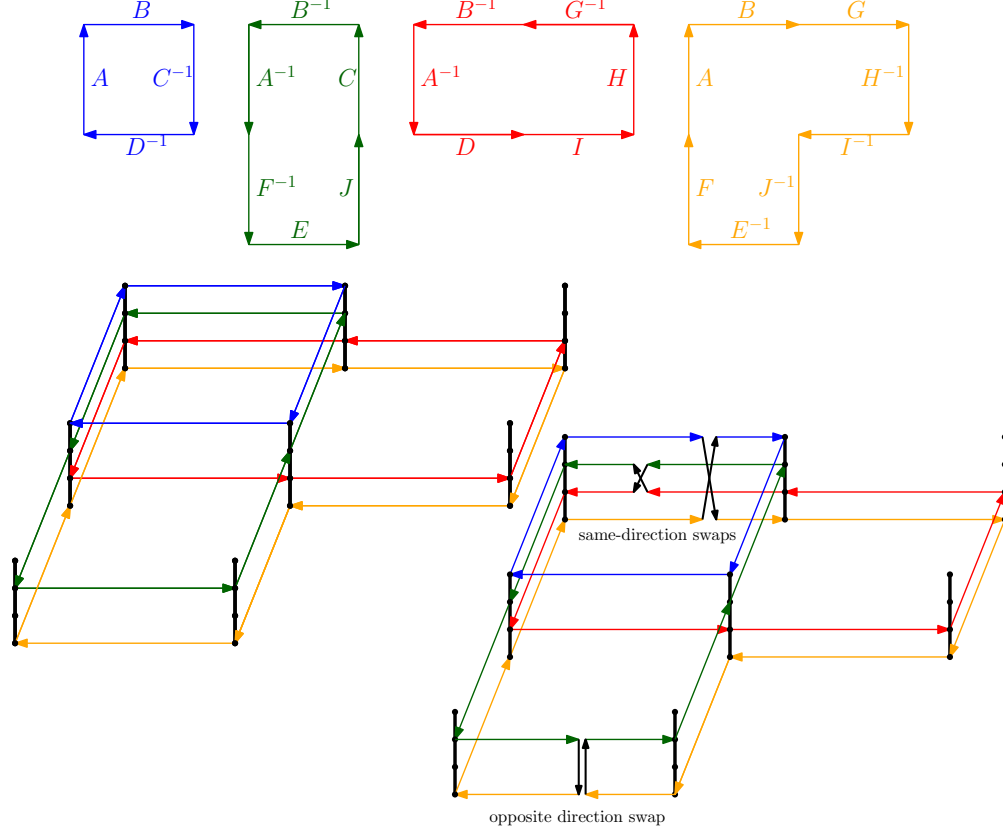


Figure 7: $\mathbb{E}\left[\text{tr}(ABC^{-1}D^{-1})\text{tr}(A^{-1}F^{-1}EJCB^{-1})\text{tr}(A^{-1}DIHG^{-1}B^{-1})\text{tr}(BGH^{-1}I^{-1}E^{-1}FA)\right]$ is the expected trace product of the four loops above, where the symbols are i.i.d. random elements of $U(N)$. [PPSY23] explains one way to compute this quantity when each symbol has the law of the time- T value of a Brownian motion on $U(N)$ started at the identity. First one stacks the strands on of each other (lower left) so that the arrows corresponding to the same symbol lie on top of each other. Then one chooses locations for “swaps” according to a certain Poisson point process (lower right). The desired expectation is a constant times $\mathbb{E}\left[(-1/N)^{\#\text{ same-dir swaps}}N^{\#\text{ components}}\right]$. As $t \rightarrow \infty$ the expected number of swaps tends to infinity. In this paper we derive the $t \rightarrow \infty$ limit by starting with the formulation above and applying simple geometric arguments and sign cancellations.

Theorem 2.5. *Let $\Gamma = (\Gamma_1, \dots, \Gamma_M)$ be a balanced collection of words on $\{\lambda_1, \dots, \lambda_L\}$. Then*

$$\lim_{T \rightarrow \infty} \mathbb{E}[\text{Tr}(B_T(\Gamma))] = \sum_{\pi = ([\sigma_\ell \tau_\ell], \ell \in [L])} \left(\prod_{\ell \in L} \text{Wg}_N(\sigma_\ell \tau_\ell^{-1}) \right) N^{\#\text{comp}(\Gamma, \pi)}.$$

Here, the sum in the right hand side is over π which can be obtained from pairs of bijections $\sigma_\ell, \tau_\ell : [n_\ell/2] \rightarrow [n_\ell/2 : n_\ell]$, $\ell \in [L]$.

Recall we defined the Weingarten function Wg_N when N is large in Section 1.4.1 (in particular, see (1.7)). We will give the definition for general values of N in Section 2.2 – see Definition 2.20.

Remark 2.6. In Theorem 2.5, it suffices to only look at balanced Γ , because if Γ is not balanced, then $\lim_{T \rightarrow \infty} \mathbb{E}[\text{Tr}(B_T(\Gamma))] = 0$, due to known properties of Haar integration.

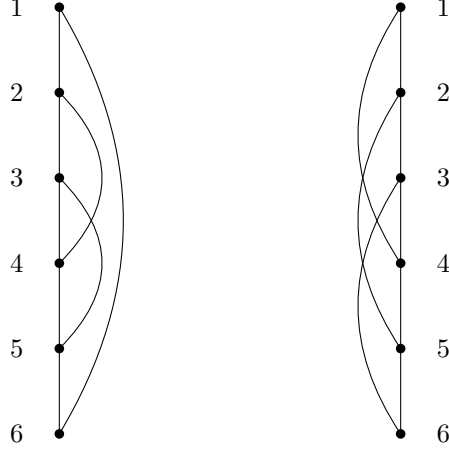


Figure 8: Example when $n_\ell = 6$. Here σ_ℓ maps $1 \mapsto 6, 2 \mapsto 4, 3 \mapsto 5$, and τ_ℓ maps $1 \mapsto 4, 2 \mapsto 5, 3 \mapsto 6$.

Since Unitary Brownian motion converges in distribution to the normalized Haar measure in the large-time limit, the combination of Lemma 2.3 and Theorem 2.5 allows us to obtain the Weingarten calculus as a corollary, which we state in the following form. Similar to existing notation, we denote $\text{Tr}(U(\mathbf{\Gamma})) := \text{Tr}(U(\Gamma_1)) \cdots \text{Tr}(U(\Gamma_k))$, where $U(\Gamma_i)$ is obtained by substituting an independent Haar-distributed matrix for each letter.

Corollary 2.7. Let $\mathbf{\Gamma} = (\Gamma_1, \dots, \Gamma_M)$ be a balanced collection of words on $\{\lambda_1, \dots, \lambda_L\}$. Then

$$\mathbb{E}[\text{Tr}(U(\mathbf{\Gamma}))] = \sum_{\pi = ([\sigma_\ell \tau_\ell], \ell \in [L])} \left(\prod_{\ell \in L} \text{Wg}_N(\sigma_\ell \tau_\ell^{-1}) \right) N^{\#\text{comp}(\mathbf{\Gamma}, \pi)}.$$

Here, the sum in the right hand side is over π which can be obtained from pairs of bijections $\sigma_\ell \tau_\ell : [n_\ell/2] \rightarrow [n_\ell/2 : n_\ell], \ell \in [L]$.

This corollary has a similar interpretation as Lemma 3.9 in terms of a weighted sum, with the previous weights $w_T(\pi_\ell)$ replaced by Weingarten weights $\text{Wg}_N(\sigma_\ell \tau_\ell^{-1})$.

We finish off this subsection with an instructive example which illustrates how one may compute $\#\text{comp}(\mathbf{\Gamma}, \pi)$ for a given $\mathbf{\Gamma}, \pi$.

Example 2.8. Suppose our letters are $\{A, B\}$, and our words are $\Gamma_1 = \Gamma_2 = ABA^{-1}B^{-1}$. Since each of A, B, A^{-1}, B^{-1} appears twice total in Γ_1, Γ_2 , we start with the diagram in Figure 9.

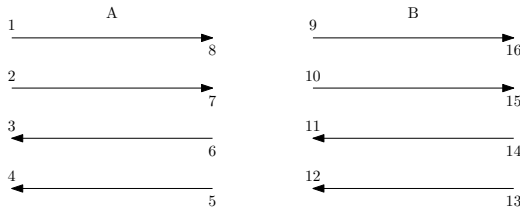


Figure 9

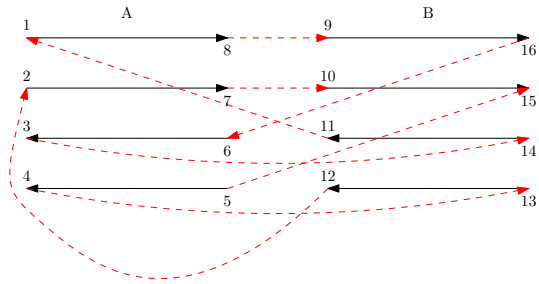


Figure 10

Notice that we have labeled the vertices of each strand by a number, which will come in handy later when we want to represent the number of connected components of the resulting diagram

after including the interior and exterior connections. The choice of words affects the exterior connections of the strand diagram. For instance, in our current example, we would include the exterior connections as illustrated in Figure 10.

Now ignoring for the moment the exterior connections, suppose we have pairs of matchings of the strand diagrams as indicated in Figure 11.

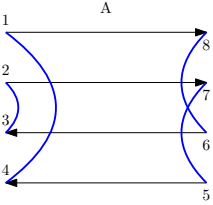


Figure 11

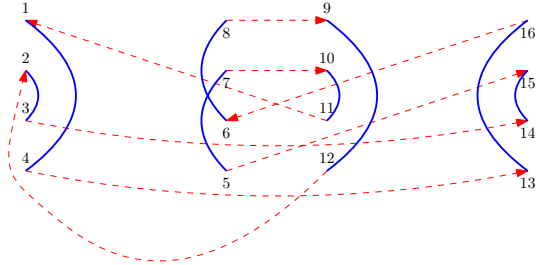


Figure 12

Now the specific statistic we need to compute is the number of connected components of the following diagram, which is essentially obtained by including both the interior (blue) and exterior (red) connections – see Figure 12.

We now make use of the vertex labels. In general, the various connected components of the diagram may be indexed by the cycles of a permutation. In this case, the permutation is on 16 elements. The cycles are obtained by starting at a given vertex and alternately following the dashed red lines and solid blue lines. For instance, in the above figure, we get a single cycle: $(1\ 11\ 10\ 7\ 5\ 15\ 14\ 3\ 2\ 12\ 9\ 8\ 6\ 16\ 13\ 4)$, which implies that there is a single connected component.

2.2 Representation theory and other preliminaries

The strand diagrams of Section 2.1 may naturally be viewed as elements of the so-called Brauer algebra, which is a well-studied object in mathematics. We proceed to introduce the Brauer algebra because this will form a convenient language when phrasing our proofs.

Definition 2.9 (Brauer algebra). For $n \geq 1$, let $\mathcal{M}(n)$ be the space of matchings of $[2n]$, i.e. partitions of $[2n]$ into two-element sets. We will view matchings pictorially as in Figure 13.

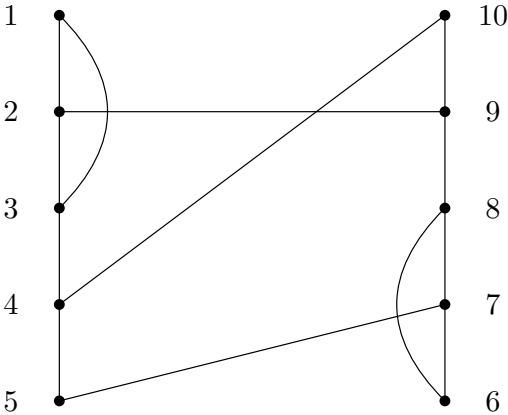


Figure 13: $\pi = \{\{1, 3\}, \{2, 9\}, \{4, 10\}, \{5, 7\}, \{6, 8\}\}$

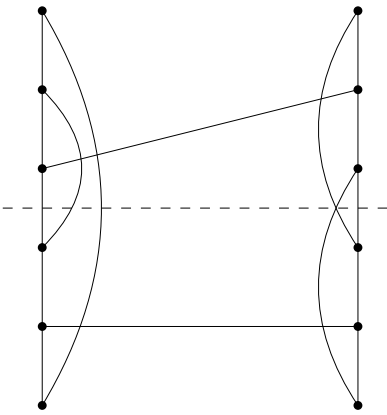


Figure 14: Element of $\mathcal{B}_{3,3}$

We refer to pairs that involve both a left and right element as “left-right pairings”, and pairs that involve two left elements or two right elements as “same-side pairings”. In the above picture, $\{1, 3\}, \{6, 8\}$ are same-side pairings, while $\{2, 9\}, \{4, 10\}, \{5, 7\}$ are left-right pairings.

Let \mathcal{B}_n be the vector space of \mathbb{C} -valued functions on $\mathcal{M}(n)$. We will often view elements $f \in \mathcal{B}_n$ as formal sums $f = \sum_{\pi} f(\pi)\pi$, where π ranges over $\mathcal{M}(n)$.

Fix $\zeta \in \mathbb{C}$. We may define a product of matchings $\pi_1, \pi_2 \in \mathcal{M}(n)$ as in Figure 15.

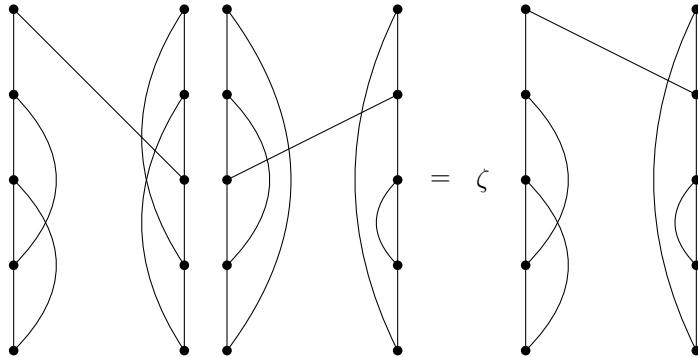


Figure 15

In words, we put π_1, π_2 together side-by-side, and then follow the lines to obtain a new matching. Any closed loops incur a factor of ζ . Observe that this product induces a product on \mathcal{B}_n which turns \mathcal{B}_n into an algebra. Explicitly, if we represent $f, g \in \mathcal{B}_n$ by formal linear combinations $f = \sum_{\pi_1 \in \mathcal{M}(n)} f(\pi_1)\pi_1$, $g = \sum_{\pi_2 \in \mathcal{M}(n)} g(\pi_2)\pi_2$, then the product fg is given by:

$$fg = \sum_{\pi_1, \pi_2 \in \mathcal{M}(n)} f(\pi_1)g(\pi_2)\pi_1\pi_2.$$

We refer to \mathcal{B}_n as the Brauer algebra.

Remark 2.10. Typically, elements of \mathcal{B}_n are drawn as top-bottom matchings, yet here we have chosen to draw them as left-right matchings.

In what follows, we always take $\zeta = N$. This is the choice of ζ which relates multiplication in the Brauer algebra with expectations of Unitary Brownian motion: note that the factor of N that we incur when we form a loop exactly matches the factor of N that we incur in the strand diagram when we add another connected component.

We specify a norm on \mathcal{B}_n , which will enable us to later talk about convergence in \mathcal{B}_n .

Definition 2.11 (Norm on \mathcal{B}_n). For $f \in \mathcal{B}_n$, define $\|f\|$ to be the L^1 norm, i.e. $\|f\| := \sum_{\pi \in \mathcal{M}(n)} |f(\pi)|$.

Next, we define a certain sub-algebra of the Brauer algebra, called the walled Brauer algebra. This arises naturally in computing expectations of Unitary Brownian motion, as it turns out that the strand diagrams of Section 2.1 are not only elements of the Brauer algebra, but even more they are elements of the walled Brauer algebra.

Definition 2.12 (Walled Brauer algebra). Let $n, m \geq 1$. Let $\mathcal{M}(n, m) \subseteq \mathcal{M}(n+m)$ be the subset of matchings of $[2(n+m)]$ such that every same-side pairing is between a top n element and bottom m element, while every left-right pairing is between two top n elements or two bottom m elements. Pictorially, one imagines a dashed line separating the top n elements from the bottom m elements,

and the only pairings which can cross this dashed line are same-side pairings. See Figure 14 for an example when $n = m = 3$.

The walled Brauer algebra $\mathcal{B}_{n,m}$ is the sub-algebra of \mathcal{B}_{n+m} consisting of functions $f \in \mathcal{B}_{n+m}$ which are supported on the matchings $\mathcal{M}(n,m)$. One may check that given two matchings $\pi_1, \pi_2 \in \mathcal{M}(n,m)$, their product $\pi_1\pi_2$ is proportional to a matching in $\mathcal{M}(n,m)$. This implies that the product on \mathcal{B}_{n+m} descends to a product on $\mathcal{B}_{n,m}$.

Observe that S_n can be embedded in $\mathcal{M}(n) \subseteq \mathcal{B}_n$ as follows. Given $\sigma \in S_n$, we can view it as an element of $\mathcal{M}(n)$ as in Figure 16.

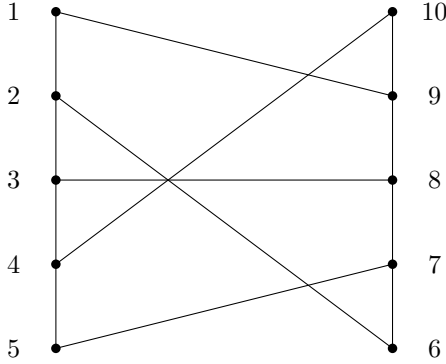


Figure 16: $\sigma = (1\ 2\ 5\ 4)$

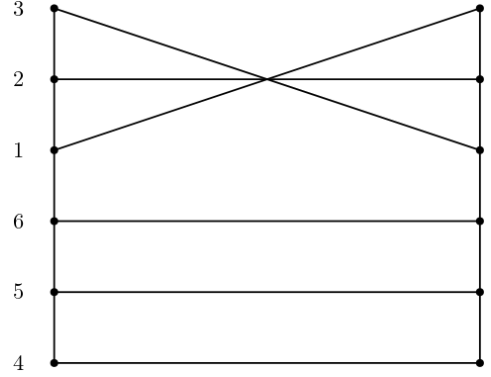


Figure 17: $(1\ 3)$

We may also embed S_n into $\mathcal{M}(n,n) \subseteq \mathcal{B}_{n,n}$ as follows. by connecting the top n vertices on the left and right as we did to embed S_n into \mathcal{B}_n , and then connecting the bottom n vertices on the left and right by straight lines.

Next, we define the following notation for certain special elements of the walled Brauer algebra $\mathcal{B}_{n,m}$. These correspond to the same-side and opposite-side swaps introduced in Section 2.1.

Definition 2.13. Given $1 \leq i < j \leq n$ or $n + 1 \leq i < j \leq n + m$, define $(i\ j) \in \mathcal{B}_{n,m}$ to be the pairing of $[2(n + m)]$ which swaps the i, j vertices with their corresponding versions on the right, while keeping the other vertices fixed. This is best explained by the example in Figure 17 when $n = m = 3$.

Given $1 \leq i \leq n$ and $n + 1 \leq j \leq n + m$, let $\langle i\ j \rangle$ be the pairing which has a same-side pairing between i, j on the left, as well as their corresponding versions on the right, while keeping the other vertices fixed. See Figure 18 for an example when $n = m = 3$.

Next, we define the following notation for another set of special elements of the walled Brauer algebra $\mathcal{B}_{n,n}$. These elements are matchings which have no left-right pairings.

Definition 2.14. Let $\sigma, \tau : [n] \rightarrow [n : 2n]$ be bijections. Define $[\sigma\ \tau] \in \mathcal{B}_{n,n}$ to be the element of the walled Brauer algebra which is given by σ on the left and τ on the right. See the Figure 19 for an example when $n = 3$.

Note the particular way we have chosen to label the vertices in Figure 19. From now on, this is how we will label vertices when working with the walled Brauer algebra $\mathcal{B}_{n,n}$. Ultimately the labeling will not matter, but we have chosen to label in this way to better relate to the Jucys-Murphy elements, which we next define.

Definition 2.15 (Jucys-Murphy elements). For $n \geq 2$, define the Jucys-Murphy element $J_n := (1\ n) + \dots + (n - 1\ n) \in \mathbb{C}[S_n]$. We also view $J_n \in \mathbb{C}[S_m]$ for any $n \leq m$. Define $J_1 := 0$.

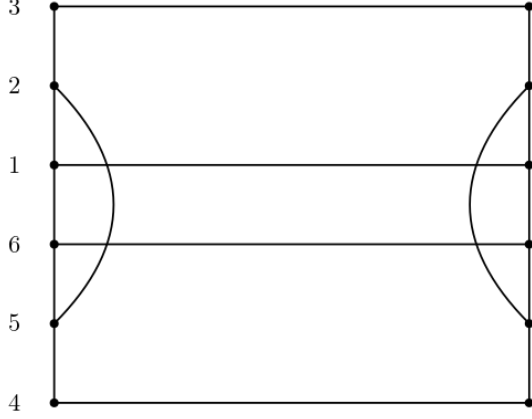


Figure 18: $\langle 2 \ 5 \rangle$

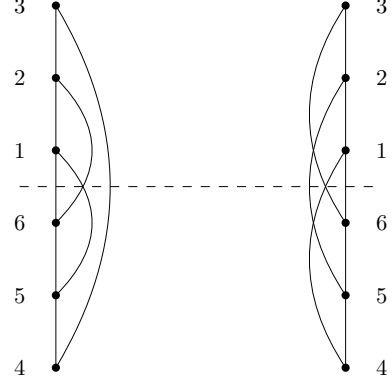


Figure 19: $\sigma = \{1 \mapsto 5, 2 \mapsto 6, 3 \mapsto 4\}$, $\tau = \{1 \mapsto 4, 2 \mapsto 5, 3 \mapsto 6\}$

Remark 2.16. One may show that the Jucys-Murphy elements commute with each other.

In the following, we will also view J_1, \dots, J_n as elements of $\mathcal{B}_{n,n}$, by using the previously mentioned embedding of $S_n \subseteq \mathcal{B}_{n,n}$. We will also need to refer to Jucys-Murphy elements which act on bottom elements rather than top elements. We define this next.

Definition 2.17. Let $n, m \geq 1$. Define $J'_1, \dots, J'_m \in \mathcal{B}_{n,m}$ by

$$J'_k := (n+1 \ n+k) + \dots + (n+k-1 \ n+k), \quad k \in [m].$$

Definition 2.18 (Norm on group algebra). For $f \in \mathbb{C}[S_n]$, we define $\|f\|$ to be the L^1 norm, i.e. $\|f\| := \sum_{\pi \in S_n} |f(\pi)|$.

Note that our norm on $\mathbb{C}[S_n]$ and on \mathcal{B}_n are compatible with our embeddings $\mathbb{C}[S_n] \subseteq \mathcal{B}_n$ and $\mathbb{C}[S_n] \subseteq \mathcal{B}_{n,n} \subseteq \mathcal{B}_{2n}$.

Remark 2.19. With this definition of the norm, we have that $\|fg\| \leq \|f\| \cdot \|g\|$ for $f, g \in \mathbb{C}[S_n]$. This implies that $\|e^f\| \leq e^{\|f\|}$, which further implies that if $\|f\| < 1$, then

$$\int_0^\infty e^{-u(\text{id}+f)} du \in \mathbb{C}[S_n]$$

converges absolutely. Moreover, one has that

$$\int_0^\infty e^{-u(\text{id}+f)} du = (\text{id} + f)^{-1}.$$

Next, we discuss an alternate form of the Weingarten function Wg_N which arises naturally in the proof of Theorem 2.5. First, suppose $N \geq n$. The case of general N will be addressed a bit later. Then $\text{Wg}_N \in \mathbb{C}[S_n]$ is the following inverse:

$$\text{Wg}_N := \left(\sum_{\sigma \in S_n} N^{\#\text{cycles}(\sigma)} \sigma \right)^{-1}.$$

Jucys [Juc74] proved the following identity:

$$\sum_{\sigma \in S_n} N^{\#\text{cycles}(\sigma)} \sigma = (N + J_n) \cdots (N + J_1). \quad (2.3)$$

Note that when $N \geq n$, each $N + J_k$ for $k \in [n]$ is invertible because then $\|J_k\| = k - 1 < N$ (recall Remark 2.19), with inverse given by:

$$(N + J_k)^{-1} = N(\text{id} + J_k/N)^{-1} = N \int_0^\infty e^{-u(\text{id} + J_k/N)} du.$$

Since the J_1, \dots, J_n commute with each other, we have that (as observed by [Nov10])

$$\text{Wg}_N = (N + J_n)^{-1} \cdots (N + J_1)^{-1}, \quad \text{when } N \geq n. \quad (2.4)$$

The reason why we introduce this formula for the Weingarten function is because the terms $(N + J_k)^{-1}$, $k \in [n]$ will appear naturally in our argument.

Next, we discuss the definition of the Weingarten function in case of general N . We follow [CS06].

Definition 2.20 (Weingarten function). Let $N, n \geq 1$. Define $\text{Wg}_N \in \mathbb{C}[\mathcal{S}_n]$ (as usual, we omit the dependence on n) by

$$\text{Wg}_N(\sigma) := \frac{1}{n!} \sum_{\substack{\lambda \vdash n \\ \ell(\lambda) \leq N}} \left[\chi_\lambda(\text{id}) \chi_\lambda(\sigma) \prod_{(i,j) \in \lambda} (N + j - i)^{-1} \right]. \quad (2.5)$$

Here, $\ell(\lambda)$ is the number of rows of λ , i.e. the number of parts in the partition of n given by λ .

Comparing with the formula (1.7) for $N \geq n$, the only difference is in the restriction $\ell(\lambda) \leq N$ when summing over Young diagrams λ . Note that when $N \geq n$, every Young diagram with n boxes has at most $n \leq N$ rows, and thus the definition (2.5) reduces to (1.7) if $N \geq n$.

2.2.1 Additional technicalities for the small N case

The following material is only needed to prove Theorem 2.5 in the case $N < 2 \max_{\ell \in [L]} n_\ell$. We encourage the reader on a first reading to skip this subsection and continue on to Section 3 to first read over the proof in the case $N \geq 2 \max_{\ell \in [L]} n_\ell$, which already contains the main probabilistic ideas. The reader may come back to this section once they are ready to read Section 3.2, where the results introduced here will be needed.

Let e_1, \dots, e_N denote the standard basis of \mathbb{C}^N . The tensor space $(\mathbb{C}^N)^{\otimes n}$ has a basis given by $(e_i, i = (i_1, \dots, i_n) \in [N]^n)$, where $e_i := e_{i_1} \otimes \cdots \otimes e_{i_n}$. The space $(\mathbb{C}^N)^{\otimes n}$ has a natural inner product which when restricted to basis elements is given by

$$\langle e_i, e_j \rangle = \delta_{ij} = \delta_{i_1 j_1} \cdots \delta_{i_n j_n}.$$

Let $M \in \text{End}((\mathbb{C}^N)^{\otimes n})$. One may think of M as an $N^n \times N^n$ matrix, whose matrix entries are given by:

$$M_{ij} = \langle e_i, M e_j \rangle, \quad i, j \in [N]^n.$$

In particular, if $M_1, \dots, M_n \in \text{End}(\mathbb{C}^N)$, then the matrix entries of the tensor product $M = M_1 \otimes \cdots \otimes M_n$ are given by

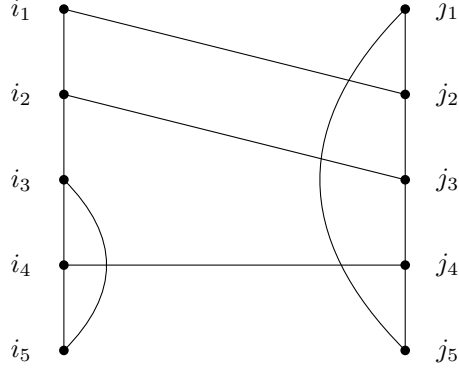
$$\begin{aligned} M_{ij} &= \langle e_i, (M_1 \otimes \cdots \otimes M_n) e_j \rangle = \langle e_{i_1} \otimes \cdots \otimes e_{i_n}, (M_1 e_{j_1}) \otimes \cdots \otimes (M_n e_{j_n}) \rangle \\ &= \langle e_{i_1}, M_1 e_{j_1} \rangle \cdots \langle e_{i_n}, M_n e_{j_n} \rangle \\ &= (M_1)_{i_1 j_1} \cdots (M_n)_{i_n j_n}, \end{aligned}$$

i.e. the product of the corresponding matrix entries of M_1, \dots, M_n .

Definition 2.21. Let $N, n \geq 1$. We define a representation ρ_+ of \mathcal{B}_n as follows. Given a pairing π of $[2n]$, define $\rho_+(\pi)$ to be the linear map in $\text{End}((\mathbb{C}^N)^{\otimes n})$ whose matrix entries are given by:

$$(\rho_+(\pi))_{(i_1, \dots, i_n), (i_{2n}, \dots, i_{n+1})} := \prod_{\{a, b\} \in \pi} \delta^{ia^i b}.$$

For notational brevity, we omit the dependence of ρ_+ on N, n . In the following, we mostly apply ρ_+ to elements of $\mathcal{B}_{n,n} \subseteq \mathcal{B}_{2n}$. The way one visualizes this definition is as follows. Suppose $n = 5$ and we are given the following pairing:



Then the matrix entry corresponding to indices $(i_1, \dots, i_5), (j_1, \dots, j_5)$ is simply 1 if all constraints indicated by the pairing are satisfied (in this case, $i_1 = j_2, i_2 = j_3, i_3 = i_5, i_4 = j_4$, and $j_1 = j_5$), and 0 otherwise.

Remark 2.22. There is an alternative definition of ρ_+ that one typically sees (e.g. [Dah16]). First, let $E_{ij} \in \text{End}(\mathbb{C}^N)$ be the elementary matrix which has a 1 in its (i, j) entry and zeros everywhere else. We may write $E_{ij} = e_i e_j^T$. Then

$$\rho_+(\pi) = \prod_{\{a, b\} \in \pi} \delta^{ia^i b} E_{i_1 i_{2n}} \otimes E_{i_2 i_{2n-1}} \otimes \dots \otimes E_{i_n i_{n+1}}.$$

Here and in the following, repeated indices are implicitly summed over. To see why this definition is equivalent, we may compute an arbitrary matrix entry:

$$\begin{aligned} (\rho_+(\pi))_{(i_1, \dots, i_n), (i_{2n}, \dots, i_{n+1})} &= \prod_{\{a, b\} \in \pi} \delta^{ja^j b} \langle e_{i_1} \otimes \dots \otimes e_{i_n}, (E_{j_1 j_{2n}} \otimes \dots \otimes E_{j_n j_{n+1}}) (e_{i_{2n}} \otimes \dots \otimes e_{i_{n+1}}) \rangle \\ &= \prod_{\{a, b\} \in \pi} \delta^{ja^j b} \langle e_{i_1}, e_{j_1} e_{j_{2n}}^T e_{i_{2n}} \rangle \dots \langle e_{i_n}, e_{j_n} e_{j_{n+1}}^T e_{i_{n+1}} \rangle \\ &= \prod_{\{a, b\} \in \pi} \delta^{ja^j b} \delta_{i_1 j_1} \delta_{j_{2n} i_{2n}} \dots \delta_{i_n j_n} \delta_{j_{n+1} i_{n+1}} \\ &= \prod_{\{a, b\} \in \pi} \delta^{ia^i b}. \end{aligned}$$

Recalling that we may view S_n as embedded in \mathcal{B}_n , the restriction of the representation ρ_+ to S_n defines a representation of S_n .

Definition 2.23. Let $N, n \geq 1$. Define the representation $\rho : \mathbb{C}[S_n] \rightarrow \text{End}((\mathbb{C}^N)^{\otimes n})$ to be the restriction of $\rho_+ : \mathcal{B}_n \rightarrow \text{End}((\mathbb{C}^N)^{\otimes n})$ to $\mathbb{C}[S_n] \subseteq \mathcal{B}_n$.

Again, we omit the dependence of ρ on N, n for notational brevity.

Remark 2.24. One may verify that ρ has the following explicit form on pure tensors:

$$\rho(\sigma)(v_1 \otimes \cdots \otimes v_n) = v_{\sigma(1)} \otimes \cdots \otimes v_{\sigma(n)}, \quad \sigma \in S_n, \quad v_1, \dots, v_n \in \mathbb{C}^N.$$

In words, $\rho(\sigma)$ acts by permutation of tensors.

Next, we discuss how the formula (2.4) needs to be modified when N is general. First, recall that when $N \geq n$, the Weingarten function may also be defined as the inverse of $\sum_{\sigma} N^{\#\text{cycles}(\sigma)} \sigma$ in $\mathbb{C}[S_n]$. For general N , this inverse may not exist. However, we quote the following result from [CS06], which says that the Weingarten function can still be interpreted as an inverse, in a suitable sense.

Lemma 2.25 (Section 2 of [CS06]). Let $N, n \geq 1$. We have that $\rho(\sum_{\sigma} N^{\#\text{cycles}(\sigma)} \sigma)$ is invertible, with inverse given by $\rho(\text{Wg}_N)$.

Remark 2.26. This is the whole point of introducing the representation ρ , in that $\rho(\sum_{\sigma} N^{\#\text{cycles}(\sigma)} \sigma)$ is always invertible as a matrix, even though $\sum_{\sigma} N^{\#\text{cycles}(\sigma)} \sigma$ may not be invertible in $\mathbb{C}[S_n]$. The simplest example of this difference is when $N = 1$ and $n = 2$, in which case $\sum_{\sigma} N^{\#\text{cycles}(\sigma)} \sigma = \text{id} + (1\ 2)$. Now clearly, $\text{id} + (1\ 2)$ is not invertible in $\mathbb{C}[S_2]$, because the inverse would be given in general by $a \cdot \text{id} + b \cdot (1\ 2)$, where $a, b \in \mathbb{C}$ solve the following system of equations:

$$\begin{aligned} a + b &= 1, \\ a + b &= 0. \end{aligned}$$

On the other hand, when $N = 1$, the space $(\mathbb{C}^N)^{\otimes n}$ is one-dimensional no matter the value of n . On this space, both $\rho(\text{id})$ and $\rho((1\ 2))$ are the identity operator. (Recall that $\rho((1\ 2))(u \otimes v) = v \otimes u$. If $u, v \in \mathbb{C}$, then $v \otimes u = u \otimes v$, so that $\rho((1, 2))(u \otimes v) = u \otimes v$.) Thus $\rho(\text{id} + (1\ 2))$ acts as multiplication by 2, and thus $\rho(\text{id} + (1\ 2))^{-1}$ is multiplication by $1/2$.

Similarly, we next show that the elements $N + J_k$, $k \in [n]$ are always invertible, if we apply the representation ρ_+ .

Lemma 2.27. Let $N, n \geq 1$. Let $\rho_+ : \mathcal{B}_{n,n} \rightarrow \text{End}((\mathbb{C}^N)^{\otimes 2n})$ be the representation⁵ from Definition 2.21. For all $k \in [n]$, all eigenvalues of $\rho_+(J_k)$ are at least $-N + 1$.

Proof. Due to our embedding of S_n into $\mathcal{B}_{n,n}$, $\rho_+(J_k)$ acts as the identity on the last n coordinates of $(\mathbb{C}^N)^{\otimes 2n}$. On the first n coordinates, $\rho_+(J_k)$ acts as $\rho(J_k)$ (as defined in Definition 2.23). Thus, it suffices to show that all eigenvalues of $\rho(J_k)$ are at least $-N + 1$. This follows from the combination of two classic results in the representation theory of the symmetric group:

1. By Schur-Weyl duality (see e.g. [CS06, Theorem 2.1]), we have that in the decomposition of ρ into irreps, only those irreps corresponding to Young diagrams λ with at most N rows (i.e. $\ell(\lambda) \leq N$) appear.
2. Let ρ^λ be the irrep corresponding to λ . The eigenvalues of $\rho^\lambda(J_k)$ are explicitly known: for each Young tableaux with shape λ , let (i, j) be the coordinates of the box which contains the integer k . Here, i is the row index and j the column index. Then $\rho^\lambda(J_k)$ has an eigenvalue equal to $j - i$. Moreover, all eigenvalues of $\rho^\lambda(J_k)$ arise this way. This result was proven by Jucys [Juc74] and independently later by Murphy [Mur81].

⁵Recall that $\mathcal{B}_{n,n} \subseteq \mathcal{B}_{2n}$. The representation ρ_+ is originally defined on \mathcal{B}_{2n} , here we restrict it to $\mathcal{B}_{n,n}$.

The second fact implies that the every eigenvalue of $\rho^\lambda(J_k)$ is at least $-\ell(\lambda) + 1$, since the box with the most negative value of $j - i$ is $(\ell(\lambda), 1)$. Combining this with the first fact, the desired result now follows. \square

This lemma shows that all for all $k \in [n]$, all eigenvalues of $\rho_+(N + J_k)$, are at least 1, and thus $\rho_+(N + J_k)$ is invertible. Moreover, we have the following lemma, which generalizes (2.4) to the case of general N .

Lemma 2.28. Let $N, n \geq 1$. We have that

$$\rho_+(\text{Wg}_N) = \rho_+(N + J_n)^{-1} \cdots \rho_+(N + J_1)^{-1}.$$

Proof. Due to our embedding of S_n into $\mathcal{B}_{n,n}$, for any element $f \in \mathbb{C}[S_n]$, the matrix $\rho_+(f) \in \text{End}((\mathbb{C}^N)^{\otimes 2n})$ acts as the identity on the last n coordinates of $(\mathbb{C}^N)^{\otimes 2n}$. On the first n coordinates, $\rho_+(f)$ acts as $\rho(f) \in \text{End}((\mathbb{C}^N)^{\otimes n})$. Thus it suffices to prove the claimed identity with ρ_+ replaced by ρ . Since ρ is a representation, we have that (using that the Jucys-Murphy elements commute with each other and applying (2.3) in the final identity)

$$\rho(N + J_n)^{-1} \cdots \rho(N + J_1)^{-1} = \rho((N + J_1) \cdots (N + J_n))^{-1} = \rho\left(\sum_{\sigma} N^{\#\text{cycles}(\sigma)} \sigma\right)^{-1}.$$

The desired result now follows by Lemma 2.25. \square

In the course of proving Theorem 2.5 for general values of N , we will also need the following technical lemma.

Lemma 2.29. Let $N, n \geq 1$. All eigenvalues of

$$\frac{1}{N} \rho(J_n + \cdots + J_1) \in \text{End}((\mathbb{C}^N)^{\otimes n})$$

are at least $-\frac{n}{2} + \frac{1}{2}$.

Proof. As noted in the proof of Lemma 2.27, by Schur-Weyl duality (see e.g. [CS06, Theorem 2.1]), we have that in the decomposition of ρ into irreps, only those irreps corresponding to Young diagrams λ with at most N rows (i.e. $\ell(\lambda) \leq N$) appear. Thus letting ρ^λ be the irrep corresponding to λ , it suffices to show the claim with ρ replaced by ρ^λ , for any Young diagram λ with at most N rows.

Towards this end, let λ be a Young diagram, for example as in Figure 20. As discussed in the proof of Lemma 2.27, for $k \in [n]$ the eigenvalues of $\rho^\lambda(J_k)$ are given by the content of the k th box when we range over standard Young tableaux with shape λ . Even more, [Juc74, Mur81] show that the $(\rho^\lambda(J_k), k \in [n])$ have a joint eigenbasis indexed by standard Young tableaux with shape λ , where the eigenvalues corresponding to a given standard Young tableaux are the contents of the boxes of the Young diagram. This discussion shows that on each eigenbasis element, $\rho^\lambda(J_n + \cdots + J_1)$ acts in the same manner, that is as a whole $\rho^\lambda(J_1 + \cdots + J_n)$ acts as a multiple c_λ of the identity, where c_λ is the sum of contents of all the boxes in λ .

To envision the computation of c_λ , we label each box of λ with its content, i.e. the number $j - i$, where (i, j) is the row-column coordinate of the box. For the Young diagram in Figure 20, we have the labeling in Figure 21.

The constant c_λ is then the sum of all box labels. For example, for the above Young diagram, $c_\lambda = 6$.

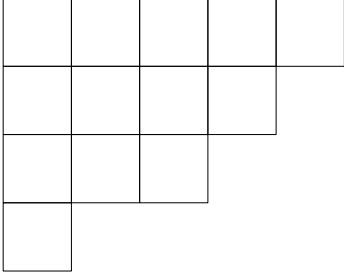


Figure 20: $5 + 4 + 3 + 1 = 13$

0	1	2	3	4
-1	0	1	2	
-2	-1	0		
-3				

Figure 21: Young diagram with content labels

Now, fix $n, N \geq 1$. To prove the lemma, we need to understand how negative the content sum c_λ may be for a Young diagram with n boxes and at most N rows. Clearly, to minimize c_λ , we want a Young diagram with as many columns of size N as possible. Thus, if $n = mN + r$ with $0 \leq r \leq N - 1$, then the Young diagram in Figure 22 minimizes c_λ .

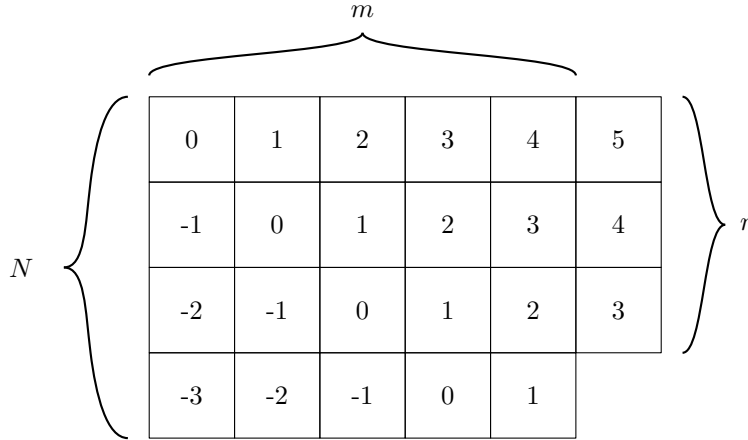


Figure 22: $n = mN + r$

The content sum c_λ of such a diagram (by first summing the contents along each column) is

$$\begin{aligned}
 c_\lambda &= -\binom{N}{2} + \left(-\binom{N}{2} + N\right) + \cdots + \left(-\binom{N}{2} + (m-1)N\right) + \left(-\binom{r}{2} + mr\right) \\
 &= -m\binom{N}{2} + \binom{m}{2}N - \binom{r}{2} + mr.
 \end{aligned}$$

Our goal is to show that $\frac{1}{N}c_\lambda \geq -\frac{1}{2}n + \frac{1}{2}$. Towards this end, note that

$$\begin{aligned}
 \frac{1}{N}c_\lambda &= -\frac{1}{2}m(N-1) + \frac{1}{2}m(m-1) - \frac{1}{2}\frac{r(r-1)}{N} + \frac{mr}{N} \\
 &= -\frac{1}{2}(mN+r) + \frac{1}{2}m^2 + \frac{1}{2}r - \frac{1}{2}\frac{r(r-1)}{N} + \frac{mr}{N}.
 \end{aligned}$$

Recalling that $n = mN + r$ with $0 \leq r \leq N - 1$, we see that if $m \geq 1$, then the above is at least $-\frac{1}{2}n + \frac{1}{2}m^2 \geq -\frac{1}{2}n + \frac{1}{2}$, as desired. Now, suppose that $m = 0$, so that $n = r$. Then the above is

equal to

$$-\frac{1}{2}n + \frac{1}{2}r \left(1 + \frac{1}{N} - \frac{r}{N}\right).$$

One may check that under the restriction $1 \leq r \leq N - 1$, the above is minimized at $r = 1$ with a value of $-\frac{1}{2}n + \frac{1}{2}$, as desired. \square

Recall the Jucys-Murphy elements acting on bottom vertices defined in Definition 2.17.

Corollary 2.30. Let $N, n \geq 1$. Let $\rho_+ : \mathcal{B}_{n, n+1} \rightarrow \text{End}((\mathbb{C}^N)^{\otimes 2n+1})$. All eigenvalues of

$$\frac{1}{N} \rho_+(J_n + \cdots + J_1 + J'_{n+1} + \cdots + J'_1)$$

are strictly greater than $-n$.

Proof. Observe that $\rho_+(J_n + \cdots + J_1)$ acts as the identity on the last $n + 1$ coordinates, and on the first n coordinates, $\rho_+(J_n + \cdots + J_1)$ acts as $\rho(J_n + \cdots + J_1)$. In other words, $\rho_+(J_n + \cdots + J_1) = \rho(J_n + \cdots + J_1) \otimes I_{n+1}$, where $I_{n+1} \in \text{End}((\mathbb{C}^N)^{\otimes (n+1)})$ is the identity. Similarly, we have that $\rho_+(J'_{n+1} + \cdots + J'_1) = I_n \otimes \rho(J'_{n+1} + \cdots + J'_1)$, where $I_n \in \text{End}((\mathbb{C}^N)^{\otimes n})$ is the identity. In general, given two matrices M_1, M_2 , the eigenvalues of $M_1 \otimes M_2$ are the products of the eigenvalues of M_1 and eigenvalues of M_2 . Combining this fact with Lemma 2.29, we obtain that all eigenvalues of $\frac{1}{N} \rho(J_n + \cdots + J_1) \otimes I_{n+1}$ are at least $-\frac{1}{2}n + \frac{1}{2}$, and all eigenvalues of $I_n \otimes \frac{1}{N} \rho(J'_{n+1} + \cdots + J'_1)$ are at least $-\frac{1}{2}(n + 1) + \frac{1}{2}$. The desired result now follows. \square

3 Poisson process exploration, the $T \rightarrow \infty$ limit, and recovery of Weingarten calculus

In this section, we prove Theorem 2.5. First, in Section 3, we define and analyze a particular exploration process that is central to our proof. We then give the proof of the theorem in the case where N is large, where it is easier to focus on the main ideas. In Section 3.2, we extend the argument to the case of general N .

3.1 Strand-by-strand exploration

We begin towards the proof of Theorem 2.5. The main difficulty is that the weights $w_T(\pi)$ appearing in Theorem 2.5, when expressed as a series in T , do not converge absolutely when $T \rightarrow \infty$. In fact, the series is of the schematic form $\sum_k \frac{(-T)^k}{k!} c_k$, for some coefficients c_k . Clearly, to show convergence as $T \rightarrow \infty$, we need to take advantage of delicate cancellations which occur, rather than any sort of absolute summability. Uncovering these cancellations is the main technical part in the argument. This will be achieved via a certain exploration of the Poisson point process introduced in Section 2.1 which will provide an alternate form for the weights $w_T(\pi)$ which makes taking the $T \rightarrow \infty$ limit trivial.

Notation 3.1. We will often refer to the opposite-direction swaps introduced in Section 2.1 as “turnarounds”. Also, we will often use the term “matching” and “partition” interchangeably.

In the following, recall the Poisson process and strand diagram material introduced in Section 2.1. Because the Poisson processes corresponding to different letters are independent, it will suffice to just analyze the portion of the strand diagram corresponding to a single letter λ .

Notation 3.2. In this section, it will be notationally convenient for us to assume that the strand diagram corresponding to λ has $2n$ total strands, with n right-directed and left-directed strands each. This corresponds to the case that λ and λ^{-1} each appear a total of n times in the given collection of words $\mathbf{\Gamma}$. This is in contrast to the notation of Definition 2.1, where n_ℓ is the total number of occurrences of a given letter λ_ℓ and its inverse λ_ℓ^{-1} . To make consistent with this previous notation, we could perhaps introduce $n_+ = n_- = n/2$ and work with n_+ . However, the parameter n often appears in subscripts or superscripts, and adding a subscript “+” to n will result in iterated subscripts, which will complicate many expressions. Therefore, we decide just to use n to denote the number of right-directed (and left-directed) strands.

Having restricted to a single letter λ , let $\mathcal{C}, \mathcal{D}, \Sigma$ (introduced in Section 2.1) correspond to the single letter λ , with a total of n positive occurrences and n negative occurrences. Let $\Sigma(T) = \Sigma_\infty \cap \mathcal{D}(T)$. By Lemma 2.3, expectations of words of Unitary Brownian motion may be expressed in terms of $w_T(\pi)$ (which is defined in (2.1)), for pairings $\pi \in \mathcal{M}(4n)$. Now that we have introduced the Brauer algebra \mathcal{B}_n in Definition 2.9, one may in fact view the pairings π as elements of \mathcal{B}_{2n} . Even more, we may restrict to the walled Brauer algebra $\mathcal{B}_{n,n} \subseteq \mathcal{B}_{2n}$, for reasons we next describe.

The weights $w_T(\pi)$ are naturally expressed in terms of a random walk on the walled Brauer algebra $\mathcal{B}_{n,n}$, as follows. We may visualize $\Sigma(T)$ as in the following picture (where $n = 3$). The green lines represent same-swaps, the blue lines represent turnarounds, and locations of the green/blue lines correspond to the points of $\Sigma(T)$. Recalling Definition 2.13, we have that each green line corresponds to an element of the form $(i j)$, and each blue line corresponds to an element of the form $\langle i j \rangle$.

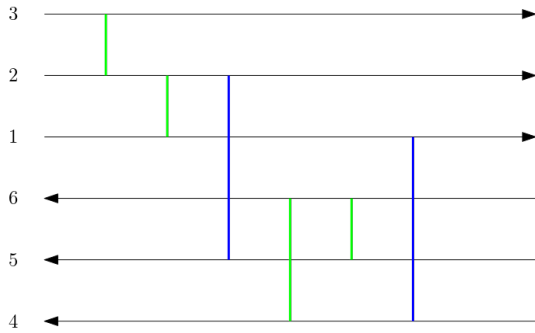


Figure 23: $(3\ 1)(2\ 1)\langle 2\ 5\rangle(6\ 4)(6\ 5)\langle 1\ 4\rangle$

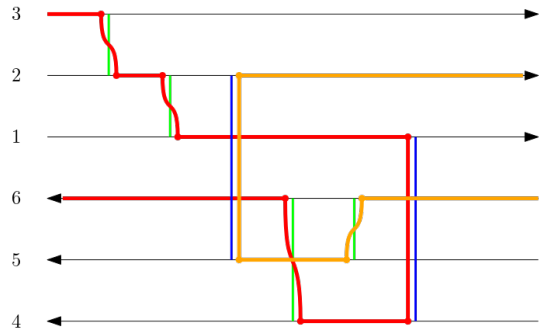


Figure 24

We can read off the element of $\mathcal{B}_{n,n}$ from the above strand diagram by exploring along each strand. For example, in Figure 24, we explore from the left of strand 3, as well as the right of strand 6. We see that 3 gets matched to 6 on the left, while 6 gets matched to 2 on the right. Clearly, if we do this for all other strands (not drawn), we can obtain the element of $\mathcal{B}_{n,n}$ that the above diagram corresponds to.

On the algebraic side, this exploration amounts to multiplying together all increments $(i j)$ or $\langle i j \rangle$ corresponding to the points of Σ , in the order that they appear. Due to the Poissonian nature of the points, each possible increment $(i j)$, $\langle i j \rangle$ is equally likely, and thus one may interpret Σ as giving a random walk on $\mathcal{B}_{n,n}$, as previously mentioned. However, there is an additional wrinkle, in that we need to keep track of more than just the final pairing, since each green line contributes a factor of $-\frac{1}{N}$ while each blue line contributes a factor of $\frac{1}{N}$. With this in mind, we make the following definition.

Definition 3.3. Given a finite collection of points $P \subseteq \mathcal{D}$, let $F(P) = F_N(P)$ be the element of $\mathcal{B}_{n,n}$ that P corresponds to, with the additional factors of $-\frac{1}{N}$ for same-direction swaps and $\frac{1}{N}$ for

turnarounds. Let $M(P)$ be the pairing corresponding to P , i.e. the element of $\mathcal{B}_{n,n}$ obtained when ignoring the additional factors.

With this definition, observe that we may express

$$w_T(\pi) = e^{\binom{2n}{2}T - nT} \mathbb{E}[F(\Sigma(T)) \mathbb{1}(M(\Sigma(T)) = \pi)]$$

Or, as elements of the walled Brauer algebra $\mathcal{B}_{n,n}$, we have the equality

$$\sum_{\pi} w_T(\pi) \pi = e^{\binom{2n}{2}T - nT} \mathbb{E}[F(\Sigma(T))]. \quad (3.1)$$

In the following, we will mainly focus on understanding $\lim_{T \rightarrow \infty} e^{\binom{2n}{2}T - nT} \mathbb{E}[F(\Sigma(T))]$. Clearly, once we understand this, we will also know $\lim_{T \rightarrow \infty} w_T(\pi)$ for any π .

We are almost done with the preliminary considerations leading up to describing our exploration of the Poisson process Σ . We make one last observation before this. Recall that for points $x \in \mathcal{D}$, $\mathfrak{l}(x) \in \binom{[2n]}{2}$ is the index of the interval which contains x .

Definition 3.4. Let $T \geq 0$. Let A_T be the event that for all $i \in [n]$, $j \in [n : 2n]$, if there is some point $x \in \Sigma(T)$ with $\mathfrak{l}(x) = \{i, j\}$, then every point thereafter $y \in \Sigma(T) \cap \sqcup_{\binom{[2n]}{2}} [x, T]$ with $\mathfrak{l}(y) \cap \mathfrak{l}(x) \neq \emptyset$ in fact also satisfies $\mathfrak{l}(y) = \{i, j\}$.

In terms of the strands, this condition says that once a blue turnaround appears, the only points which can thereafter appear that touch either of the matched strands must be the blue turnaround between the same two strands.

Lemma 3.5. We have that

$$\mathbb{E}[F(\Sigma(T))] = \mathbb{E}[F(\Sigma(T)) \mathbb{1}_{A_T^c}].$$

Proof. We show that for any integer $k \geq 0$,

$$\mathbb{E}[F(\Sigma(T)) \mathbb{1}_{A_T^c} \mid |\Sigma(T)| = k] = 0.$$

The above is trivial when $k = 0, 1$, because in this case A_T^c cannot occur. Thus, suppose that $k \geq 2$. Let Ω_k be the set of length- k sequences of elements of the set

$$\{(i j) : 1 \leq i < j \leq n\} \cup \{(i j) : n + 1 \leq i < j \leq 2n\} \cup \{\langle i j \rangle : i \in [n], j \in [n : 2n]\},$$

such that there exists some $\langle i j \rangle$ in the sequence, as well as some transposition which appears afterwards that involves either i or j . For each $(x_1, \dots, x_k) \in \Omega_k$, let $n_T(x_1, \dots, x_k)$ be the number of transpositions (i.e. elements of the form $(i j)$) in the sequence. Observe that

$$\mathbb{E}[F(\Sigma(T)) \mathbb{1}_{A_T^c} \mid |\Sigma(T)| = k] = \frac{1}{\binom{2n}{2}^k N^k} \sum_{(x_1, \dots, x_k) \in \Omega_k} (-1)^{n_T(x_1, \dots, x_k)} x_1 \cdots x_k.$$

We now define a bijection $h : \Omega_k \rightarrow \Omega_k$ such that if $h(x_1, \dots, x_k) = (y_1, \dots, y_k)$, then $(-1)^{n_T(y_1, \dots, y_k)} y_1 \cdots y_k = -(-1)^{n_T(x_1, \dots, x_k)} x_1 \cdots x_k$. Note that this immediately implies that

$$\sum_{(x_1, \dots, x_k) \in \Omega_k} (-1)^{n_T(x_1, \dots, x_k)} x_1 \cdots x_k = - \sum_{(x_1, \dots, x_k) \in \Omega_k} (-1)^{n_T(x_1, \dots, x_k)} x_1 \cdots x_k,$$

which implies that the above is zero, which would give the desired result. To define h , given a sequence (x_1, \dots, x_k) , let $2 \leq r \leq k$ be index of the first element x_r which causes the sequence (x_1, \dots, x_n) to be in Ω_k . There are two cases: (1) $x_r = \langle i j \rangle$ and there exists some $1 \leq m < r$ with $x_m = \langle i k \rangle$, (2) $x_r = \langle i j \rangle$ and there exists $1 \leq m < r$ with $x_m = \langle i k \rangle$. In the first case, we define

$$h(x_1, \dots, x_k) := (x_1, \dots, x_{r-1}, \langle j k \rangle, x_{r+1}, \dots, x_k),$$

and in the second case, we define

$$h(x_1, \dots, x_k) := (x_1, \dots, x_{r-1}, (j k), x_{r+1}, \dots, x_k).$$

Note that h is an involution, and thus a bijection. Also, we clearly have by construction that

$$(-1)^{n_T(x_1, \dots, x_k)} = -(-1)^{n_T(h(x_1, \dots, x_k))}.$$

Thus to finish, it suffices to show that with $h(x_1, \dots, x_k) = (y_1, \dots, y_k)$, we have that $x_1 \cdots x_k = y_1 \cdots y_k$. By construction of h , it just suffices to show that $x_m \cdots x_r = x_m \cdots x_{r-1} y_r$. By the assumption on r , we have that $x_{m+1} \cdots x_{r-1}$ commutes with x_m , and so

$$x_m \cdots x_{m-1} x_r = x_{m+1} \cdots x_{m-1} x_m x_r.$$

The desired result now follows because $\langle i k \rangle \langle i j \rangle = \langle i k \rangle \langle j k \rangle$ and $\langle i k \rangle \langle i j \rangle = \langle i k \rangle \langle j k \rangle$. For the first identity, observe that the two products of matchings in Figure 25 are equal.

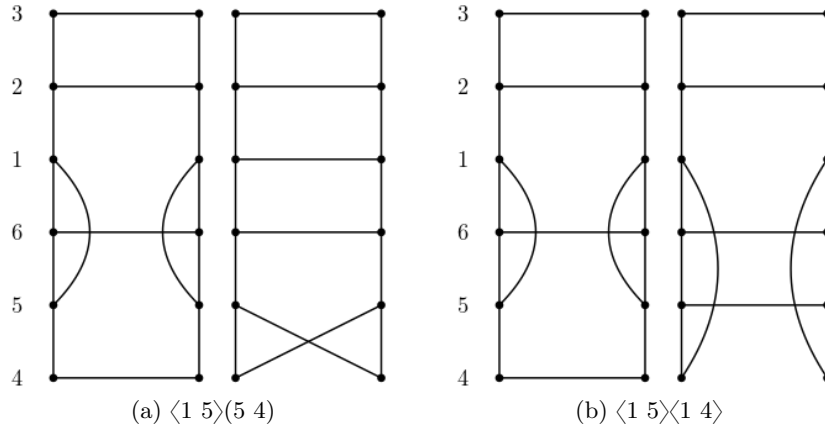


Figure 25

The second identity follows similarly. □

We now finally describe our exploration of the strand diagram corresponding to Σ . The exploration proceeds strand-by-strand. We first give an informal description with accompanying figures before proceeding to the formal mathematical definition. The main feature of the exploration is that we explore only a single strand at a time, rather than all strands at once. That is, we start at (say) the top strand, and explore left-to-right until we see a swap or a turnaround involving this strand. If we see a swap between the top strand and another strand, then we begin exploring this other strand. If we see a turnaround, then the current exploration era ends, and we begin to explore the next strand. To visualize this exploration, suppose we want to explore the the diagram in Figure 26.

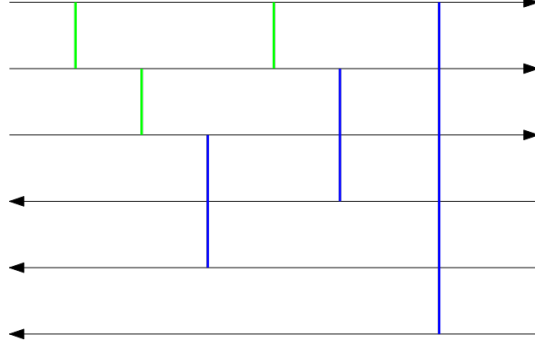


Figure 26

Our exploration proceeds in three separate eras, drawn as in Figure 27.

Note that at the start of the second era, we begin exploring the top strand instead of the second-to-top strand, because of the previous swap between these two strands. Likewise, at the start of the third era, we also begin exploring from the top strand, because this is effectively the bottom strand due to the previously seen swaps. Another thing to note is that in principle, during the first exploration era, it is certainly possible for the point process to have swaps that involve two non-top strands. However, our exploration process does not see these swaps. It turns out that by exploring the random environment in the manner we described, we can in fact assume that in every exploration era, every swap in the point process involves the current exploration strand, so that we don't need to worry about such "unseen swaps". This property is due to certain cancellations that we may take advantage of, which are very similar in spirit to the cancellations observed in the proof of Lemma 3.5.

At the end of the last exploration era, we have built up an element of $\mathcal{B}_{n,n}$ (we have omitted the additional factors of $\pm \frac{1}{N}$ and only drawn the left and right matchings), as displayed in Figure 28.

Here, the colors are for visual purposes and don't affect the end element of $\mathcal{B}_{n,n}$: we have colored the matching edges to denote the exploration era in which these pairing were discovered. Now here is why we chose to explore as we did: conditioned on everything we have seen up to the end of the last exploration era, the expectation of $F(\Sigma(T))$ is essentially given⁶ by the matching in Figure 28. This property is intimately related to our previous comment that we can assume that there are no unseen swaps, i.e. swaps which do not involve the current exploration strand. This key property of our exploration enables us to give a rather explicit closed-form expression for the overall expectation of $F(\Sigma(T))$. Even more, it is almost trivial to take the $T \rightarrow \infty$ limit of the closed-form expression, and this allows us to recover the Weingarten calculus.

We now proceed to the precise definition of the exploration. First, for $i \in [2n]$, define

$$\Sigma_i := \bigcup_{j \in [2n] \setminus \{i\}} \Sigma_{\{i,j\}},$$

i.e. Σ_i collects all Poisson processes with which i is involved. In terms of the strands, Σ_i collects all swaps and turnarounds touching the i th strand. The exploration is described by two processes $(E_t)_{t \geq 0}$, $(\pi_t)_{t \geq 0}$, the first of which takes values in $[n]$, and the second of which takes values in S_n (which we view as the set of bijections of $[n]$). One should think of E_t as tracking the current exploration era, and π_t as tracking the current strand of exploration.

⁶Technically, this is only true up to some explicit factors, but this is more of a technical detail.

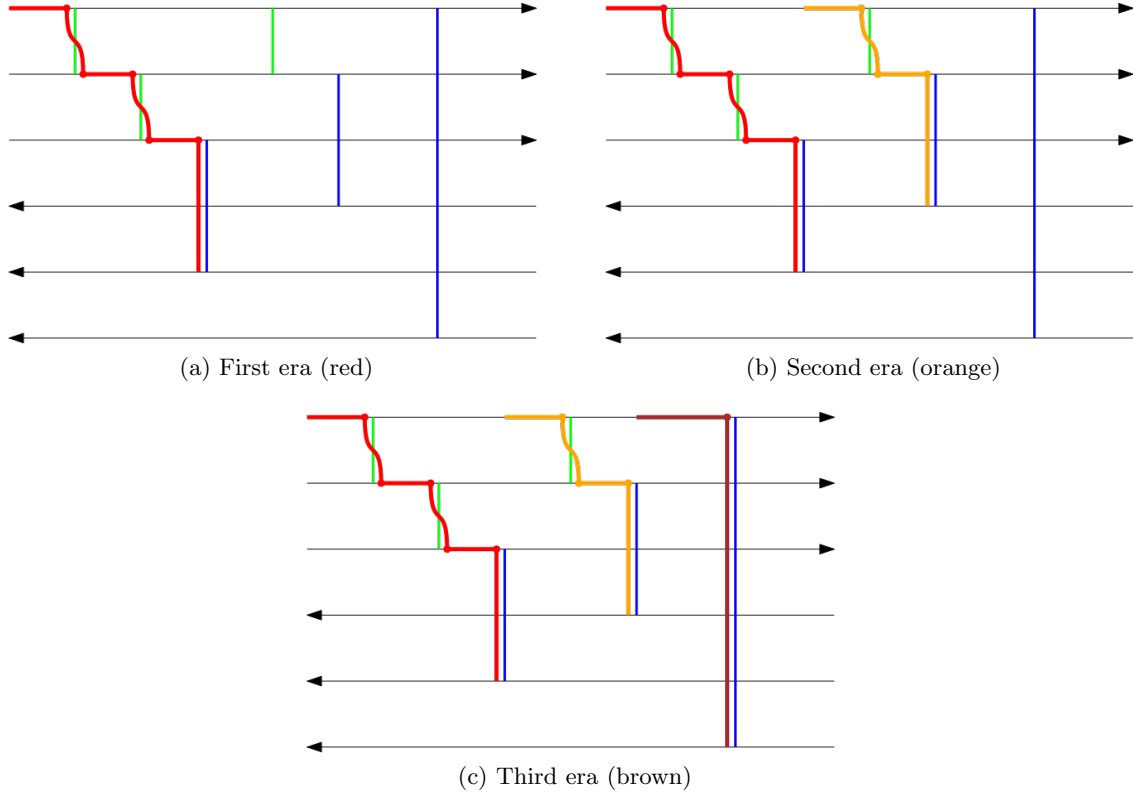


Figure 27

We start with $E_0 := 1$, $\pi_0 := \text{id}$. We begin exploring $\Sigma_{\pi_0(E_0)} = \Sigma_1$ until we see the first point, which we denote by U_1 . At time U_1 , we update E and π as follows. There is some $j \in [2n] \setminus \{E_0\}$ such that $\mathfrak{l}(U_1) = \pi_0(E_0, j)$. For $t \in (0, U_1)$, we set $E_t := E_0$, $\pi_t := \pi_0$. Now if $j \in [n]$, then we set $E_{U_1} := E_0$ and $\pi_{U_1} := (\pi_0(1) j)\pi_0$. We then continue exploring $\Sigma_{\pi_{U_1}(E_{U_1})}$ from time U_1 . Otherwise, if $j \in [n : 2n]$, then we set $E_{U_1} := E_0 + 1$ (i.e. a new exploration era begins) and $\pi_{U_1} := \pi_0$. Additionally, we remove all points of $\Sigma_{\pi_0(E_0)} \cup \Sigma_j$ from Σ . The exploration then continues on this reduced point process. In terms of the strands, the removal of points corresponds to only looking at those swaps or turnarounds which do not involve $\pi_0(E_0), j$. The exploration stops once all exploration eras have ended, i.e. once we have explored all strands up to their first time of turnaround. This is the first time t such that $E_t = n + 1$.

For $i \in [n]$, let $T_i := \inf\{t \geq 0 : E_t = i + 1\}$, i.e. the time at which the i th exploration era ends. Let \mathcal{Q}_t be the set of points that the exploration has seen up to time t . Let $(\mathcal{F}_t, t \geq 0)$ be the filtration generated by the processes E, π .

The following key proposition makes precise the key property of our exploration that we described earlier.

Proposition 3.6. We have that

$$e^{\binom{2n}{2}T - nT} \mathbb{E}[F(\Sigma(T)) \mathbb{1}_{A_T} \mathbb{1}(T_n \leq T)] = \mathbb{E}[F(\mathcal{Q}(T_n)) \mathbb{1}(T_n \leq T) e^{2(n-1)T_1} e^{2(n-2)(T_2 - T_1)} \dots e^{2(n-n)(T_n - T_{n-1})}].$$

Proof. Fix N . We proceed by induction on n . When $n = 1$, the result is true for all $T \geq 0$, because then A_T always occurs, and furthermore when $T_1 \leq T$, we have that $F(\Sigma(T)) = F(\mathcal{Q}(T_1))$. Now

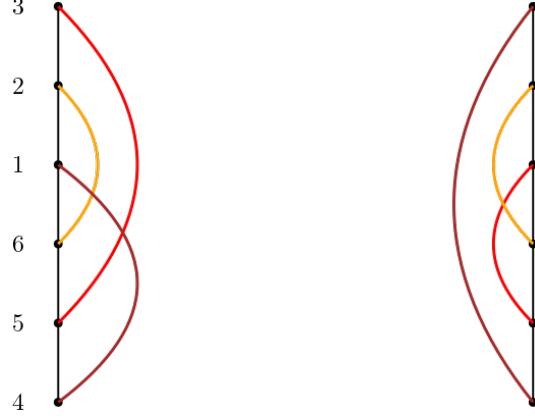


Figure 28

suppose that for some general $n \geq 1$, the result is true for all $T \geq 0$. We proceed to show that the case $n + 1$ also holds. We start by conditioning on \mathcal{F}_{T_1} . Pictorially, this corresponds to exploring until the end of the first era, see Figure 29. One should think of the two parallel vertical red lines

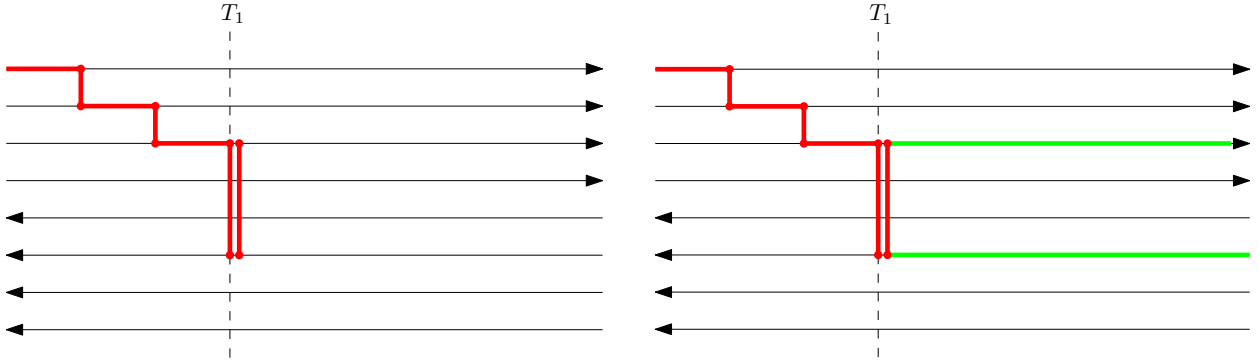


Figure 29

Figure 30

as occurring at the same time (namely T_1), although for visual purposes we have drawn them to be slightly separated. Next, naturally, we may split the diagram in Figure 29 into two parts: the part to the left of T_1 , and the part to the right of T_1 . This corresponds to splitting

$$\Sigma(T) = \Sigma(T_1) \cup (\Sigma(T) \setminus \Sigma(T_1)).$$

Since the Poisson processes before T_1 and after T_1 are conditionally independent, we have that

$$\begin{aligned} \mathbb{E}[F(\Sigma(T)) \mathbb{1}_{A_T} \mathbb{1}(T_{n+1} \leq T) \mid \mathcal{F}_{T_1}] = \\ \mathbb{E}[F(\Sigma(T_1)) \mid \mathcal{F}_{T_1}] \mathbb{E}[F(\Sigma(T) \setminus \Sigma(T_1)) \mathbb{1}_{A_T} \mathbb{1}(T_{n+1} - T_1 \leq T - T_1) \mid \mathcal{F}_{T_1}]. \end{aligned}$$

We first use our inductive assumption to rewrite the second conditional expectation on the right hand side above. Note that on the event A_T , we have that after T_1 , the two strands which have been matched cannot be involved in any more swaps or turnarounds, besides the turnaround of the same type. Pictorially, after T_1 , the two segments which are colored bright green are no longer connected to the other strands in the diagram, see Figure 30.

Since each individual strand is connected to $2(n+1) - 1 = 2n + 1$ other strands, the total number of independent Poisson processes which are forced to be zero is $2(2n + 1) - 2 = 4n$. Moreover,

any additional turnarounds between the two green strands has no effect, since every additional turnaround creates a new component, which incurs a factor of N , which cancels out the factor of $\frac{1}{N}$ that is associated to each turnaround. Thus, we may ignore the two green strands. The point now is that after having taken out the two green strands, the expectation of the remainder of the diagram after T_1 is exactly given by our inductive assumption:

$$e^{\binom{2n}{2}(T-T_1)-n(T-T_1)} \mathbb{E}[F(\Sigma(T) \setminus \Sigma(T_1)) \mathbb{1}_{A_T} \mathbb{1}(T_{n+1} - T_1 \leq T - T_1) \mid \mathcal{F}_{T_1}] = e^{-4n(T-T_1)} \mathbb{E}[F(\mathcal{Q}_T \setminus \mathcal{Q}_{T_1}) \mathbb{1}(T_{n+1} - T_1 \leq T - T_1) e^{2(n-1)(T_2-T_1)} e^{2(n-2)(T_3-T_2)} \dots e^{2(n-n)(T_{n+1}-T_n)}].$$

Applying this identity, as well as the identity $\binom{2(n+1)}{2} - (n+1) = 4n + \binom{2n}{2} - n$, we obtain

$$e^{\binom{2(n+1)}{2}T - (n+1)T} \mathbb{E}[F(\Sigma(T)) \mathbb{1}_{A_T} \mathbb{1}(T_{n+1} \leq T)] = \mathbb{E}[F(\Sigma(T_1)) F(\mathcal{Q}_{T_{n+1}} \setminus \mathcal{Q}_{T_1}) \mathbb{1}(T_{n+1} \leq T) e^{(4n + \binom{2n}{2} - n)T_1} e^{2(n+1-2)(T_2-T_1)} \dots e^{2(n+1-(n+1))(T_{n+1}-T_n)}].$$

To finish, we now argue that

$$e^{(4n + \binom{2n}{2} - n)T_1} \mathbb{E}[F(\Sigma(T_1)) F(\mathcal{Q}_{T_{n+1}} \setminus \mathcal{Q}_{T_1}) \mid \mathcal{F}_{T_{n+1}}] = e^{2nT_1} F(\mathcal{Q}_{T_1}) F(\mathcal{Q}_{T_{n+1}} \setminus \mathcal{Q}_{T_1}) \quad (3.2) \\ = e^{2nT_1} F(\mathcal{Q}_{T_{n+1}}).$$

Note that this would complete the proof of the inductive step. For a picture of what we have in mind when conditioning on $\mathcal{F}_{T_{n+1}}$, see Figure 31.

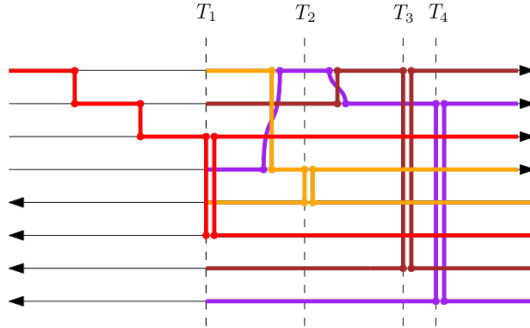


Figure 31

In Figure 31, we treat the portion of the diagram to the right of T_1 as fixed, whereas the portions of the strands before T_1 which are black have not been fully explored. The identity (3.2) says that after averaging over this randomness, we may simply assume that there are no additional swaps or turnarounds in $[0, T_1]$, so that the expectation is given by the diagram in Figure 32 (which corresponds to the right hand side of the identity).

The identity (3.2) follows due to certain cancellations, which allow us to assume that the only things that occur before T_1 are those turnarounds connecting a top and bottom strand which are connected by the diagram to the right of T_1 . This follows by similar arguments as in the proof of Lemma 3.5. Indeed, observe that the two diagrams in Figure 33 equal, in the sense that the top strands get matched to the same bottom strands (the red and orange strands are unchanged, so one only needs to track the brown and purple strands). Note however that the left diagram will have an opposite sign compared to the right diagram, because swaps incur a factor of -1 while turnarounds do not. This gives the desired cancellation between swaps and turnaround which do not connect two strands which have been matched by the portion of the diagram after T_1 .

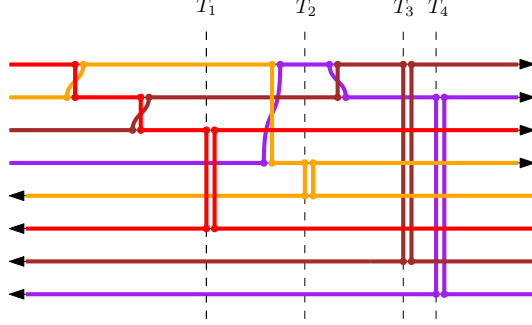


Figure 32

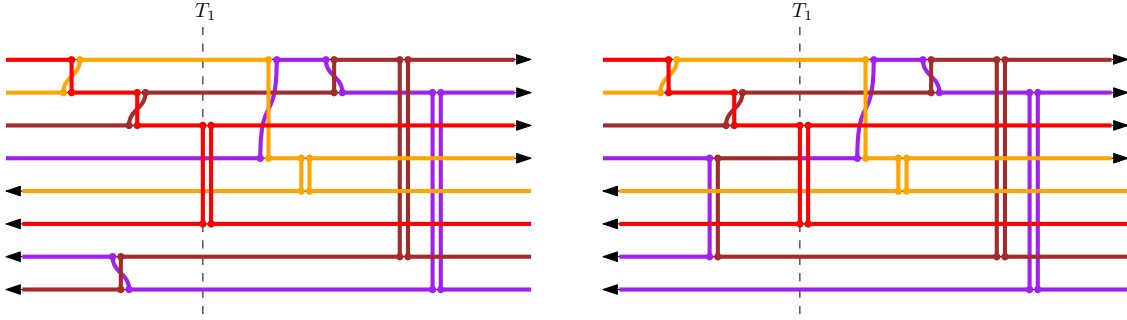


Figure 33: The above two diagrams are equal as elements of $\mathcal{B}_{n,n}$

Thus the total number of Poisson processes which must have zero points is $\binom{n}{2} + \binom{n+1}{2} + n^2$. Here, $\binom{n}{2}$ counts the possible swaps between two top strands, $\binom{n+1}{2}$ counts the possible swaps between two bottom strands, and $n^2 = n(n+1) - n$ counts the turnarounds which connect a top and bottom strand which are not already connected by the diagram to the right of T_1 . We now finish by noting the identity

$$4n + \binom{2n}{2} - n - \binom{n}{2} - \binom{n+1}{2} - n^2 = 2n. \quad \square$$

Next, to extract the Jucys-Murphy elements, it is helpful to think of all the swaps in the i th exploration era as involving the i th strand. Towards this end, we show that the expectation of $F(\mathcal{Q}(T_n))$ appearing in Proposition 3.6 may be computed by following a slightly different exploration, one in which each exploration era stays on a single strand, and in each era, we keep track of all swaps that touch the strand we are currently exploring. Towards this end, we define processes $(\bar{E}_t)_{t \geq 0}$ and $(\bar{\pi}_t)_{t \geq 0}$ as follows. As before, we start with $\bar{E}_0 = 1$ and $\bar{\pi}_0 = \text{id}$. We proceed to explore $\mathcal{P}_{\bar{E}_0}$ (in contrast to before, where we explored $\mathcal{P}_{\pi_0(E_0)}$). When we see a swap of the form $\{1, j\}$, $j \in [n]$, we update $\bar{\pi} \mapsto \bar{\pi}(1 \ j)$. When we see a turnaround $\langle 1 \ j \rangle$, $j \in [n : 2n]$, the first exploration era ends, we update \bar{E} to be 2, and we remove from \mathcal{P} all points in \mathcal{P}_{E_0} . We then continue until the end of the n th exploration era. See Figure 34 for how one may visually compare this alternative exploration with our original exploration.

Formally, we may define a bijection on sets of points $P \mapsto P'$, which preserves the Poisson measure, and moreover if we follow our original exploration process on the set P , then that amounts to following the alternative exploration on the set P' . Under this bijection, the left matching found by the original exploration is equal to the left matching found by the alternative exploration,

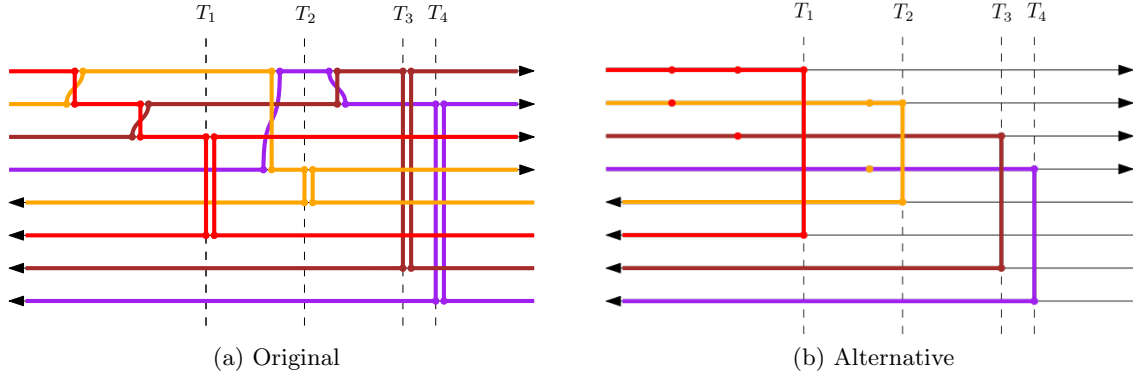


Figure 34

whereas the right matchings of the two explorations differ in a precise way, which is exactly encoded in the process $\bar{\pi}$. As an example, observe that in the previous picture, just before time T_1 , we have that $\bar{\pi}_t = (4\ 3)(4\ 2) = (2\ 3\ 4)$. Observe that $\bar{\pi}_t(4) = 2$, and on the right hand side of the original exploration, 2 is matched to 6. More generally, the rule is as follows. Let $\sigma(\mathcal{Q})$ be the left matching found by the alternative exploration process. Then the right matching $\tau(\mathcal{Q})$ is given by $\sigma(\mathcal{Q})\bar{\pi}_t$. Finally, because the bijection preserves the Poisson measure, when we apply the two explorations to a Poisson process, then they have the same law. We have thus arrived at the following result.

Lemma 3.7. We have that

$$\mathbb{E}[F(\mathcal{Q}(T_n))\mathbb{1}(T_n \leq T)e^{2(n-1)T_1}e^{2(n-2)(T_2-T_1)} \dots e^{2(n-n)(T_n-T_{n-1})}] = \frac{1}{N^n n!} \sum_{\sigma: [n] \rightarrow [n:2n]} [\sigma \sigma \mathbb{E}[\bar{\pi}_{T_n} \mathbb{1}(T_n \leq T)]]$$

Remark 3.8. The factor of $\frac{1}{N^n}$ arises because each turnaround incurs factor of $\frac{1}{N}$, and there are n total turnarounds on the event $T_n \leq T$. The factor $\frac{1}{n!}$ arises because the first turnaround is equally likely to touch any of the n bottom strands, the second turnaround is equally likely to touch any of the $n-1$ remaining bottom strands, etc.

Lemma 3.9. Let $U_1, \dots, U_n \stackrel{i.i.d.}{\sim} \text{Exp}(1)$. We have that

$$\mathbb{E}[\bar{\pi}_{T_n} \mathbb{1}(T_n \leq T)] = n! \mathbb{E}[\exp(-U_n J_n / N) \dots \exp(-U_1 J_1 / N) \mathbb{1}(U_1 + \dots + U_n \leq T)].$$

Proof. Note that the duration $T_k - T_{k-1}$ of the k th exploration process is an exponential random variable with rate $n - k + 1$. We thus have the explicit formula

$$\mathbb{E}[\bar{\pi}_{T_n} \mathbb{1}(T_n \leq T)] = \int_0^T dt_1 \int_{t_1}^T dt_2 \dots \int_{t_{n-1}}^T dt_n (ne^{-nt_1}) ((n-1)e^{-(n-1)(t_2-t_1)}) \dots e^{-(t_n-t_{n-1})} \times f_n(t_1) f_{n-1}(t_2-t_1) \dots f_1(t_n-t_{n-1}).$$

Here, $f_n(t_1)$ is the expected contribution of all same-side swaps in the first exploration era, conditioned on $T_1 = t_1$, $f_{n-1}(t_2-t_1)$ is the expected contribution of all same-side swaps in the second exploration era, conditioned on $T_2 - T_1 = t_2 - t_1$, etc. Conditioned on $T_1 = t_1$, the number of total same-side swaps is $\text{Poi}((n-1)t_1)$, and conditional on the total number of same-side swaps being

equal to k , the expected contribution is uniformly distributed on all possible sequences of k swaps, i.e. $(-J_n/N(n-1))^k$. We thus have the explicit formula

$$\begin{aligned} f_n(t_1) &= e^{-(n-1)t_1} \sum_{k=0}^{\infty} \frac{((n-1)t_1)^k}{k!} \left(\frac{-J_n}{N(n-1)} \right)^k \\ &= e^{-(n-1)t_1} \sum_{k=0}^{\infty} \frac{(-t_1 J_n/N)^k}{k!} = e^{-(n-1)t_1} e^{-t_1 J_n/N}. \end{aligned}$$

More generally, we have the formula

$$f_{n-k}(t_k - t_{k-1}) = e^{-(n-k)(t_k - t_{k-1})} e^{-(t_k - t_{k-1})J_{n-k+1}/N}, \quad k \in [n].$$

Inserting this into our first display, we obtain

$$\begin{aligned} \mathbb{E}[\bar{\pi}_{T_n} \mathbb{1}(T_n \leq T)] &= \\ n! \int_0^T dt_1 \int_{t_1}^T dt_2 \cdots \int_{t_{n-1}}^T dt_n & e^{-t_1} \cdots e^{-(t_n - t_{n-1})} e^{-t_1 J_n/N} e^{-(t_2 - t_1)J_{n-1}/N} \cdots e^{-(t_n - t_{n-1})J_1/N}. \end{aligned}$$

To finish, observe that the right hand side above is precisely the right hand side of the claimed identity. \square

Up to now, we did not need to make any assumption on the size of N . We begin to do so here. Later, in Section 3.2, we will show how to remove these assumptions, but for now we prefer to work in a simplified setting where the main ideas are more transparent.

Lemma 3.10. Suppose that $N \geq n$. Then

$$\lim_{T \rightarrow \infty} \mathbb{E}[\bar{\pi}_{T_n} \mathbb{1}(T_n \leq T)] = n! N^n (N + J_n)^{-1} \cdots (N + J_1)^{-1}.$$

Proof. By Lemma 3.9, we may compute

$$\mathbb{E}[\bar{\pi}_{T_n} \mathbb{1}(T_n \leq T)] = n! \int_0^T du_n \int_0^{T-u_n} du_{n-1} \cdots \int_0^{T-(u_n+\cdots+u_2)} du_1 (e^{-u_n} e^{-u_n J_n/N}) \cdots (e^{-u_1} e^{-u_1 J_1/N}).$$

Since $N \geq n$, we have that $\|J_k/N\| < 1$ for all $k \in [n]$. This implies that the following integral is absolutely convergent (recall Remark 2.19):

$$\int_0^\infty du_n \int_0^\infty du_{n-1} \cdots \int_0^\infty du_1 (e^{-u_n} e^{-u_n J_n/N}) \cdots (e^{-u_1} e^{-u_1 J_1/N}),$$

and moreover, $\lim_{T \rightarrow \infty} \mathbb{E}[\bar{\pi}_{T_n} \mathbb{1}(T_n \leq T)]$ is equal to $n!$ times the above. To finish, simply observe that the above splits into a product of n integrals, where the k th integral may be evaluated:

$$\int_0^\infty du_k e^{-u_k} e^{-u_k J_k/N} = \int_0^\infty du_k e^{-u_k (\text{id} + J_k/N)} = \left(\text{id} + \frac{J_k}{N} \right)^{-1} = N(N + J_k)^{-1}.$$

The desired result follows. \square

Next, we argue why the contribution to the partition function $e^{\binom{2n}{2}T - nT} \mathbb{E}[F(\Sigma(T))]$ coming from the event $\{T_n > T\}$ vanishes in the $T \rightarrow \infty$ limit (that is, as T becomes large, we can assume that all exploration eras have finished by time T). We first show that when the numbers of top strands and bottom strands are mismatched, the expectation vanishes as $T \rightarrow \infty$. This will be needed in the proof of Proposition 3.19 later.

Lemma 3.11. Suppose that $n \geq 2$ and $N \geq 2n$. Suppose that Σ is a Poisson process arising from having $n - 1$ top strands and n bottom strands. Then

$$\sup_{T \geq 0} e^{(2n-1)T - (n-1)T} \|\mathbb{E}[F(\Sigma(T))]\| < \infty.$$

Proof. We proceed by induction. First, consider the base case $n = 2$. In this case, by conditioning on the first time of turnaround, we can explicitly compute

$$e^{2T} \mathbb{E}[F(\Sigma(T))] = e^{2T} \int_0^T 2e^{-2u} X(u) Y Z(u) du + e^{2T} e^{-2T} e^{-T} e^{-T J'_2/N},$$

where $X(u)$ is the expected contribution of all swaps up to time u , and $Z(u)$ is the expected contribution of all points after time u , where both are conditioned on the first turnaround happening at time u . Also, $Y = \frac{1}{2}(\langle 1 \ 2 \rangle + \langle 1 \ 3 \rangle)$ is the expected contribution of the turnaround, since each of the two turnarounds is equally likely. Note that the time of first turnaround is exponential of rate 2, which explains the presence of the $2e^{-2u}$ term. The second term above corresponds to the case where the first turnaround happens after time T .

We have the explicit formulas

$$X(u) = e^{-u} e^{-u J'_2/N}, \quad Z(u) = e^{-2(T-u)},$$

where J'_2 is the Jucys-Murphy element which we view as acting on the bottom two strands (recall Definition 2.17). This formula follows because the number of swaps up to time u is $\text{Poisson}(u)$, and each swap incurs a factor $-J'_2/N$. The fact that $Z(u) = e^{-2(T-u)}$ follows because once a turnaround occurs, we can argue via cancellation as in the proof of Lemma 3.5 that the only points which can occur thereafter are turnarounds between the same two strands. Plugging in the formulas for $X(u), Z(u)$, we may obtain the expression

$$\int_0^T e^{-u(\text{id} + J'_2/N)} du (\langle 1 \ 2 \rangle + \langle 1 \ 3 \rangle) + e^{-T(\text{id} + J'_2/N)}.$$

Since $N \geq 2n$ is sufficiently large, as $T \rightarrow \infty$ the above stays bounded (in fact, it converges to some explicit expression involving $(\text{id} + J'_2/N)^{-1}$, as in the proof of Lemma 3.9). This shows the case $n = 2$.

Now suppose the claim is true for some n . Suppose also that $N \geq 2(n+1)$. We show that the claim is true for $n+1$. As in the base case, by conditioning on the first time of turnaround, we may express (note that $\binom{2n+1}{2} - n = 2n^2$)

$$\begin{aligned} e^{(2n+1)T - nT} \mathbb{E}[F(\Sigma(T))] &= e^{2n^2 T} \int_0^T n(n+1) e^{-n(n+1)u} X_n(u) Y_n Z_n(u) du + \\ &e^{2n^2 T} e^{-n(n+1)T} e^{-\binom{n}{2}T} e^{-T(J_n + \dots + J_1)/N} e^{-\binom{n+1}{2}T} e^{-T(J'_{n+1} + \dots + J'_1)/N}, \end{aligned} \quad (3.3)$$

where $X_n(u)$ is the expected contribution of all swaps up to time u and $Z_n(u)$ is the expected contribution of all points after time u , where both are conditioned on the first turnaround happening at time u . Also, $Y_n = \frac{1}{n(n+1)} \sum_{i \in [n], j \in [n:2n+1]} \langle i \ j \rangle$ is the expectation of the first turnaround. Let J'_1, \dots, J'_{n+1} be the Jucys-Murphy elements which act on the bottom $n+1$ strands, as in Definition 2.17. Similar to before, we may explicitly compute

$$X_n(u) = e^{-\binom{n}{2}u} e^{-\binom{n+1}{2}u} e^{-u(J_n + \dots + J_1)/N} e^{-u(J'_{n+1} + \dots + J'_1)/N},$$

$$Z_n(u) = e^{-2(2n-1)(T-u)} f_n(T-u),$$

where $f_n(T-u)$ is the expected contribution of the points involving the remaining $n-1$ top and n bottom strands after time u , conditioned on the first turnaround happening at time u . Observe that the $e^{-2(2n-1)(T-u)}$ factor in $Z_n(u)$ arises due to similar cancellations as in the proof of Lemma 3.5, which allows us to restrict to the event that after the first turnaround $\langle i j \rangle$, the only points which can involve either of the two matched strands are exactly the turnarounds of the form $\langle i j \rangle$. This means that a total of $2(2n-1)$ rate-1 Poisson processes must have zero points on the interval $[u, T]$.

Plugging in our formulas for $X_n(u)$, $Z_n(u)$, and using the identities $2n^2 - n(n+1) - \binom{n}{2} - \binom{n+1}{2} = -n$, $2n^2 - 2(2n-1) = 2(n-1)^2$, we have that the first term on the right hand side of (3.3) is equal to

$$n(n+1) \int_0^T e^{-nu} e^{-u(J_n + \dots + J_1)/N} e^{-u(J'_{n+1} + \dots + J'_1)/N} Y e^{2(n-1)^2(T-u)} f_n(T-u) du.$$

By the inductive assumption, we have that $\sup_{S \geq 0} e^{2(n-1)^2 S} \|f_n(S)\| < \infty$. Also, since $N \geq 2(n+1)$, we have that $\|(J_n + \dots + J_1)/N\| < n/2$ and $\|(J'_{n+1} + \dots + J'_1)/N\| < n/2$, which implies

$$\int_0^\infty e^{-nu} \|e^{-u(J_n + \dots + J_1)/N} e^{-u(J'_{n+1} + \dots + J'_1)/N}\| du < \infty.$$

Combining the two facts, we obtain that the first term on the right hand side of (3.3) is uniformly bounded in T . The second term in the right hand side of (3.3) may be expressed

$$e^{-nT} e^{-T(J_n + \dots + J_1)/N} e^{-T(J'_{n+1} + \dots + J'_1)/N}.$$

By arguing as before, we may show that this stays bounded as $T \rightarrow \infty$ (in fact, it converges to zero). This completes the proof of the inductive step. \square

Combining this lemma with an inductive argument, we can obtain the following.

Proposition 3.12. Suppose that $N \geq 2n$. We have that

$$\lim_{T \rightarrow \infty} e^{\binom{2n}{2}T - nT} \mathbb{E}[F(\Sigma(T)) \mathbb{1}_{A_T} \mathbb{1}(T_n > T)] = 0.$$

Proof. Fix N . First, when $n = 1$, we have that

$$\mathbb{E}[F(\Sigma(T)) \mathbb{1}_{A_T} \mathbb{1}(T_1 > T)] = e^{-T} \text{id},$$

where id here denotes the identity element of $\mathcal{B}_{n,n}$. The right hand side above clearly goes to zero as $T \rightarrow \infty$. This shows the base case $n = 1$. Now suppose the result is true for some general $n \geq 1$. Suppose also that $N \geq 2(n+1)$. We proceed to show that the $n+1$ case is true. Towards this end, observe that we may decompose

$$\mathbb{1}(T_{n+1} > T) = \mathbb{1}(T_1 > T) + \mathbb{1}(T_1 \leq T < T_{n+1}).$$

We split into the two cases indicated above. In the first case, we condition on the exploration at time T :

$$e^{\binom{2(n+1)}{2}T - (n+1)T} \mathbb{E}[\mathbb{E}[F(\Sigma(T)) \mathbb{1}_{A_T} \mid \mathcal{F}_T] \mathbb{1}(T_1 > T)]].$$

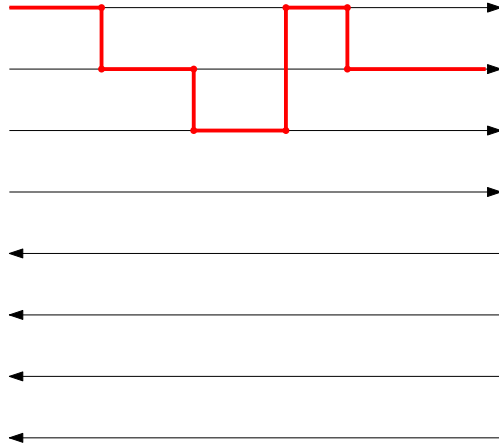


Figure 35

To help visualize, imagine we have the situation in Figure 35, where we explore the first strand until time T , and we have not yet seen a turnaround.

Conditioned on this picture, the expectation of the diagram can be computed as follows. First, since we have already explored one strand, the remaining points effectively form a Poisson process corresponding to n top strands and $n + 1$ bottom strands. Call this modified process $\bar{\Sigma}(T)$. We visualize this in Figure 36, where the top-most strand in the left diagram is dashed, to signify that there are no points touching this strand.

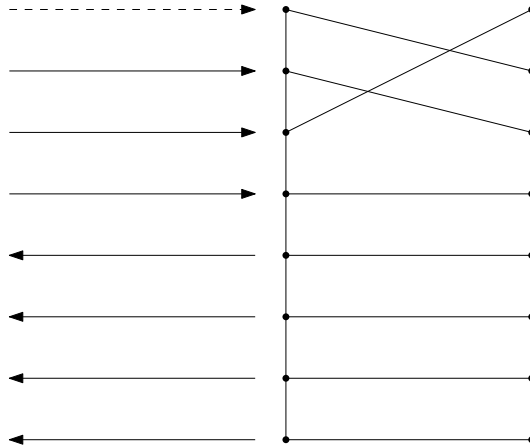


Figure 36: Left: $F(\bar{\Sigma}(T))$. Right: $F(\mathcal{Q}(T))$.

Having computed the expectation of the modified diagram in the left of Figure 36, to obtain the conditional expectation of $F(\Sigma(T))$ we simply need to multiply by the right diagram in the figure, which captures the effect of all swaps seen by our exploration up to time T . This discussion corresponds to the following identity for the conditional expectation:

$$\mathbb{E}[F(\Sigma(T))\mathbb{1}_{A_T} \mid \mathcal{F}_T] = \mathbb{E}[F(\bar{\Sigma}(T))]F(\mathcal{Q}_T).$$

We may then compute

$$\begin{aligned}
& e^{\binom{2(n+1)}{2}T-(n+1)T} \mathbb{E}[\mathbb{E}[F(\Sigma(T)) \mathbb{1}_{A_T} \mid \mathcal{F}_T] \mathbb{1}(T_1 > T)] \\
&= e^{\binom{2(n+1)}{2}T-(n+1)T} \mathbb{E}[F(\bar{\Sigma}(T))] \mathbb{E}[F(Q_T) \mathbb{1}(T_1 > T)] \\
&= e^{\binom{2(n+1)}{2}T-(n+1)T} \mathbb{E}[F(\bar{\Sigma}(T))] e^{-(n+1)T} e^{-nT} e^{-T J_{n+1}/N} \\
&= (e^{\binom{2(n+1)}{2}T-nT} \mathbb{E}[F(\bar{\Sigma}(T))]) e^{-T} e^{-T J_{n+1}/N}.
\end{aligned}$$

As $T \rightarrow \infty$, the right hand side above goes to zero, since by Lemma 3.11 (and our assumption that $N \geq 2(n+1)$), the term in the parentheses above is $O(1)$, and since $N \geq n+1$, we have that $\|J_{n+1}/N\| < 1$, so that $e^{-T} e^{-T J_{n+1}/N} \rightarrow 0$. This shows the inductive step in the first case.

Next, we consider the case corresponding to $\mathbb{1}(T_1 \leq T < T_{n+1})$. We condition on the exploration at time T_1 . Consider the diagram in Figure 37 which corresponds to $n+1 = 4$.

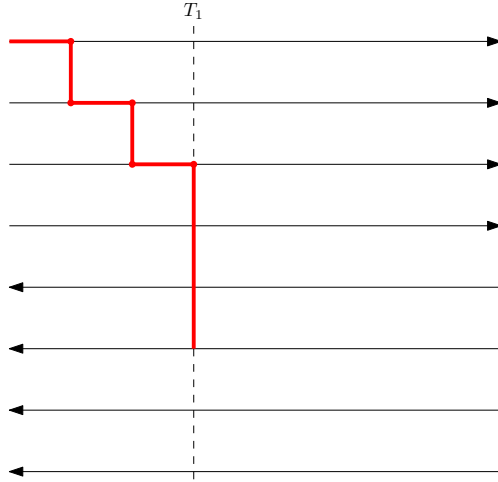


Figure 37

On the event that $T_1 \leq T < T_{n+1}$, the portion of the diagram to the right of T_1 can be treated as having n top strands and n bottom strands, since we are on the event A_T . By arguing similarly to the previous case, i.e. by splitting our strand diagrams into the portion before T_1 and the portion after T_1 , we may compute the conditional expectation:

$$\mathbb{E}[F(\Sigma(T)) \mathbb{1}_{A_T} \mathbb{1}(T_1 \leq T < T_{n+1}) \mid \mathcal{F}_{T_1} = u] = \mathbb{E}[F(\bar{\Sigma}(u))] e^{-4n(T-u)} F(Q_{T_1}) f_n(T-u),$$

where $\bar{\Sigma}$ is a Poisson process corresponding to having n top strands and $n+1$ bottom strands, and $f_n(T-u)$ is the expectation of the remaining n top and n bottom strands after time u , on the event that not all n exploration eras end before time is up. Observe that by our inductive assumption, we have that for any $u \geq 0$,

$$\lim_{T \rightarrow \infty} e^{\binom{2n}{2}(T-u)-n(T-u)} f_n(T-u) = 0. \tag{3.4}$$

Since T_1 is an exponential random variable of rate $n+1$, we may compute the expectation:

$$e^{\binom{2(n+1)}{2}T-(n+1)T} \mathbb{E}[F(\Sigma(T)) \mathbb{1}_{A_T} \mathbb{1}(T_1 \leq T < T_{n+1})] =$$

$$e^{\binom{2(n+1)}{2}T-(n+1)T} \int_0^T du (n+1)e^{-(n+1)u} (\mathbb{E}[F(\bar{\Sigma}(u))]) (e^{-nu} e^{-uJ_{n+1}/N}) Y(e^{-4n(T-u)} f_n(T-u))$$

Here, the term $e^{-nu} e^{-uJ_{n+1}/N}$ arises from taking the expectation of all swaps in the first exploration era (i.e. $F(\mathcal{Q}(T_1))$), conditioned on $T_1 = u$, and Y is the expectation of the first turnaround. Since

$$\begin{aligned} \binom{2(n+1)}{2} - (n+1) &= 2n^2 + 2n \\ \binom{2(n+1)}{2} - (n+1) - 4n &= \binom{2n}{2} - n, \end{aligned}$$

we have that the above is further equal to

$$(n+1) \int_0^T du (e^{2n^2u} \mathbb{E}[F(\bar{\Sigma}(u))]) (e^{-u} e^{-uJ_{n+1}/N}) Y e^{-4n(T-u)} f_n(T-u).$$

Now since $N \geq 2n$, by Lemma 3.11, we have that $e^{2n^2u} \mathbb{E}[F(\bar{\Sigma}(u))] = O(1)$ and $e^{-u} e^{-uJ_{n+1}/N}$ is integrable. Combining this with (3.4) and dominated convergence, we finally obtain

$$\lim_{T \rightarrow \infty} e^{\binom{2(n+1)}{2}T-(n+1)T} \mathbb{E}[F(\Sigma(T)) \mathbb{1}_{A_T} \mathbb{1}(T_1 \leq T < T_{n+1})] = 0.$$

This completes the proof of the inductive step, and thus the desired result now follows. \square

We can now finally take the $T \rightarrow \infty$ limit.

Proposition 3.13. Suppose that $N \geq 2n$. Then as $T \rightarrow \infty$, we have that

$$\lim_{T \rightarrow \infty} e^{\binom{2n}{2}T-nT} \mathbb{E}[F(\Sigma(T))] = \sum_{\sigma, \tau: [n] \rightarrow [n:2n]} \text{Wg}_N(\sigma\tau^{-1})[\sigma \tau].$$

Proof. By combining Lemma 3.5, Proposition 3.6, Lemmas 3.7 and 3.10, and Proposition 3.12, we obtain

$$\begin{aligned} \lim_{T \rightarrow \infty} e^{\binom{2n}{2}T-nT} \mathbb{E}[F(\Sigma(T))] &= \sum_{\sigma: [n] \rightarrow [n:2n]} [\sigma \sigma \text{Wg}_N] \\ &= \sum_{\sigma: [n] \rightarrow [n:2n]} \sum_{\pi \in \mathbb{S}_n} [\sigma \sigma \pi] \text{Wg}_N(\pi) \\ &= \sum_{\sigma, \tau: [n] \rightarrow [n:2n]} [\sigma \tau] \text{Wg}_N(\sigma^{-1}\tau). \end{aligned}$$

To finish, recall that $\text{Wg}_N(\sigma^{-1}\tau) = \text{Wg}_N(\sigma\tau^{-1})$, because Wg_N is a class function. \square

We can now prove Theorem 2.5 in the case $N \geq 2n$.

Proof of Theorem 2.5 when $N \geq n$. Recall from (3.1) that

$$e^{\binom{2n}{2}T-nT} \mathbb{E}[F(\mathcal{P}(T))] = \sum_{\pi} w_T(\pi) \pi.$$

By Proposition 3.13, we obtain

$$\lim_{T \rightarrow \infty} w_T(\pi) = \mathbb{1}(\pi = [\sigma \tau] \text{ for some } \sigma, \tau : [n] \rightarrow [n : 2n]) \text{Wg}_N(\sigma\tau^{-1}).$$

Since $w_T(\pi_1, \dots, \pi_L) = w_T(\pi_1) \cdots w_T(\pi_L)$, the desired result now follows. \square

3.2 Extension to general values of N

Recall that in the proof of Proposition 3.13, we deduced the existence of $\lim_{T \rightarrow \infty} e^{\binom{2n}{2}T - nT} \mathbb{E}[F(\Sigma(T))]$ from the existence of $\lim_{T \rightarrow \infty} \mathbb{E}[\bar{\pi}_{T_n} \mathbb{1}(T_n \leq T)] \in \mathbb{C}[\mathbb{S}_n]$. However, when $N \leq n$, the trouble is that the latter limit no longer exists. Thus to prove Theorem 2.5 in the case where N is small, we need some alternative argument which does not rely on convergence in the group algebra. Indeed, we will show that although $\lim_{T \rightarrow \infty} \mathbb{E}[\bar{\pi}_{T_n} \mathbb{1}(T_n \leq T)]$ does not necessarily exist in $\mathbb{C}[\mathbb{S}_n]$, once we apply the representation ρ_+ (Definition 2.21), the limit *does exist*. Moreover, the limit $\lim_{T \rightarrow \infty} \rho_+(\mathbb{E}[\bar{\pi}_{T_n} \mathbb{1}(T_n \leq T)])$ already contains enough information in order to compute expectations of traces of words. Once we have built up enough background, the actual proof of Theorem 2.5 for general values of N will be a small variation of the proof for large N , as the major technical steps were already covered in Section 3 (and any additional background covered in Section 2.2).

Towards this end, it will be useful to recall why expectations of traces of words may be reduced to weighted sums over the Brauer algebra, i.e. why Lemma 2.3 is true. Let Γ be a word on letters $\{\lambda_1, \dots, \lambda_L\}$. We may assume $\Gamma = \lambda_{c(1)}^{\varepsilon(1)} \cdots \lambda_{c(n)}^{\varepsilon(n)}$, where $\varepsilon : [n] \rightarrow \{\pm 1\}$ and $c : [n] \rightarrow [L]$. Let $M = (M_1, \dots, M_L)$ be a given collection of $N \times N$ Unitary matrices. The computation of $\text{Tr}(M(\Gamma)) = \text{Tr}(M_{c(1)}^{\varepsilon(1)} \cdots M_{c(n)}^{\varepsilon(n)})$ may be visualized in terms of the strand diagram as in Figure 38, where we consider the concrete case $\Gamma = \lambda_1^2 \lambda_2 \lambda_1^{-2} \lambda_2^{-1}$.

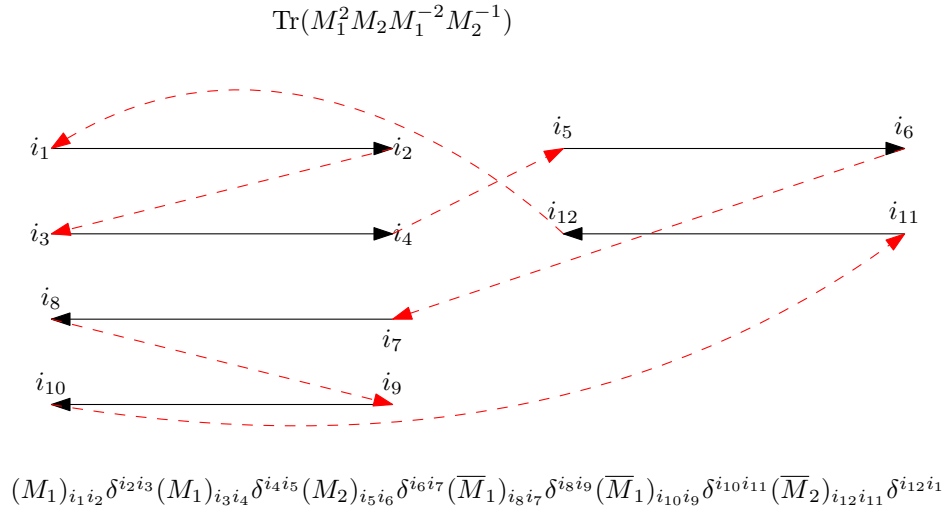


Figure 38

In Figure 38, we can imagine we are traversing the strand diagram. Every black strand contributes a matrix element, and every dashed red strand enforces an identification of indices. In the end we sum over all indices which appear. Of course, we could have written the trace more succinctly as

$$\text{Tr}(M_1^2 M_2 M_1^{-2} M_2^{-1}) = (M_1)_{i_1 i_2} (M_1)_{i_2 i_3} (M_2)_{i_3 i_4} (\overline{M}_1)_{i_5 i_4} (\overline{M}_1)_{i_6 i_5} (\overline{M}_2)_{i_1 i_6},$$

but we prefer to keep the δ functions because they correspond to the dashed red lines. We now want to give an expression as above for general words and strand diagrams. Given the strand diagram of a word Γ , note that the diagram has a single component, with a unique ordering of its vertices x_1, \dots, x_V up to cyclic equivalence. This ordering is such that the edges alternate between black strands and dashed red lines. Let $B(\Gamma)$ be the set of black strands, and $R(\Gamma)$ be the set of dashed

red lines. Further split $B(\Gamma) = B_+(\Gamma) \cup B_-(\Gamma)$, where $B_+(\Gamma), B_-(\Gamma)$ are the set of positive (i.e. right) and negative (i.e. left)-oriented black strands. In the previous example,

$$B_+(\Gamma) = \{(x_1, x_2), (x_3, x_4), (x_5, x_6)\}, \quad B_-(\Gamma) = \{(x_7, x_8), (x_9, x_{10}), (x_{11}, x_{12})\}, \\ R(\Gamma) = \{(x_2, x_3), (x_4, x_5), (x_6, x_7), (x_8, x_9), (x_{10}, x_{11})\}.$$

Given a collection of indices $i = (i_1, \dots, i_V) \in [N]^V$, and an edge $e = (x_j, x_{j+1})$, let $i_e = (i_j, i_{j+1})$, $i_{-e} = (i_{j+1}, i_j)$. Let $r(e) \in [L]$ be the index of the letter that e corresponds to. Then the general formula for $\text{Tr}(M(\Gamma))$ in terms of the strand diagram is:

$$\text{Tr}(M(\Gamma)) = \prod_{e \in B_+(\Gamma)} (M_{r(e)})_{i_e} \prod_{e \in B_-(\Gamma)} (\overline{M}_{r(e)})_{i_{-e}} \prod_{e \in R(\Gamma)} \delta^{i_e},$$

where we implicitly sum over $i = (i_1, \dots, i_V) \in [N]^V$. Now the point is as follows. If M_1, \dots, M_L are independent $U(N)$ -valued Brownian motions, then upon taking expectations of the above, we may obtain that $\mathbb{E}[\text{Tr}(M(\Gamma))]$ is equal to a weighted sum of diagrams as follows.

First, for $\ell \in [L]$, let $B_+(\Gamma, \ell), B_-(\Gamma, \ell)$ be the sets of positively and negatively oriented edges corresponding to the letter λ_ℓ . Since the M_1, \dots, M_L are independent, we have that

$$\mathbb{E}[\text{Tr}(M(\Gamma))] = \prod_{\ell \in [L]} \mathbb{E} \left[\prod_{e \in B_+(\Gamma, \ell)} (M_{r(e)})_{i_e} \prod_{e \in B_-(\Gamma, \ell)} (\overline{M}_{r(e)})_{i_{-e}} \right] \prod_{e \in R(\Gamma)} \delta^{i_e}.$$

We recall the following lemma from [PPSY23] (see also (2.1)) which gives a formula for each of the expectations appearing in the right hand side above.

Proposition 3.14. Let $i_1, \dots, i_n, i'_1, \dots, i'_n, j_1, \dots, j_n, j'_1, \dots, j'_n \in [N]$. We have that

$$\mathbb{E}[(B_T)_{i_1 j_1} \cdots (B_T)_{i_n j_n} (\overline{B}_T)_{i'_1 j'_1} \cdots (\overline{B}_T)_{i'_n j'_n}] = \sum_{\pi} w_T(\pi) \mathbb{1}(\text{indices match with } \pi).$$

Here, the sum is over walled pairings $\pi \in \mathcal{M}(n, n)$ (recall Definition 2.12).

Using this, we may write

$$\mathbb{E}[\text{Tr}(M(\Gamma))] = \sum_{\pi = (\pi_1, \dots, \pi_L)} w_T(\pi_1) \cdots w_T(\pi_L) \prod_{\ell \in [L]} \prod_{\{a, b\} \in \pi_\ell} \delta^{i_a i_b} \prod_{e \in R(\Gamma)} \delta^{i_e}.$$

Now, observe that

$$\prod_{\ell \in [L]} \prod_{\{a, b\} \in \pi_\ell} \delta^{i_a i_b} \prod_{e \in R(\Gamma)} \delta^{i_e} = N^{\#\text{comp}(\Gamma, \pi)},$$

where recall $\#\text{comp}(\Gamma, \pi)$ is the number of components obtained by deleting all black strands but including all interior matchings specified by π_1, \dots, π_L . For instance, in our previous example, suppose our matchings were as in Figure 39. Since each edge in Figure 39 (be it red or black) imposes a constraint on the indices, the total number of free summation indices is exactly equal to the number of connected components in the above diagram. Each free summation index may take one of N values, whence the term $N^{\#\text{comp}(\Gamma, \pi)}$. Lemma 2.3 follows directly from these considerations⁷.

⁷In our discussion, we have only considered a single word, but everything extends directly to the case of multiple words.

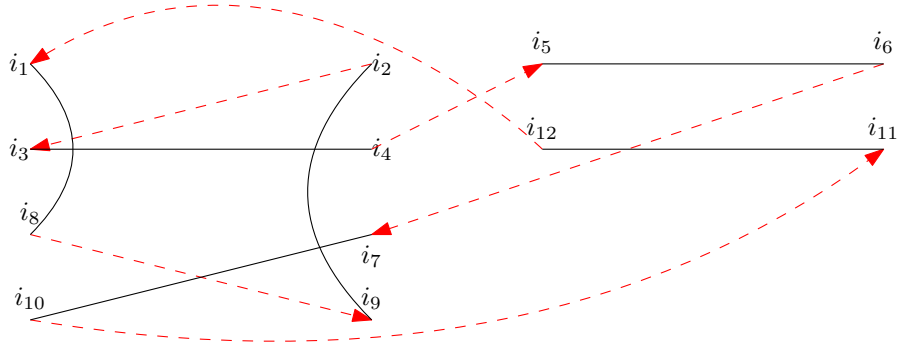


Figure 39

Now recall from Definition 2.21 that the matrix elements of the representation $\rho_+(\pi)$ are exactly given by

$$(\rho_+(\pi))_{i \sqcup i', j \sqcup j'} = \mathbb{1}(\text{indices match with } \pi).$$

Here, $i \sqcup i'$ denotes the length- $2n$ vector of indices given by concatenation: $(i_1, \dots, i_n, i'_1, \dots, i'_n)$, and similarly for $j \sqcup j'$. Combining this with the previous discussion, we have the following result. First, for some notation, let $\mathbf{i}_\ell, \mathbf{j}_\ell$ respectively collect all left and right indices which appear in the strand diagram corresponding to λ_ℓ . For the example in Figure 39, we have that $\mathbf{i}_1 = (i_1, i_3, i_8, i_7)$, $\mathbf{j}_1 = (i_2, i_4, i_7, i_9)$, $\mathbf{i}_2 = (i_5, i_{12})$, $\mathbf{j}_2 = (i_6, i_{11})$.

Lemma 3.15. Let Γ be a balanced collection of words on letters $\{\lambda_1, \dots, \lambda_L\}$. Let $\pi = (\pi_\ell, \ell \in [L])$. Then

$$\prod_{\ell \in [L]} \rho_+(\pi_\ell)_{\mathbf{i}_\ell \mathbf{j}_\ell} \prod_{e \in R(\Gamma)} \delta^{i_e} = N^{\#\text{comp}(\Gamma, \pi)}.$$

Using this lemma and the previous discussion, we could have written $\mathbb{E}[\text{Tr}(M(\Gamma))]$ in terms of $\rho_+(\pi_1), \dots, \rho_+(\pi_L)$, as follows.

Lemma 3.16. Let $\Gamma = (\Gamma_1, \dots, \Gamma_n)$ be a balanced collection of words with letters $\{\lambda_1, \dots, \lambda_L\}$. We have that

$$\mathbb{E}[\text{Tr}(B_T(\Gamma))] = \left(\sum_{\pi_1 \in \mathcal{B}_{n_1, n_1}} w_T(\pi_1) \rho_+(\pi_1) \right)_{\mathbf{i}_1 \mathbf{j}_1} \cdots \left(\sum_{\pi_L \in \mathcal{B}_{n_L, n_L}} w_T(\pi_L) \rho_+(\pi_L) \right)_{\mathbf{i}_L \mathbf{j}_L} \prod_{e \in R(\Gamma)} \delta^{i_e},$$

As mentioned at the beginning of this subsection, we have rewritten expectations of traces of words of Unitary Brownian motion in terms of some function (namely, ρ_+) of weighted sums over the Brauer algebra. The point now is that $\lim_{T \rightarrow \infty} \rho_+(\mathbb{E}[\bar{\pi}_{T_n} \mathbb{1}(T_n \leq T)])$ exists for all N . Once we show this, the rest of the proof of Theorem 2.5 in the case of general N is exactly the same.

Lemma 3.17 (Analog of Lemma 3.10). We have that

$$\lim_{T \rightarrow \infty} \rho_+(\mathbb{E}[\bar{\pi}_{T_n} \mathbb{1}(T_n \leq T)]) = n! N^n \rho_+(\text{Wg}_N).$$

Proof. By Lemma 3.9, we may compute

$$\begin{aligned} \rho_+ (\mathbb{E}[\bar{\pi}_{T_n} \mathbb{1}(T_n \leq T)]) &= \\ n! \int_0^T du_n \int_0^{T-u_1} du_{n-1} \cdots \int_0^{T-(u_1+\cdots+u_{n-1})} du_1 & e^{-u_n \rho_+(\text{id}+J_n/N)} \cdots e^{-u_1 \rho_+(\text{id}+J_1/N)}. \end{aligned}$$

By Lemma 2.27, for all $k \in [n]$, all eigenvalues of $\rho_+(J_k)$ are at least $-N+1$, and thus all eigenvalues of $\rho_+(\text{id}+J_k/N)$ are at least $1/N$, and in particular all eigenvalues are strictly positive. Thus as we send $T \rightarrow \infty$ the above converges to (applying Lemma 2.28 in the final identity)

$$\begin{aligned} n! \int_0^\infty e^{-u_n \rho_+(\text{id}+J_n/N)} du_n \cdots \int_0^\infty e^{-u_1 \rho_+(\text{id}+J_1/N)} du_1 &= n! \rho_+(\text{id}+J_n/N)^{-1} \cdots \rho_+(\text{id}+J_1/N)^{-1} \\ &= n! N^n \rho_+(N+J_n)^{-1} \cdots \rho_+(N+J_1)^{-1} \\ &= n! N^n \rho_+(\text{Wg}_N), \end{aligned}$$

as desired. \square

We also have the following analogs of Lemma 3.11 and Proposition 3.12.

Lemma 3.18 (Analog of Lemma 3.11). Suppose that Σ is a Poisson process arising from having $n-1$ top strands and n bottom strands. Then

$$\sup_{T \geq 0} e^{(2n-1)T - (n-1)T} \|\rho_+(\mathbb{E}[F(\Sigma(T))])\| < \infty.$$

Proof. In the proof of Lemma 3.11, the condition on N was needed to show that

$$\begin{aligned} \int_0^\infty e^{-nu} \|e^{-u(J_n+\cdots+J_1)/N} e^{-u(J'_{n+1}+\cdots+J'_1)/N}\| du &< \infty, \\ \sup_{T \geq 0} e^{-nT} \|e^{-T(J_n+\cdots+J_1)/N} e^{-T(J'_{n+1}+\cdots+J'_1)/N}\| &< \infty. \end{aligned}$$

When we apply ρ_+ , we instead need to show that

$$\begin{aligned} \int_0^\infty e^{-nu} \|e^{-u\rho_+(J_n+\cdots+J_1)/N} e^{-u\rho_+(J'_{n+1}+\cdots+J'_1)/N}\| du &< \infty, \\ \sup_{T \geq 0} e^{-nT} \|e^{-T\rho_+(J_n+\cdots+J_1)/N} e^{-T\rho_+(J'_{n+1}+\cdots+J'_1)/N}\| &< \infty. \end{aligned}$$

These claims both follow from Corollary 2.30, which gives that the eigenvalues of $\frac{1}{N}\rho_+(J_n+\cdots+J_1) + \frac{1}{N}\rho_+(J'_{n+1}+\cdots+J'_1)$ are all strictly greater than $-n$. \square

Proposition 3.19 (Analog of Proposition 3.12). We have that

$$\lim_{T \rightarrow \infty} e^{(2n)T - nT} \rho_+(\mathbb{E}[F(\Sigma(T)) \mathbb{1}_{A_T} \mathbb{1}(T_n > T)]) = 0.$$

Proof. The points in the proof of Proposition 3.12 where we needed N to be large were in the application of Lemma 3.11 and in arguing that $e^{-u} e^{-uJ_{n+1}/N}$ is integrable. For the present proposition, we may apply Lemma 3.18 which does not require N to be large. The fact that $e^{-u} e^{-u\rho_+(J_{n+1})/N}$ is integrable follows from Lemma 2.27, as noted in the proof of Lemma 3.17. \square

Proposition 3.20 (Analog of Proposition 3.13). We have that

$$\lim_{T \rightarrow \infty} e^{\binom{2n}{2} T - nT} \mathbb{E}[\rho_+(F(\Sigma(T)))] = \sum_{\sigma, \tau: [n] \rightarrow [n:2n]} \rho_+([\sigma \ \tau]) \text{Wg}_N(\sigma \tau^{-1}).$$

Proof. We argue exactly as in the proof of Proposition 3.13, except we replace the applications of Lemma 3.10 and Proposition 3.12 with Lemma 3.17 and Proposition 3.19. \square

Proof of Theorem 2.5. Combining Lemma 3.16 and Proposition 3.20, we have that

$$\lim_{T \rightarrow \infty} \mathbb{E}[\text{Tr}(B_T(\mathbf{\Gamma}))] = \prod_{\ell \in L} \left(\sum_{\sigma_\ell, \tau_\ell: [n] \rightarrow [n:2n]} \rho_+([\sigma_\ell \ \tau_\ell]) \text{Wg}_N(\sigma_\ell \tau_\ell^{-1}) \right) \prod_{i \in \mathbf{j} \ell} \delta^{i_e}.$$

By Lemma 3.15, the right hand side above may be written

$$\sum_{\pi = ([\sigma_\ell \ \tau_\ell], \ell \in [L])} \left(\prod_{\ell \in L} \text{Wg}_N(\sigma_\ell \tau_\ell^{-1}) \right) N^{\#\text{comp}(\Gamma, \pi)},$$

as desired. \square

4 Schwinger-Dyson/Master loop equation

In this section, we utilize the Process process formulation described in Section 2.1 and analyzed in Section 3 to prove a recursion relation (Proposition 4.2) on expectations of products of traces of words in independent Haar-distributed Unitary matrices. We then apply this recursion to deduce the Schwinger-Dyson/Master loop equations (Theorem 4.6) for Wilson loop expectations.

First, we describe the terms which will appear in our recursion. Let $\mathbf{\Gamma} = (\Gamma_1, \dots, \Gamma_k)$ be a collection of words on $\{\lambda_1, \dots, \lambda_L\}$. Our collections of words are unordered, so that $(\Gamma_1, \dots, \Gamma_k) = (\Gamma_k, \dots, \Gamma_1)$. We will often refer to the edge at the (i, j) location of $\mathbf{\Gamma}$, which is meant to be the j th letter of Γ_i .

Definition 4.1 (Splittings and mergers). Let $\mathbf{\Gamma} = (\Gamma_1, \dots, \Gamma_k)$ be a collection of words on $\{\lambda_1, \dots, \lambda_L\}$. Let (i, j) be a location of $\mathbf{\Gamma}$. Define the set of positive and negative splittings $\mathbb{S}_+((i, j), \mathbf{\Gamma})$ and $\mathbb{S}_-((i, j), \mathbf{\Gamma})$, as well as the set of positive and negative mergers $\mathbb{M}_+((i, j), \mathbf{\Gamma})$ and $\mathbb{M}_-((i, j), \mathbf{\Gamma})$, as follows.

The set of positive splittings $\mathbb{S}_+((i, j), \mathbf{\Gamma})$ is the set of collections of words $\mathbf{\Gamma}'$ obtained by splitting Γ_i into two words as follows. Let (i, k) , $k \neq j$ be another location of Γ_i which has the same letter as at location (i, j) . Suppose Γ_i is of the form $A\lambda B\lambda C$, where λ is the letter at locations (i, j) and (i, k) . We may split Γ_i into $\Gamma_{i,1} = A\lambda C$ and $\Gamma_{i,2} = B\lambda$. The set $\mathbb{S}_+((i, j), \mathbf{\Gamma})$ is the set of all collections of words that may be obtained this way.

Similarly, the set of negative splittings $\mathbb{S}_-((i, j), \mathbf{\Gamma})$ is the set of collections of words $\mathbf{\Gamma}'$ obtained by splitting Γ_i into two words as follows. Let (i, k) , $k \neq j$ be a location of Γ_i which has inverse of the letter at location (i, j) . We may write $\Gamma_i = A\lambda B\lambda^{-1}C$ or $\Gamma_i = A\lambda^{-1}B\lambda C$. In either case, we split Γ_i into $\Gamma_{i,1} = AC$ and $\Gamma_{i,2} = B$. The set $\mathbb{S}_-((i, j), \mathbf{\Gamma})$ is the set of all collections of words that may be obtained this way.

The set of positive mergers $\mathbb{M}_+((i, j), \mathbf{\Gamma})$ is the set of collections of words $\mathbf{\Gamma}'$ obtained by merging Γ_i with some Γ_ℓ , $\ell \neq i$, as follows. Let (ℓ, m) be a location which has the same letter as at location (i, j) . Suppose $\Gamma_i = A\lambda B$ and $\Gamma_\ell = C\lambda D$. Then Γ_i, Γ_ℓ are replaced by their positive merger $A\lambda DC\lambda B$. The set $\mathbb{M}_+((i, j), \mathbf{\Gamma})$ is the set of all collections of words that may be obtained this way.

Similarly, the set of negative mergers $\mathbb{M}_-((i, j), \mathbf{\Gamma})$ is the set of collections of collections of words $\mathbf{\Gamma}'$ obtained by merging Γ_i with some Γ_ℓ , $\ell \neq i$, as follows. Let (ℓ, m) be a location which has the inverse of the letter at location (i, j) . Suppose $\Gamma_i = A\lambda B$ and $\Gamma_\ell = C\lambda^{-1}D$. Then Γ_i, Γ_ℓ are replaced by their negative merger $ADC B$. The set $\mathbb{M}_-((i, j), \mathbf{\Gamma})$ is the set of all collections of words that may be obtained this way.

In the following, let $\text{tr}(U(\mathbf{\Gamma})) = \prod_{i \in [k]} \text{tr}(U(\Gamma_i))$, where $U(\Gamma_i)$ is obtained by substituting into Γ_i an independent Haar-distributed Unitary matrix for each letter $\{\lambda_1, \dots, \lambda_L\}$. Note that in contrast to previous results, we are using the normalized trace here, which we find to be more natural for stating the recursion.

Proposition 4.2 (Word recursion). Let $\mathbf{\Gamma} = (\Gamma_1, \dots, \Gamma_k)$ be a collection of words on $\{\lambda_1, \dots, \lambda_L\}$. For any location (i, j) of $\mathbf{\Gamma}$, we have that

$$\begin{aligned} \mathbb{E}[\text{tr}(U(\mathbf{\Gamma}))] &= - \sum_{\mathbf{\Gamma}' \in \mathbb{S}_+((i, j), \mathbf{\Gamma})} \mathbb{E}[\text{tr}(U(\mathbf{\Gamma}'))] + \sum_{\mathbf{\Gamma}' \in \mathbb{S}_-((i, j), \mathbf{\Gamma})} \mathbb{E}[\text{tr}(U(\mathbf{\Gamma}'))] \\ &\quad - \frac{1}{N^2} \sum_{\mathbf{\Gamma}' \in \mathbb{M}_+((i, j), \mathbf{\Gamma})} \mathbb{E}[\text{tr}(U(\mathbf{\Gamma}'))] + \frac{1}{N^2} \sum_{\mathbf{\Gamma}' \in \mathbb{M}_-((i, j), \mathbf{\Gamma})} \mathbb{E}[\text{tr}(U(\mathbf{\Gamma}'))]. \end{aligned}$$

Proof. Without loss of generality, take $(i, j) = (1, 1)$, so that we look at the first letter of Γ_1 . Let $\lambda \in \{\lambda_1, \dots, \lambda_L\}$ be this letter. Recall from Corollary 2.7 that $\mathbb{E}[\text{Tr}(U(\mathbf{\Gamma}))]$ is equal to a sum over pairs of matchings of strand diagrams, weighted by the Weingarten function applied to each pair, as well as N raised to the number of components of the resulting strand diagram. For each strand diagram corresponding to a letter $\lambda' \neq \lambda$, fix a pair of matchings $\sigma_{\lambda'}, \tau_{\lambda'}$. We apply our strand-by-strand Poisson process exploration from Section 3 to the strand diagram corresponding to λ , but stop at the first time we see any point in the first exploration era. This will result in the claimed recursion.

Let n be the number of times that λ appears in $\mathbf{\Gamma}$, so that the portion of the strand diagram corresponding to λ has n right-directed strands and n left-directed strands. Let all notation be as in Section 3. Now, suppose that $N \geq 2n$. (As was the case for the proof of Theorem 2.5, the case of general N will follow by small modifications from the case of large N , by applying the representation ρ_+ and using the various general N results proven in Section 3.2.) By combining Lemma 3.5 and Propositions 3.6, 3.12, and Proposition 3.13, we have that

$$\begin{aligned} \sum_{\sigma, \tau: [n] \rightarrow [n:2n]} \text{Wg}_N(\sigma\tau^{-1})[\sigma \ \tau] &= \\ \lim_{T \rightarrow \infty} \mathbb{E}[F(\mathcal{Q}(T_n)) \mathbb{1}(T_n \leq T) e^{2(n-1)T_1} e^{2(n-2)(T_2-T_1)} \dots e^{2(n-n)(T_n-T_{n-1})}]. \end{aligned}$$

We will derive a recursion for the left hand side above by looking at the first point seen by our exploration process \mathcal{Q} . For brevity, let

$$f_n(T) := \mathbb{E}[F(\mathcal{Q}(T_n)) \mathbb{1}(T_n \leq T) e^{2(n-1)T_1} e^{2(n-2)(T_2-T_1)} \dots e^{2(n-n)(T_n-T_{n-1})}].$$

Let U_1 be the time of the first swap seen by \mathcal{Q} . Note that U_1 is an exponential random variable with rate $2n-1$ (since there are $n-1$ possible same-side swaps and n possible opposite-side swaps). By conditioning on this time, we may obtain a recursion like

$$f_n(T) = -\frac{1}{N} \sum_{j=1}^{n-1} \int_0^T e^{-(2n-1)u} (n \ j) e^{2(n-1)u} f_n(T-u) du +$$

$$\frac{1}{N} \sum_{j=n+1}^{2n} \int_0^T e^{-(2n-1)u} \langle n \ j \rangle e^{2(n-1)u} f_{n-1}(j, T-u) du.$$

Note the factor $e^{2(n-1)u}$ comes from the $e^{2(n-1)T_1}$ term. The first sum corresponds to the case that we first see a same-side swap, and the second sum corresponds to the case that we first see an opposite-side swap. Here, $f_{n-1}(j, T-u)$ denotes the corresponding expectation where we take out the top and bottom strand which are matched by the opposite-side swap $\langle n \ j \rangle$ and continue the exploration on the remaining strands. The point now is that when we send $T \rightarrow \infty$, we obtain the recursion:

$$\begin{aligned} \sum_{\sigma, \tau: [n] \rightarrow [n:2n]} \text{Wg}_N(\sigma\tau^{-1})[\sigma \ \tau] &= -\frac{1}{N} \sum_{j=1}^{n-1} \sum_{\sigma, \tau: [n] \rightarrow [n:2n]} \text{Wg}_N(\sigma\tau^{-1})(n \ j)[\sigma \ \tau] + \\ &\quad \frac{1}{N} \sum_{j=n+1}^{2n} \sum_{\substack{\sigma, \tau: [n] \rightarrow [n:2n] \\ \sigma(n)=\tau(n)=j}} \text{Wg}_N(\sigma\tau^{-1})[\sigma \ \tau]. \end{aligned}$$

(In the case of general N the above is true after applying ρ_+ to both sides.) We now claim that by inserting this equation into the sum over pairs of matchings in the portion of the strand diagram corresponding to λ (and then applying Corollary 2.7 to compute the expectation), we obtain the claimed recursion. To help visualize why, note that before having explored the Poisson process, the strand diagram looks as in Figure 40.

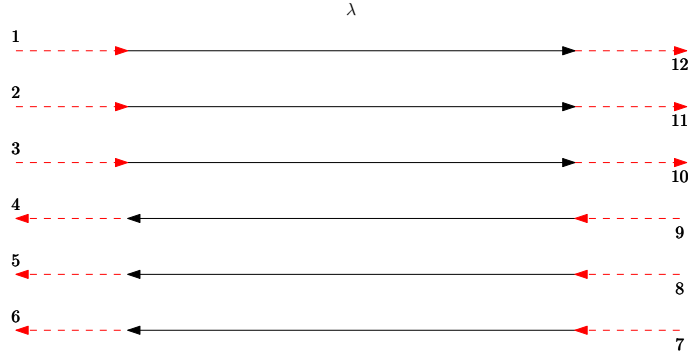


Figure 40

Here, the top strand corresponds to the first letter of Γ_1 . The dashed red strands indicate the exterior connections which are determined by the words involving the letter λ . When we follow our exploration process until the first point of any kind, there are several possibilities that can occur. The first point can be (1) a same-side swap which connects the top-most strand with another right-directed strand (2) an opposite-side swap (i.e. turnaround) which connects the top-most strand with a left-directed strand. Also, the two strands which are connected can (1) be in the same word (2) be in different words. Any combination of these two things can happen, and so all told there are four different scenarios to account for. These four scenarios correspond to the four different categories of strings appearing in the right hand side of the loop equation: positive/negative splittings and positive/negative mergers. We proceed on a case-by-case basis. Throughout, let U_1 denote the time of the first point.

Suppose that the first point we see is a swap which connects the top-most strand with another right-directed strand, and moreover the two strands are in the same word. See Figure 41.

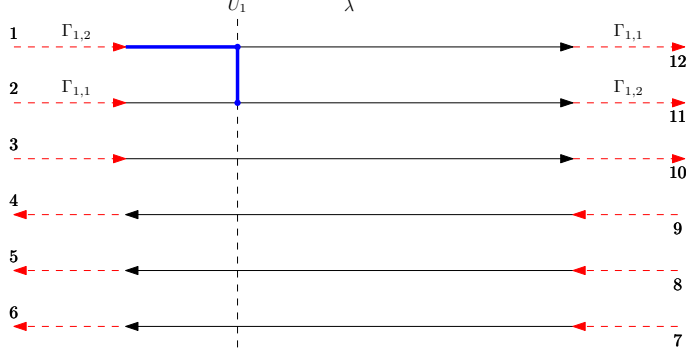


Figure 41

Since the top two strands belong in the same word Γ_1 , we can write $\Gamma_1 = \lambda\Gamma_{1,1}\lambda\Gamma_{1,2}$, where $\Gamma_{1,1}$ collects all letters which appear in between the dashed red line labeled 12 and the dashed red line labeled 2, while $\Gamma_{1,2}$ collects all letters which appear in between the dashed red line labeled 11 and the dashed red line labeled 1. After accounting for the same-side swap we saw, we may treat the part of the diagram after time U_1 as in Figure 42.

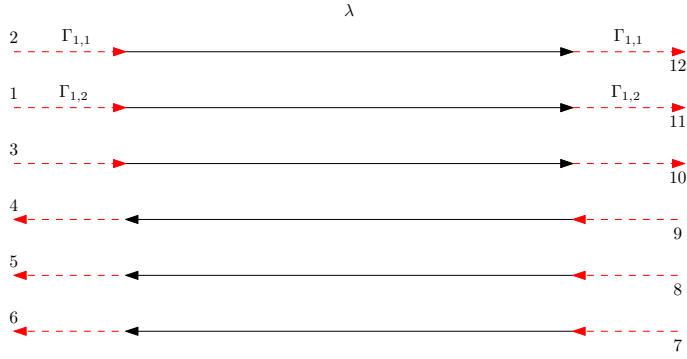


Figure 42

Notice here that the dashed red lines labeled 1 and 2 have been swapped. The effect of this is that the top and second-top strands are now in different words: $\lambda\Gamma_{1,1}$ and $\lambda\Gamma_{1,2}$. Note that the resulting string $s' = (\lambda\Gamma_{1,1}, \lambda\Gamma_{1,2}, \Gamma_2, \dots, \Gamma_k)$ is precisely a positive splitting of s at λ . We thus see that this case contributes the term

$$-\frac{1}{N} \sum_{\Gamma' \in \mathbb{S}_+((i,j), \Gamma)} \mathbb{E}[\text{Tr}(U(\Gamma'))].$$

If the first point is a swap but the two matched strands are in different words (say $\Gamma_1 = \lambda\Gamma'$ and $\Gamma_2 = \lambda\Gamma'_2$), then we would have the two diagrams in Figure 43.

Note that the two matched strands are now effectively in the same word: $\lambda\Gamma'_1\lambda\Gamma'_2$. Thus the case where the first point is a swap and the two matched strands are in different words contributes the positive merger term:

$$-\frac{1}{N} \sum_{\Gamma' \in \mathbb{M}_+(\lambda, \Gamma)} \mathbb{E}[\text{Tr}(U(\Gamma'))].$$

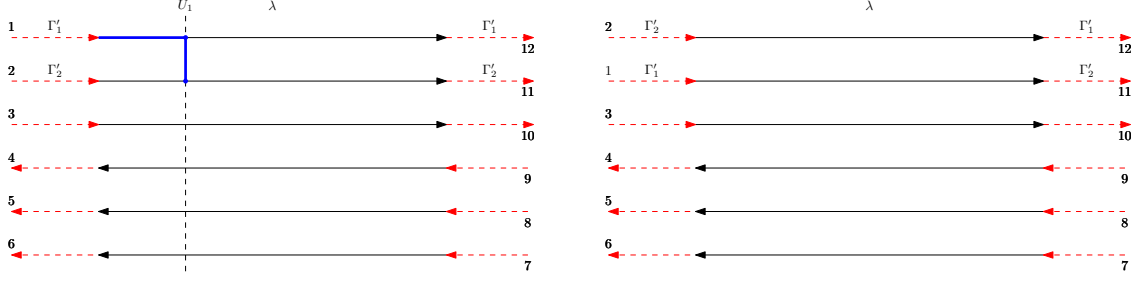


Figure 43

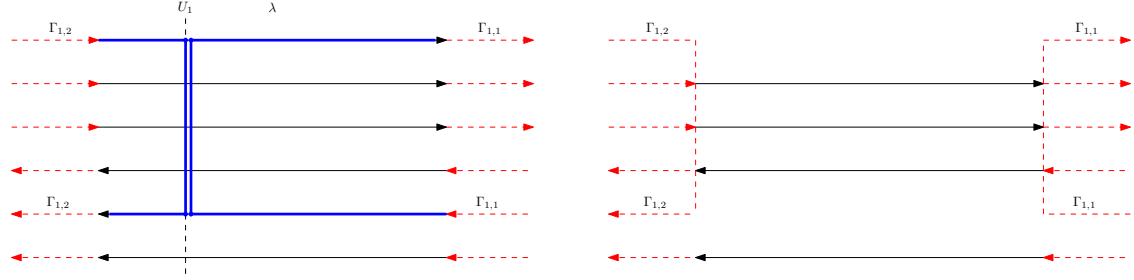


Figure 44

Next, suppose that the first point is a turnarround and the two matched strands are in the same word. We then have the two diagrams in Figure 44.

Originally, we have the word $\Gamma = \lambda\Gamma_{1,1}\lambda^{-1}\Gamma_{1,2}$. After seeing the turnarround swap, we may treat the rest of the diagram after U_1 as in the right figure, where the two matched strands have been deleted, and the word Γ has been replaced by two words $\Gamma_{1,1}$ and $\Gamma_{1,2}$. This case corresponds to a negative splitting, and contributes the term

$$\frac{1}{N} \sum_{\Gamma' \in \mathbb{S}_-(\lambda, \Gamma)} \mathbb{E}[\text{Tr}(U(\Gamma'))].$$

The final case is when the first point is a parallel swap and the two matched strands are in different words. The two pictures are as in Figure 45.

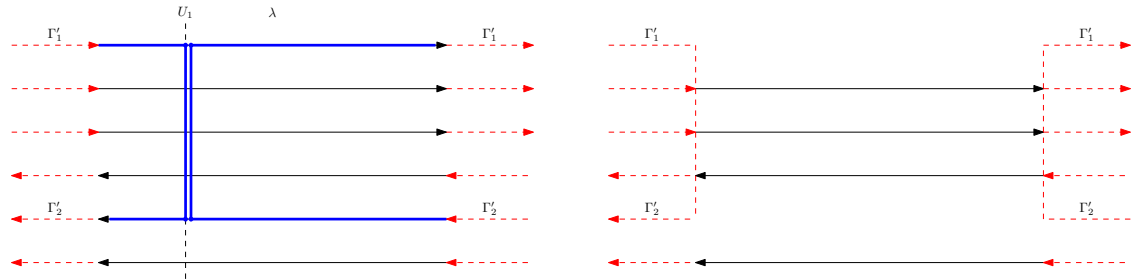


Figure 45

Originally, the top strand is part of the word $\Gamma_1 = \lambda\Gamma'_1$, while the bottom strand is part of the word $\Gamma_2 = \lambda\Gamma'_2$. After the turnarround swap, the two words Γ_1, Γ_2 merge to form the word $\Gamma'_1\Gamma'_2$.

Thus, this case contributes the term

$$\frac{1}{N} \sum_{\Gamma' \in \mathbb{M}_-(\lambda, \Gamma)} \mathbb{E}[\text{Tr}(U(\Gamma'))].$$

In summary, we have obtained the following recursion (stated using the usual trace):

$$\begin{aligned} \mathbb{E}[\text{Tr}(U(\Gamma))] &= -\frac{1}{N} \sum_{\Gamma' \in \mathbb{S}_+((i, j), \Gamma)} \mathbb{E}[\text{Tr}(U(\Gamma'))] + \frac{1}{N} \sum_{\Gamma' \in \mathbb{S}_-((i, j), \Gamma)} \mathbb{E}[\text{Tr}(U(\Gamma'))] \\ &\quad - \frac{1}{N} \sum_{\Gamma' \in \mathbb{M}_+((i, j), \Gamma)} \mathbb{E}[\text{Tr}(U(\Gamma'))] + \frac{1}{N} \sum_{\Gamma' \in \mathbb{M}_-((i, j), \Gamma)} \mathbb{E}[\text{Tr}(U(\Gamma'))]. \end{aligned}$$

To convert to the normalized trace, we need to multiply both sides by $N^{-|k|}$, and then observe that in the splitting terms, a factor of $\frac{1}{N}$ gets absorbed due to the fact that $\Gamma' \in \mathbb{S}_\pm((i, j), \Gamma)$ has one more word than Γ , and in the merger terms, a factor of $\frac{1}{N}$ pops out because $\Gamma' \in \mathbb{M}_\pm((i, j), \Gamma)$ has one less word than Γ . \square

Next, we apply the loop recursion Proposition 4.2 to obtain a recursion for Wilson loop expectations. In contrast to the notation of Section 1, we denote collections of loops by s instead of \mathcal{L} , and we refer to s as a string. Recall the notation that $W_s(Q) = \prod_{k \in [n]} \text{tr}(Q_{\ell_k})$.

Notation 4.3. Given a string $s = (\ell_1, \dots, \ell_n)$, let $\phi(s) := \langle W_s \rangle_{\Lambda, \beta}$, where $\langle \cdot \rangle_{\Lambda, \beta}$ denotes expectation with respect to the lattice Yang-Mills measure defined in (1.1). We omit the dependence of ϕ on Λ, β, N .

Note that Definition 4.1 specializes to the case of loops on a lattice: given a string s , we have the sets of positive/negative splittings/mergers $\mathbb{S}_\pm((k, i), s)$ and $\mathbb{M}_\pm((k, i), s)$.

Remark 4.4. We remark that our definition of the set of splittings and mergers is slightly different than what appears in [Cha19a, SSZ22]. In our definition, we consider all possible splittings/mergers that involve the specific location (k, i) , whereas in the earlier works, the authors consider any splitting/merger that involves any two locations of the string which correspond to the same lattice edge as the edge of (k, i) . The master loop equation of the previous works may be recovered from our equation (stated in the upcoming Theorem 4.6) by summing over all locations of s .

We need to define another type of string operation which appears for lattice Yang-Mills.

Definition 4.5 (Deformations). Let $s = (\ell_1, \dots, \ell_n)$ be a string. Let (k, i) be a location in s . We define the sets of positive and negative deformations $\mathbb{D}_+((k, i), s)$ and $\mathbb{D}_-((k, i), s)$ as follows.

The set of positive deformations $\mathbb{D}_+((k, i), s)$ is the set of all possible strings which can be obtained by a positive merger between s at location (k, i) and some oriented plaquette $p \in \mathcal{P}$. The set of negative deformations $\mathbb{D}_-((k, i), s)$ is the set of possible strings which can be obtained by a negative merger between s at location (k, i) and some oriented plaquette $p \in \mathcal{P}$.

Let e be the oriented edge of Λ that is at location (k, i) in s . Let $p \in \mathcal{P}$. In order for there to exist a positive merger between s and p , note that p must contain e . In this case, we denote by $s \oplus_{(k, i)} p$ to be the positive merger of s and p at location (k, i) . Similarly, in order for there to exist a negative merger between s and p , note that p must contain $-e$. In this case, we denote by $s \ominus_{(k, i)} p$ to be the negative merger of s and p at location (k, i) .

Let $p > e$ denote that the plaquette p contains the edge e . Note then that (here e is the edge at location (k, i) of s)

$$\begin{aligned} \mathbb{D}_+((k, i), s) &= \{s \oplus_{(k, i)} p : p \in \mathcal{P}, p > e\} \\ \mathbb{D}_-((k, i), s) &= \{s \ominus_{(k, i)} p : p \in \mathcal{P}, p > -e\}. \end{aligned} \tag{4.1}$$

Theorem 4.6 (Master loop/Schwinger-Dyson equation). *Let $s = (\ell_1, \dots, \ell_n)$ be a string. Let (k, i) be a location in s . We have that*

$$\begin{aligned} \phi(s) = & - \sum_{s' \in \mathbb{S}_+((k, i), s)} \phi(s') + \sum_{s' \in \mathbb{S}_-((k, i), s)} \phi(s') - \frac{1}{N^2} \sum_{s' \in \mathbb{M}_+((k, i), s)} \phi(s') + \frac{1}{N^2} \sum_{s' \in \mathbb{M}_-((k, i), s)} \phi(s') \\ & - \beta \sum_{s' \in \mathbb{D}_+((k, i), s)} \phi(s') + \beta \sum_{s' \in \mathbb{D}_-((k, i), s)} \phi(s'). \end{aligned}$$

Remark 4.7. Recall Remark 1.1 that our scaling is so that β in our paper corresponds to 2β in previous papers. This explains why β appears in the above recursion, while $\beta/2$ appears in [SSZ22, Equation (1.7)].

Proof. Recall from equation (1.5) that

$$\phi(s) = Z_{\Lambda, \beta}^{-1} \sum_{K: \mathcal{P} \rightarrow \mathbb{N}} \frac{(N\beta)^K}{K!} \int W_s(Q) \prod_{p \in \mathcal{P}} \text{Tr}(Q_p)^{K(p)} \prod_{e \in E_\Lambda} dQ_e.$$

For brevity, let

$$I(s, K) := \int W_s(Q) \prod_{p \in \mathcal{P}} \text{Tr}(Q_p)^{K(p)} \prod_{e \in E_\Lambda} dQ_e.$$

Fix $K: \mathcal{P} \rightarrow \mathbb{N}$. It may help to keep in mind that $K(p)$ counts the number of copies of p that are present. Before we apply Proposition 4.2, let us set some notation. Let e be the oriented edge of Λ that is traversed at location (k, i) in the string s . Recall that $p > e$ means that p contains e , and $p > -e$ means that p contains e with the opposite orientation. Recall also that if $p > e$ or $p > -e$, let $s \oplus_{(k, i)} p$ and $s \ominus_{(k, i)} p$ be the positive and negative deformations of s by p at location (k, i) . For $p \in \mathcal{P}$, let $\delta_p: \mathcal{P} \rightarrow \mathbb{N}$ be the delta function at p . Now applying the word recursion Proposition 4.2, we have that

$$\begin{aligned} I(s, K) = & - \frac{1}{N} \sum_{s' \in \mathbb{S}_+((k, i), s)} I(s', K) + \frac{1}{N} \sum_{s' \in \mathbb{S}_-((k, i), s)} I(s', K) \\ & - \frac{1}{N} \sum_{s' \in \mathbb{M}_+((k, i), s)} I(s', K) + \frac{1}{N} \sum_{s' \in \mathbb{M}_-((k, i), s)} I(s', K) \\ & - \frac{K(p)}{N} \sum_{\substack{p \in \mathcal{P} \\ p > e}} I(s \oplus_{(k, i)} p, K - \delta_p) + \frac{K(p)}{N} \sum_{\substack{p \in \mathcal{P} \\ p > -e}} I(s \ominus_{(k, i)} p, K - \delta_p). \end{aligned}$$

(Here, the factor of $K(p)$ arising in the last two terms arises because there are $K(p)$ copies of the plaquette p which can possibly be used to deform s .) From this, we obtain (note that in the splitting terms, the $1/N$ factor gets absorbed due to the fact that s' has one more loop than s , while in the merging terms, there is an extra $1/N$ factor because s' has one less loop than s)

$$\begin{aligned} \phi(s) = & - \sum_{s' \in \mathbb{S}_+((k, i), s)} \phi(s') + \sum_{s' \in \mathbb{S}_-((k, i), s)} \phi(s') - \frac{1}{N^2} \sum_{s' \in \mathbb{M}_+((k, i), s)} \phi(s') + \frac{1}{N^2} \sum_{s' \in \mathbb{M}_-((k, i), s)} \phi(s') \\ & + D_1 + D_2, \end{aligned}$$

where

$$D_1 := -Z_{\Lambda, \beta}^{-1} \frac{1}{N} \sum_{\substack{p \in \mathcal{P} \\ p > e}} \sum_{\substack{K: \mathcal{P} \rightarrow \mathbb{N} \\ K(p) \geq 1}} \frac{(N\beta)^K}{K!} K(p) I(s \oplus_{(k, i)} p, K - \delta_p),$$

$$D_2 := Z_{\Lambda, \beta}^{-1} \frac{1}{N} \sum_{\substack{p \in \mathcal{P} \\ p > -e}} \sum_{\substack{K: \mathcal{P} \rightarrow \mathbb{N} \\ K(p) \geq 1}} \frac{(N\beta)^K}{K!} K(p) I(s \ominus_{(k,i)} p, K - \delta_p)$$

Observe that we may write (by changing variables $K \mapsto K - \delta_p$ and then recalling (4.1))

$$\begin{aligned} D_1 &= -Z_{\Lambda, \beta}^{-1} \frac{1}{N} (N\beta) \sum_{\substack{p \in \mathcal{P} \\ p > e}} \sum_{K: \mathcal{P} \rightarrow \mathbb{N}} \frac{(N\beta)^K}{K!} I(s \oplus_{(k,i)} p, K) \\ &= -\beta \sum_{\substack{p \in \mathcal{P} \\ p > e}} \phi(s \oplus_{(k,i)} p) = -\beta \sum_{s' \in \mathbb{D}_+((k,i), s)} \phi(s'), \end{aligned}$$

and similarly

$$D_2 = \beta \sum_{\substack{p \in \mathcal{P} \\ p > -e}} \phi(s \ominus_{(k,i)} p) = \beta \sum_{s' \in \mathbb{D}_-((k,i), s)} \phi(s').$$

The desired result now follows. \square

5 Wilson loop expectations as sums over edge-plaquette embeddings

In this section, we show how to apply Corollary 2.7 to express Wilson loop expectations as sums over edge-plaquette embeddings (which were introduced in Section 1.4). We first prove a more abstract result about expectations of traces of words of Haar distributed Unitary matrices (Theorem 5.6) which has no reference to a lattice, and then apply this result to Wilson loop expectations to obtain Corollary 5.8.

Definition 5.1. Define the normalized Weingarten function $\overline{\text{Wg}}_N$ by:

$$\overline{\text{Wg}}_N(\pi) := N^{n + \|\pi\|} \text{Wg}_N(\pi), \quad \pi \in S_n.$$

Here, $\|\pi\| := n - \#\text{cycles}(\pi)$.

Remark 5.2. We will see later on that the normalized Weingarten function is the more natural quantity to work with, as it leads to nicer statements of our formulas. Another nice thing about $\overline{\text{Wg}}_N$ is that with this choice of normalization, the limit as $N \rightarrow \infty$ exists and depends on π . Indeed, we in fact have (see e.g. [CS06, Corollary 2.7])

$$\overline{\text{Wg}}_N(\pi) = \text{Möb}(\pi) + O(N^{-2}) \text{ as } N \rightarrow \infty,$$

where if π is decomposed into cycles of lengths C_1, \dots, C_k , then

$$\text{Möb}(\pi) := \prod_{i \in [k]} c_{C_i-1} (-1)^{C_i-1}, \quad \text{where } c_n := \frac{(2n)!}{n!(n+1)!} \text{ is the } n\text{th Catalan number.}$$

Recall from Corollary 2.7 that expectations of traces of words with respect to Haar measure may be expressed in terms of sums over pairs of matchings of strand diagrams, with matchings weighted by the Weingarten function. In this section, we will use this to express Wilson loop expectations in lattice gauge theories as weighted sums over edge-plaquette embeddings. The main step is to

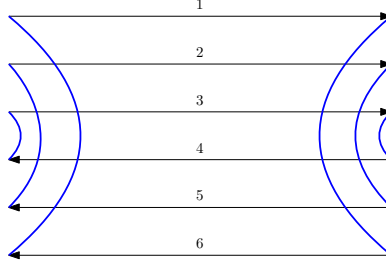


Figure 46

describe how to obtain a bipartite map from a given collection of words Γ along with a collection of matchings of strand diagrams. Let us start with some examples. Consider the following pair of left-right matchings of a strand diagram as in Figure 46. One can imagine that the two endpoints of each blue line are identified (this corresponds to “shrinking” each blue line away). In this case, one is then left with a collection of faces as in Figure 47.

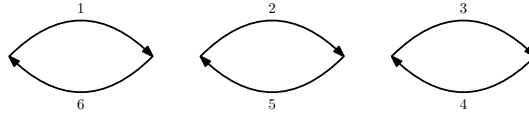


Figure 47

In Figure 48, we give another example of a pair of matchings of the strand diagram, and the corresponding collection of faces. We thus naturally have two collections of faces: the set of faces

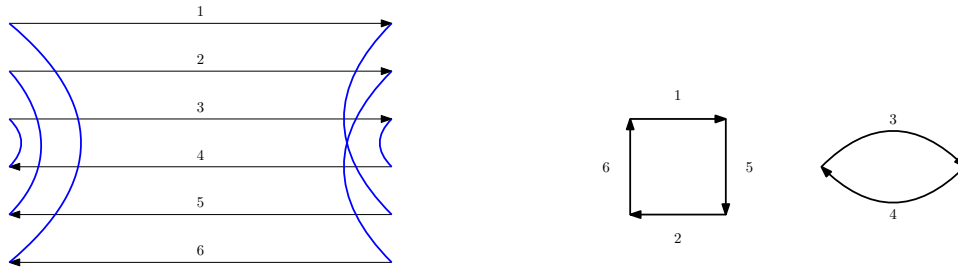


Figure 48

which correspond to words in Γ , and the set of faces obtained as above for every strand diagram. Observe that every edge is incident to exactly two faces, and moreover it is incident to one of each type of face. Therefore, we obtain a bipartite map from this data. Now the point is that the number of vertices of this bipartite map is precisely the number of components of the strand diagram. This relation is captured in the following lemma.

Lemma 5.3. Let $\Gamma = (\Gamma_1, \dots, \Gamma_k)$ be a balanced collection of words on $\{\lambda_1, \dots, \lambda_L\}$. Suppose that for each $\ell \in [k]$, the number of occurrences of λ_ℓ is n_ℓ . For $\ell \in [k]$, let $\sigma_\ell, \tau_\ell : [n_\ell] \rightarrow [n_\ell : 2n_\ell]$ be a pair of matchings of the portion of the strand diagram corresponding to Γ_k . Then $\#\text{comp}(\Gamma, ((\sigma_\ell, \tau_\ell), \ell \in [L]))$ is equal to the number of vertices in the corresponding bipartite map.

Proof. To compute the number of vertices in the bipartite map, we can proceed as follows. Recalling that the bipartite map arises from combining an interior connection with an exterior connection

of the strand diagrams, we may begin by giving the vertices of the strands separate labels. For the portion of the strand diagram corresponding to λ_ℓ , we give a total of $4n_\ell$ labels, since there are $2n_\ell$ strands. Each connection (be it interior or exterior) results in the identification of two labels. In terms of the bipartite map, labels which have been identified are in fact the same vertex. Therefore the number of vertices in the bipartite map corresponds to the number of different equivalence classes of labels, after performing all label identifications indicated by the connections. The equivalence class of a given label may be obtained by starting at the label, and alternately following the exterior and interior connections, until we arrive back at the initial label. Recalling Example 2.8, observe that this is precisely the same method for computing the number of connected components of a given strand diagram with interior and exterior connections. Thus the connected components of the strand diagram are in bijection (moreover, there is a canonical identification) with the vertices of the bipartite map. \square

Definition 5.4. Let $\mathbf{\Gamma} = (\Gamma_1, \dots, \Gamma_k)$ be a balanced collection of words on $\{\lambda_1, \dots, \lambda_L\}$. Define $\text{BPM}(\mathbf{\Gamma})$ to be the set of all possible bipartite maps which can be obtained from adding interior matchings to the strand diagram corresponding to $\mathbf{\Gamma}$. For a given bipartite map $\mathcal{M} \in \text{BPM}(\mathbf{\Gamma})$, and $\ell \in [L]$, let $\mu_\ell(\mathcal{M})$ be the partition of n_ℓ (the total number of occurrences of λ_ℓ) given by $1/2$ times the degrees of the blue faces which are glued in to the strand diagram of λ_ℓ .

Remark 5.5. Observe that for any $\mathcal{M} \in \text{BPM}(\mathbf{\Gamma})$, we have that

$$E(\mathcal{M}) = 2 \sum_{i \in [L]} n_i, \quad F(\mathcal{M}) = k + \sum_{i \in [L]} \ell(\mu_i(\mathcal{M})). \quad (5.1)$$

Here, $\ell(\mu_i(\mathcal{M}))$ is the number of parts of the partition $\mu_i(\mathcal{M})$. The first identity says that the number of edges is equal to the total number of strands in the strand diagrams, and the second identity says that the total number of faces is equal to the number of words (note each word gives a yellow face) plus the total number of cycles of the interior matching of the strand diagram (these correspond to blue faces).

Theorem 5.6. *Let $\mathbf{\Gamma} = (\Gamma_1, \dots, \Gamma_k)$ be a balanced collection of words on $\{\lambda_1, \dots, \lambda_L\}$. We have that*

$$\mathbb{E}[\text{Tr}(U(\mathbf{\Gamma}))] = \sum_{\mathcal{M} \in \text{BPM}(\mathbf{\Gamma})} \left(\prod_{\ell \in [L]} \overline{\text{Wg}}_N(\mu_\ell(\mathcal{M})) \right) N^{\chi(\mathcal{M}) - k}.$$

Proof. By Corollary 2.7, the definition of $\text{BPM}(\mathbf{\Gamma})$, and Lemma 5.3, we have that

$$\mathbb{E}[\text{Tr}(U(\mathbf{\Gamma}))] = \sum_{\mathcal{M} \in \text{BPM}(\mathbf{\Gamma})} \left(\prod_{\ell \in [L]} \text{Wg}_N(\mu_\ell(\mathcal{M})) \right) N^{V(\mathcal{M})}.$$

Applying the identities (5.1), we further obtain

$$\mathbb{E}[\text{Tr}(U(\mathbf{\Gamma}))] = \sum_{\mathcal{M} \in \text{BPM}(\mathbf{\Gamma})} \left(\prod_{i \in [L]} N^{n_i + \|\mu_i(\mathcal{M})\|} \text{Wg}_N(\mu_i(\mathcal{M})) \right) N^{V(\mathcal{M}) - E(\mathcal{M}) + F(\mathcal{M}) - k}.$$

The desired result now follows. \square

We now apply the previous considerations to lattice Yang-Mills. Let $s = (\ell_1, \dots, \ell_n)$ be a string. Recall equation (1.5), which we reproduce here:

$$\langle W_s \rangle_{\Lambda, \beta} = Z_{\Lambda, \beta}^{-1} \sum_{K: \mathcal{P} \rightarrow \mathbb{N}} \frac{(N\beta)^K}{K!} \int W_s(Q) \prod_{p \in \mathcal{P}} \text{Tr}(Q_p)^{K(p)} \prod_{e \in E_\Lambda} dQ_e. \quad (5.2)$$

For each fixed $K : \mathcal{P} \rightarrow \mathbb{N}$, we may apply Theorem 5.6 to obtain an expression for the integral above in terms of a sum over edge-plaquette embeddings. We first set some notation.

Definition 5.7. Let $s = (\ell_1, \dots, \ell_n)$ be a string, and let $K : \mathcal{P} \rightarrow \mathbb{N}$. Define the set $\text{EPE}(s, K)$ of edge-plaquette embeddings associated to s, K to be as follows. If s, K is unbalanced, then $\text{EPE}(s, K) := \emptyset$. If s, K is balanced, we define $\text{EPE}(s, K)$ to be the set of edge-plaquette embeddings (\mathcal{M}, ψ) such that for each $p \in \mathcal{P}$, there are exactly $K(p)$ faces of \mathcal{M} which are mapped by ψ to p , and for each $i \in [n]$, there is exactly one face of \mathcal{M} mapped by ψ to ℓ_i . In words, $\text{EPE}(s, K)$ is the set of edge-plaquette embeddings with plaquette counts specified by K .

Next, define

$$\text{EPE}(s) := \bigsqcup_{K: \mathcal{P} \rightarrow \mathbb{N}} \text{EPE}(s, K).$$

For $(\mathcal{M}, \psi) \in \text{EPE}(s)$, and $e \in E_\Lambda$, let $\mu_e(\psi)$ be the partition of $|\psi^{-1}(e)|/2$ induced by $1/2$ times the degrees of the faces of $\psi^{-1}(e)$. Define

$$\begin{aligned} \text{area}(\mathcal{M}, \psi) &:= \sum_{p \in \mathcal{P}} |\psi^{-1}(p)|, \\ (\psi^{-1})! &:= \prod_{p \in \mathcal{P}} |\psi^{-1}(p)|!. \end{aligned}$$

Note that if $(\mathcal{M}, \psi) \in \text{EPE}(s, K)$, then $\text{area}(\mathcal{M}, \psi) = \sum_p K(p)$ and $(\psi^{-1})! = K!$. Note also that $\text{area}(\mathcal{M}, \psi)$ is equal to the total number of yellow faces of \mathcal{M} , minus n .

Corollary 5.8. Let $s = (\ell_1, \dots, \ell_n)$ be a string. We have that

$$\langle W_s \rangle_{\Lambda, \beta} = Z_{\Lambda, \beta}^{-1} \sum_{(\mathcal{M}, \psi) \in \text{EPE}(s)} \frac{\beta^{\text{area}(\mathcal{M}, \psi)}}{(\psi^{-1})!} \left(\prod_{e \in E_\Lambda} \overline{\text{Wg}}_N(\mu_e(\psi)) \right) N^{\chi(\mathcal{M}) - 2n}.$$

Proof. Combining equation (5.2) with Theorem 5.6, we have that (recall that our Wilson loops are defined using the normalized trace)

$$\langle W_s \rangle_{\Lambda, \beta} = Z_{\Lambda, \beta}^{-1} \sum_{K: \mathcal{P} \rightarrow \mathbb{N}} \frac{(N\beta)^K}{K!} \sum_{(\mathcal{M}, \psi) \in \text{EPE}(s, K)} \left(\prod_{e \in E_\Lambda} \overline{\text{Wg}}_N(\mu_e(\psi)) \right) N^{\chi(\mathcal{M}) - 2n} N^{-K}.$$

Recalling that $\text{area}(\mathcal{M}, \psi) = \sum_p K(p)$ and $(\psi^{-1})! = K!$ for $(\mathcal{M}, \psi) \in \text{EPE}(s, K)$, the desired result now follows. \square

6 Open problems

Although lattice gauge theory has been very thoroughly studied in physics, there are many simple ideas about the relationship between random surfaces and Yang-Mills theory that have not been so thoroughly explored on the math side. There is also room for innovation: producing clever variants and toy models whose limits might be easier to describe in terms of continuum random surfaces (including those related to Liouville quantum gravity and conformal field theory). If the ultimate goal is to get a handle on a continuum theory, there is a good deal of flexibility in how one sets up the discrete models that are meant to approximate that theory. We present a series of open problems along those lines, ranging from very general and open-ended to very technical and specific.

1. For which lattice models can we establish a version of the area law (related to “quark confinement”) using the surface sum point of view? Many such results are known (from various points of view) for small β , see e.g. the discussion in [CJ16] which explains string-trajectory-based derivation of such a result in the $N \rightarrow \infty$ and small β setting.
2. For which lattice models can we establish exponential decay of correlations for the Wilson loop traces using the surface sum point of view? This is related to the so-called “mass gap” problem, see e.g. discussion in [Cha19b].
3. What can we say about the *conditional* law of the surface *given* the number and type of blue plaquettes at each edge? Once the blue plaquettes are fixed, we no longer need to consider the Weingarten function, and the remain combinatorics are simpler: in fact one obtains precisely the sort of model used to study words in GUE matrices using Wick’s formula [Zvo97]. In this setting all ways of hooking up yellow to blue along edges are allowed and all contribute with the same sign, but there is still a weighting according to the genus, which leads the surface to concentrate around minimal genus configurations in the large N limit. As a simplified model, we could even imagine that we fix the number of blue faces of each type to be exactly the same at each edge. Can we say anything about the scaling limits in this setting? Is the GUE correspondence at all helpful here?
4. Within a three-dimensional lattice like \mathbb{Z}^3 , one way to try to understand the scaling limit of an oriented random surface (which could become space-filling in the fine mesh limit, with genus tending to infinity) is to try to understand the limit of the “height function” on the dual lattice that changes by ± 1 (depending on orientation) each time one crosses a layer of the surface. Is there a setting in which such a limit can be obtained? The gradient of such a function is in some sense the normal vector field corresponding to the surface. (It is a flow in which one unit of current is assigned for each face of the surface, in the direction orthogonal to that face; the flow is not divergence free but it is curl-free except along the boundary loops.) Is there a qualitative difference between $N = 1$ and general N in the limit? The $N = 1$ case has been understood by Fröhlich and Spencer [FS82] and has an interesting β -dependent phase transition that one we would not expect to see for larger N .
5. Can we prove anything interesting about the variants in which there are many plaquettes but only three can meet along any given edge? For example \mathcal{L} might be the truncated octahedron tessellation, and \mathcal{P} can be the collection of square and hexagonal faces in the tessellation. If we require that each plaquette appears zero times or once, then the only non-zero terms come about when two of the three plaquettes along each non-interior face are present. In this case the surfaces we obtain are somehow simpler (all of the blue faces are 2-gons and the surfaces are self-avoiding), and moreover there is no need for the Weingarten function.
6. Can we reduce our sums to the study of *connected* surfaces even when β is large? What if we just fix a large number of plaquettes of each type at each edge (or say have n or $n + 1$ for some big n)?
7. Is there a clean way to simplify the problem by taking advantage of the sign cancellation that takes place as we sum over the Weingarten function?
8. Instead of weighting by genus, we can imagine we want a label 1 to N on every vertex of the final surface (which amounts to weighting by N to the number of vertices). The labeled surface is more complex than the unlabeled surface, but it also has Markov properties

that the unlabeled surface lacks and can be described without directly appealing to the Weingarten function. Can one make sense of a continuum version of this Markov property in any continuum model?

9. Is there a clear expression (or at least asymptotic expression in the limit of a large number of plaquettes) for the Weingarten function in the case that N is a small integer and one is restricting to representations corresponding to Young tableaux with at most N rows?
10. What happens if we assume a finite t for all plaquettes? What is the most natural way to express the finite- t analog of the Weingarten function and the corresponding random planar maps? Note that adding a few single-edge loops can have a similar effect to switching to finite t (in the sense that it biases the measure on $U(N)$ toward the identity).
11. Are there any natural random surface models emerging in the lattice Yang-Mills framework that lead to planar maps similar to those whose limits (can be conjectured to) correspond to Liouville quantum gravity surfaces with $c \in (1, 25)$? Those surfaces are multi-ended and infinite.
12. There have been many recent results about random planar maps of high genus and/or random hyperbolic planar maps, see, e.g. [ACCR13, Cur16, BL21, BL22, DGZZ22, JL23]. Which of these results can be extended to embedded random planar maps of the type that emerge in our analysis?
13. Can we interpret Wilson loops in terms of Liouville quantum gravity at least in the critical $c = 1$ setting where we have a “ladder graph” and have gauge fixed so that we have the identity on the left and right sides of the ladder, and each yellow plaquette can be treated as a 2-gon (since the left and right edges can be shrunk to points)? Since the yellow plaquettes are all 2-gons, we can interpret them as edges between blue faces: each blue face comes with a “height” (the height of the ladder rung) and its neighboring blue faces have heights that are one unit higher or one unit lower. Essentially one has a planar map of blue faces decorated by a one-dimensional height function, which one might expect to converge to Liouville quantum gravity with parameter $c = 1$ in the $N = \infty$ limit.
14. Two-dimensional lattice gauge theory can also be reduced to a ladder graph (if one gauge fixes along a spiral, one essentially obtains a ladder). But is there any sense in the Liouville quantum gravity surfaces for $c \in (1, 25)$, as defined in [GHPR20, DG23, DG21] can be recovered in these models?
15. What happens when one adds some correlation between the noise defining distinct edges, so that the analogs of the blue faces are perhaps not mapped to a single edge?
16. What is the fine-mesh scaling random surface we obtain when we fix exactly b yellow plaquettes of each type and take $N = \infty$ (so that the surface is simply connected)? Does it look like a continuum random tree (a.k.a. Brownian tree or branched polymer) conditioned to fill out Λ in some even way?
17. We alert the reader that the “spin-foam” constructions in [OP01, Con05] provide another approach for converting non-Abelian lattice gauge theory into a statistical physical model. We can then pose a general question: what new properties of lattice Yang-Mills theory and/or its continuum scaling limits can be deduced from the spin-foam perspective?

18. The abelian versions of “spin foam” are simpler and were used e.g. by Frölich and Spencer [FS82] to understand the phase transition structure of $U(1)$ lattice gauge theory. Can an alternative proof of these results be given using the surface expansion described in this paper?
19. Note that adding extra single-face edges in both directions has the effect of changing the underlying measure from Haar measure to another conjugation-invariant measure on $U(N)$ (which can be a signed measure if we add associate sign weights to different edge configurations). Can one obtain a natural connection between a signed-measure variant of Yang-Mills theory and the sort of random surfaces that arise in conformal field theory?
20. What can one say about supersymmetric variants of this question? Can a super-symmetric version of Yang-Mills theory be connected to random planar maps whose scaling limits can be understood in terms of Liouville quantum gravity or some other probabilistic continuum random surface model? What about fermionic variants or variants involving Higgs fields?

References

- [ACCR13] O. Angel, G. Chapuy, N. Curien, and G. Ray. The local limit of unicellular maps in high genus. 2013.
- [App11] D. Applebaum. Infinitely divisible central probability measures on compact Lie groups—regularity, semigroups and transition kernels. *The Annals of Probability*, 39(6):2474–2496, 2011.
- [BC23] B. Bringmann and S. Cao. A para-controlled approach to the stochastic Yang-Mills equation in two dimensions. *arXiv preprint arXiv:2305.07197*, 2023.
- [Bd23] T. Buc-d’Alché. Topological expansion of unitary integrals and maps. *arXiv preprint arXiv:2304.12785*, 2023.
- [BDFG02] J. Bouttier, P. Di Francesco, and E. Guitter. Census of planar maps: from the one-matrix model solution to a combinatorial proof. *Nuclear Physics B*, 645(3):477–499, 2002.
- [BIPZ78] E. Brézin, C. Itzykson, G. Parisi, and J.-B. Zuber. Planar diagrams. *Communications in Mathematical Physics*, 59:35–51, 1978.
- [BIZ80] D. Bessis, C. Itzykson, and J.-B. Zuber. Quantum field theory techniques in graphical enumeration. *Advances in Applied Mathematics*, 1(2):109–157, 1980.
- [BL21] T. Budzinski and B. Louf. Local limits of uniform triangulations in high genus. *Inventiones mathematicae*, 223:1–47, 2021.
- [BL22] T. Budzinski and B. Louf. Local limits of bipartite maps with prescribed face degrees in high genus. *The Annals of Probability*, 50(3):1059–1126, 2022.
- [CC21] S. Cao and S. Chatterjee. A state space for 3D Euclidean Yang-Mills theories. *arXiv preprint arXiv:2111.12813*, 2021.
- [CC23] S. Cao and S. Chatterjee. The Yang-Mills heat flow with random distributional initial data. *Communications in Partial Differential Equations*, 48(2):209–251, 2023.

- [CCHS20] A. Chandra, I. Chevyrev, M. Hairer, and H. Shen. Langevin dynamic for the 2D Yang–Mills measure. *arXiv preprint arXiv:2006.04987*, 2020.
- [CCHS22a] A. Chandra, I. Chevyrev, M. Hairer, and H. Shen. Langevin dynamic for the 2D Yang–Mills measure. *Publications mathématiques de l’IHÉS*, pages 1–147, 2022.
- [CCHS22b] A. Chandra, I. Chevyrev, M. Hairer, and H. Shen. Stochastic quantisation of Yang–Mills–Higgs in 3d. *arXiv preprint arXiv:2201.03487*, 2022.
- [CDK18] B. Collins, A. Dahlqvist, and T. Kemp. The spectral edge of unitary Brownian motion. *Probability Theory and Related Fields*, 170(1-2):49–93, 2018.
- [CGMS09] B. Collins, A. Guionnet, and E. Maurel-Segala. Asymptotics of unitary and orthogonal matrix integrals. *Advances in Mathematics*, 222(1):172–215, 2009.
- [Cha19a] S. Chatterjee. Rigorous solution of strongly coupled $SO(N)$ lattice gauge theory in the large N limit. *Communications in Mathematical Physics*, 366(1):203–268, 2019.
- [Cha19b] S. Chatterjee. Yang–Mills for probabilists. In *Probability and Analysis in Interacting Physical Systems*, pages 1–16. Springer, Cham: Springer, 2019.
- [Che19] I. Chevyrev. Yang–Mills measure on the two-dimensional torus as a random distribution. *Communications in Mathematical Physics*, 372(3):1027–1058, 2019. MR4034782
- [Che22] I. Chevyrev. Stochastic quantization of Yang–Mills. *Journal of Mathematical Physics*, 63(9):091101, 2022.
- [CJ16] S. Chatterjee and J. Jafarov. The $1/N$ expansion for $SO(N)$ lattice gauge theory at strong coupling. *arXiv preprint arXiv:1604.04777*, 2016.
- [CM17] B. Collins and S. Matsumoto. Weingarten calculus via orthogonality relations: new applications. *arXiv preprint arXiv:1701.04493*, 2017.
- [CMN22] B. Collins, S. Matsumoto, and J. Novak. The weingarten calculus. *arXiv preprint arXiv:2109.14890*, 2022.
- [CMŚS07] B. Collins, J. A. Mingo, P. Śniady, and R. Speicher. Second order freeness and fluctuations of random matrices. III: Higher order freeness and free cumulants. *Documenta Mathematica*, 12:1–70, 2007.
- [Con05] F. Conrady. Geometric spin foams, Yang–Mills theory and background-independent models. *arXiv preprint gr-qc/0504059*, 2005.
- [CŚ06] B. Collins and P. Śniady. Integration with respect to the Haar measure on unitary, orthogonal and symplectic group. *Communications in Mathematical Physics*, 264(3):773–795, 2006.
- [Cur16] N. Curien. Planar stochastic hyperbolic triangulations. *Probability Theory and Related Fields*, 165:509–540, 2016.
- [Dah16] A. Dahlqvist. Free energies and fluctuations for the unitary Brownian motion. *Communications in Mathematical Physics*, 348(2):395–444, 2016.

- [Dah17] A. Dahlqvist. Integration formulas for Brownian motion on classical compact Lie groups. *Annales de l'Institut Henri Poincaré. Probabilités et Statistiques*, 53(4):1971–1990, 2017.
- [DFGZJ95] P. Di Francesco, P. Ginsparg, and J. Zinn-Justin. 2D gravity and random matrices. *Physics Reports*, 254(1-2):1–133, 1995.
- [DG21] J. Ding and E. Gwynne. Regularity and confluence of geodesics for the supercritical Liouville quantum gravity metric. *arXiv preprint arXiv:2104.06502*, 2021.
- [DG23] J. Ding and E. Gwynne. Uniqueness of the critical and supercritical Liouville quantum gravity metrics. *Proceedings of the London Mathematical Society*, 126(1):216–333, 2023.
- [DGZZ22] V. Delecroix, E. Goujard, P. Zograf, and A. Zorich. Large genus asymptotic geometry of random square-tiled surfaces and of random multicurves. *Inventiones mathematicae*, 230(1):123–224, 2022.
- [DHK17] B. K. Driver, B. C. Hall, and T. Kemp. Three proofs of the Makeenko-Migdal equation for Yang-Mills theory on the plane. *Communications in Mathematical Physics*, 351(2):741–774, 2017.
- [DL22] A. Dahlqvist and T. Lemoine. Large N limit of the Yang-Mills measure on compact surfaces II: Makeenko-Migdal equations and planar master field. *arXiv preprint arXiv:2201.05886*, 2022.
- [DM22] T. Diez and L. Miaskiowski. Expectation values of polynomials and moments on general compact Lie groups. *arXiv preprint arXiv:2203.11607*, 2022.
- [DN20] A. Dahlqvist and J. R. Norris. Yang-Mills measure and the master field on the sphere. *Communications in Mathematical Physics*, 377(2):1163–1226, 2020.
- [Dri89] B. K. Driver. YM_2 : Continuum expectations, lattice convergence, and lassos. *Communications in Mathematical Physics*, 123(4):575–616, 1989.
- [Dri19] B. K. Driver. A Functional Integral Approaches to the Makeenko–Migdal Equations. *Communications in Mathematical Physics*, 370:49–116, 2019.
- [E⁺16] B. Eynard et al. Counting surfaces. *Progress in Mathematical Physics*, 70:414, 2016.
- [EO08] B. Eynard and N. Orantin. Algebraic methods in random matrices and enumerative geometry. *arXiv preprint arXiv:0811.3531*, 2008.
- [Eyn11a] B. Eynard. Formal matrix integrals and combinatorics of maps. In *Random matrices, random processes and integrable systems*, CRM Ser. Math. Phys., pages 415–442. Berlin: Springer, 2011. MR2858440
- [Eyn11b] B. Eynard. Formal matrix integrals and combinatorics of maps. In *Random matrices, random processes and integrable systems*, pages 415–442. Springer, 2011.
- [Fin91] D. S. Fine. Quantum Yang-Mills on a Riemann surface. *Communications in Mathematical Physics*, 140(2):321–338, 1991.
- [FS82] J. Fröhlich and T. Spencer. Massless phases and symmetry restoration in abelian gauge theories and spin systems. *Communications in Mathematical Physics*, 83:411–454, 1982.

- [GHPR20] E. Gwynne, N. Holden, J. Pfeffer, and G. Remy. Liouville quantum gravity with matter central charge in $(1, 25)$: a probabilistic approach. *Communications in Mathematical Physics*, 376(2):1573–1625, 2020.
- [GKS89] L. Gross, C. King, and A. Sengupta. Two dimensional Yang–Mills theory via stochastic differential equations. *Annals of Physics*, 194(1):65–112, 1989.
- [GMS05] A. Guionnet and E. Maurel-Segala. Combinatorial aspects of matrix models. *arXiv preprint math/0503064*, 2005.
- [GN15] A. Guionnet and J. Novak. Asymptotics of unitary multimatrix models: The Schwinger–Dyson lattice and topological recursion. *Journal of Functional Analysis*, 268(10):2851–2905, 2015.
- [GPW91] D. J. Gross, T. Piran, and S. Weinberg. *Two dimensional quantum gravity and random surfaces-8th Jerusalem winter school for theoretical physics*, volume 8. World Scientific, 1991.
- [IZ80] C. Itzykson and J.-B. Zuber. The planar approximation. II. *Journal of Mathematical Physics*, 21(3):411–421, 1980.
- [Jaf16] J. Jafarov. Wilson loop expectations in $SU(N)$ lattice gauge theory. *arXiv preprint arXiv:1610.03821*, 2016.
- [JL23] S. Janson and B. Louf. Unicellular maps vs. hyperbolic surfaces in large genus: Simple closed curves. *The Annals of Probability*, 51(3):899–929, 2023.
- [Juc74] A.-A. Jucys. Symmetric polynomials and the center of the symmetric group ring. *Reports on Mathematical Physics*, 5(1):107–112, 1974.
- [JW06] A. Jaffe and E. Witten. Quantum Yang–Mills theory. *The millennium prize problems*, 1:129–152, 2006.
- [Lév03] T. Lévy. *Yang–Mills measures on compact surfaces*, volume 790 of *Mem. Am. Math. Soc.* Providence, RI: American Mathematical Society (AMS), 2003.
- [Lév10] T. Lévy. *Two-dimensional Markovian holonomy fields.*, volume 329 of *Astérisque*. Paris: Société Mathématique de France (SMF), 2010.
- [Lév17] T. Lévy. The master field on the plane. *Asterisque*, 388, 2017.
- [LT20] B. Lees and L. Taggi. Site monotonicity and uniform positivity for interacting random walks and the spin $O(N)$ model with arbitrary N . *Communications in Mathematical Physics*, 376(1):487–520, 2020.
- [LT21] B. Lees and L. Taggi. Exponential decay of transverse correlations for $O(N)$ spin systems and related models. *Probability Theory and Related Fields*, 180(3-4):1099–1133, 2021.
- [Meh81] M. L. Mehta. A method of integration over matrix variables. *Communications in Mathematical Physics*, 79:327–340, 1981.
- [Mig96] A. A. Migdal. Recursion equations in gauge field theories. In *30 Years Of The Landau Institute—Selected Papers*, pages 114–119. World Scientific, 1996.

- [MM79] Y. M. Makeenko and A. A. Migdal. Exact equation for the loop average in multicolor QCD. *Physics Letters B*, 88(1-2):135–137, 1979.
- [MN13] S. Matsumoto and J. Novak. Jucys–Murphy elements and unitary matrix integrals. *International Mathematics Research Notices*, 2013(2):362–397, 2013.
- [MP19] M. Magee and D. Puder. Matrix group integrals, surfaces, and mapping class groups. I. $U(N)$. *Inventiones Mathematicae*, 218(2):341–411, 2019.
- [MP21] M. Magee and D. Puder. Surface words are determined by word measures on groups. *Israel Journal of Mathematics*, 241(2):749–774, 2021.
- [MP22] M. Magee and D. Puder. Matrix Group Integrals, Surfaces, and Mapping Class Groups II: $O(N)$ and $Sp(N)$. *Mathematische Annalen*, 2022, 1904.13106.
- [MRS93] J. Magnen, V. Rivasseau, and R. Sénéor. Construction of YM 4 with an infrared cutoff. *Communications in mathematical physics*, 155:325–383, 1993.
- [MS06] E. Maurel-Segala. High order expansion of matrix models and enumeration of maps. *arXiv preprint math/0608192*, 2006.
- [Mur81] G. E. Murphy. A new construction of Young’s seminormal representation of the symmetric groups. *Journal of Algebra*, 69(2):287–297, 1981.
- [Nov10] J. Novak. Jucys–Murphy elements and the unitary Weingarten function. *Banach Center Publications*, 1(89):231–235, 2010.
- [Oko00] A. Okounkov. Random matrices and random permutations. *International Mathematics Research Notices*, 2000(20):1043–1095, 2000.
- [OP01] R. Oeckl and H. Pfeiffer. The dual of pure non-Abelian lattice gauge theory as a spin foam model. *Nuclear Physics B*, 598(1-2):400–426, 2001.
- [Pol81] A. M. Polyakov. Quantum geometry of bosonic strings. *Physics Letters B*, 103(3):207–210, 1981.
- [PPSY23] M. Park, J. Pfeiffer, S. Sheffield, and P. Yu. Wilson loop expectations as sums over surfaces on the plane. *arXiv preprint arXiv:2305.02306*, 2023.
- [QT23] A. Quitmann and L. Taggi. Macroscopic loops in the Bose gas, Spin $O(N)$ and related models. *Communications in Mathematical Physics*, pages 1–56, 2023.
- [Sen97] A. Sengupta. *Gauge theory on compact surfaces*, volume 600 of *Mem. Am. Math. Soc.* Providence, RI: American Mathematical Society (AMS), 1997.
- [She21] H. Shen. Stochastic quantization of an abelian gauge theory. *Communications in Mathematical Physics*, 384(3):1445–1512, 2021.
- [She22] S. Sheffield. What is a random surface? *arXiv preprint arXiv:2203.02470*, 2022.
- [SSZ22] H. Shen, S. A. Smith, and R. Zhu. A new derivation of the finite N master loop equation for lattice Yang–Mills. *arXiv preprint arXiv:2202.00880*, 2022.

- [tH93] G. 't Hooft. A planar diagram theory for strong interactions. In *The Large N Expansion In Quantum Field Theory And Statistical Physics: From Spin Systems to 2-Dimensional Gravity*, pages 80–92. World Scientific, 1993.
- [Tut68] W. T. Tutte. On the enumeration of planar maps. 1968.
- [Wei78] D. Weingarten. Asymptotic behavior of group integrals in the limit of infinite rank. *Journal of Mathematical Physics*, 19(5):999–1001, 1978.
- [WG01] R. Wilson and J. Gray. *Mathematical conversations: selections from The mathematical intelligencer*. Springer Science & Business Media, 2001.
- [Wil74] K. G. Wilson. Confinement of quarks. *Physical review D*, 10(8):2445, 1974.
- [Wil04] K. G. Wilson. The origins of lattice gauge theory. *arXiv preprint hep-lat/0412043*, 2004.
- [Wit91] E. Witten. On quantum gauge theories in two dimensions. *Communications in Mathematical Physics*, 141(1):153–209, 1991.
- [ZJ09] P. Zinn-Justin. Jucys-Murphy elements and Weingarten matrices. *arXiv preprint arXiv:0907.2719*, 2009.
- [ZJZ03] P. Zinn-Justin and J.-B. Zuber. On some integrals over the $U(N)$ unitary group and their large N limit. *Journal of Physics A: Mathematical and General*, 36(12):3173, 2003.
- [Zvo97] A. Zvonkin. Matrix integrals and map enumeration: an accessible introduction. *Mathematical and Computer Modelling*, 26(8-10):281–304, 1997.